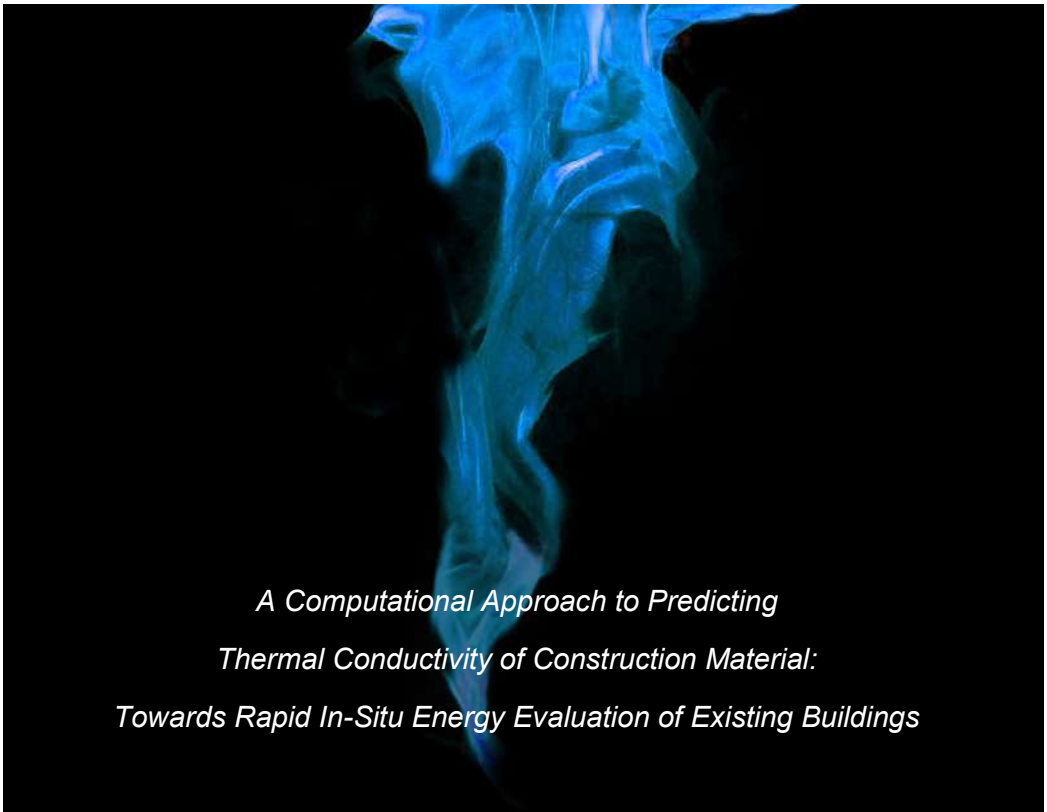

A Computational Approach to Predicting

Thermal Conductivity of Construction Material:

Towards Rapid In-Situ Energy Evaluation of Existing Buildings

SUBMITTED IN PARTIAL FULFILLMENT OF THE REQUIREMENTS FOR A

DOCTOR OF PHILOSOPHY IN COMPUTATIONAL DESIGN

School of Architecture,

College of Fine Arts

Submitted by:

Noreen Saeed

For Abu Jee

Advisory Committee

Ramesh Krishnamurti
Chair
Professor, Computational Design
School of Architecture,
Carnegie Mellon University

Jonathan A. Malen
Professor, Mechanical Engineering & Material Sciences
Carnegie Mellon University

Chris Harrison
Associate Professor, Human-Computer Interaction Institute
Carnegie Mellon University

Abstract

Thermal conductivity of the building envelope is the basis for building energy simulation and gives key information about its energy performance. Accurate assumptions about thermal conductivity contribute to accurate energy labelling of buildings, provide insights for retrofit strategies and are instrumental in energy policy making at an urban level. However, physically establishing the thermal conductivity of the external walls of a building is difficult and is often a time-consuming process. Currently available measurement methods are extremely technical with restrictive boundary conditions. To avoid this dilemma, thermal conductivity is often inferred from published standards, which gives significantly different values compared to in-situ measurement. It is therefore important not only to measure thermal conductivity of buildings in-situ, but also to make the means for evaluating thermal conductivity ubiquitous, accessible and uncomplicated for architects, surveyors and building engineers.

Aiming to bridge the identified gap, this thesis presents a study of material properties, how they interrelate, and how these relationships can be exploited to assess the building fabric. It presents a computational approach, which is a data-driven method motivated by experimental results. In this method thermal conductivity is predicted using computation on experimental data of relevant material properties rather than direct measurement. During this work, extensive experiments were conducted to measure thermal conductivity, dielectric and mechanical material properties to determine their correlation. These experiments were conducted on two categories of materials. One that represents wood-frame construction, which is the most prevalent form of construction for residential use here in the United States. The materials studied for this category included solid wood, plywood, OSB, chipboard, MDF and gypsum drywall. The other category of materials is the ceramic family and is representative of clay brick construction. Clay bricks, concrete, naturally occurring stone and gypsum were included in this study. Apart from the categories described above, work was also conducted on multiple-layered materials so that the effect of stacking layers together could be studied. A final study was performed to explore the effects of moisture on materials thermal conductivity and dielectric properties.

The empirical data collected during this study suggests a strong correlation between thermal conductivity and dielectric properties. This correlation has not been systematically studied previously and experimental data on the subject is extremely scarce. The correlation found through this study identifies the potential of using handheld meters or antenna-based devices that can quickly measure capacitance and dielectric properties, to measure thermal conductivity instead. If successful, this method will eliminate the need to create steady-state conditions required for thermal conductivity measurement and simplify the measurement enough to bring a useful gadget not only for experts, but also for the layperson.

Keywords:

Thermal Conductivity, in-situ measurement, relative permittivity, dielectric constant, material properties, correlation, materials properties, experimental data collection

Table of Contents

List of tables

List of Figures

PART I

1 Introduction

Thermal conductivity is a material property that defines the rate at which thermal energy is transported through a material due to a temperature gradient [1]. Thermal conductivity of walls signals the amount of heat lost through a building envelope; thus, it is an important indicator of building energy efficiency. In the current context of a worldwide call towards sustainable practices, buildings and construction are responsible for 30% of the global energy consumption [2]. As such, accurate and reliable in-situ diagnostic tools for evaluating and predicting building energy consumption are becoming increasingly imperative.

Although thermal conductivity is important to measure, its difficult measurement process [3] makes it an elusive number. In-situ measurements of the building envelope add further complications to the process. The methods available for this measurement are slow or expensive, typically requiring technical expertise. The most commonly used method is known as the heat flow meter method (HFM), which requires a minimum of three days to complete. The other more commonly used technique is infra-red thermography, which has additionally restrictive boundary conditions that depend on weather and environmental conditions. Results may deviate by up to 200% from the actual value [4]. Both methods require considerable temperature difference of at least 10°C between indoors and outdoors and steady state conditions be ensured at the time of measurement. Results improve with a higher temperature difference between indoors and outdoors [5] in each case, making environmental conditions a pre-requisite for accuracy.

Thermal conductivity of building walls is often inferred from published standards or from literature provided by manufacturers [6]. It is assessed from the properties of constituent material layers and components. However, numerous studies have demonstrated that in-situ measurements of thermal conductivity are significantly different from the calculations based on relevant standards [7]. Asdrubali concludes that several factors may be at play. Manufacturers may report an exaggerated performance of their products for marketing reasons, or that installation may not have been carried out correctly. Measurement under controlled lab conditions may also be a factor. Furthermore, environmental conditions, moisture migration, workmanship, and substitution of materials during construction can also affect thermal conductivity in-situ.

Inaccuracies in the assumption of thermal conductivity lead to poor energy predictions. Studies show that actual energy consumption deviates from predicted values considerably [8]. Doran [9] showed that existing methods of energy calculations for regulatory purposes underestimate true heat losses in walls by more than 30% in some cases. Prada et al [10] has demonstrated that the precision of energy models of buildings depends largely on the inaccuracy of the assumed thermo-physical properties of the building envelope. Majcen et al showed that in every energy efficient building, actual gas consumption exceeded predicted levels [11]. He showed that a slight deviation in the estimate of U-values can account for a large part of the gap between the predicted and actual energy consumption [12].

To address the gap in the evaluation of thermal conductivity of building walls, this thesis presents a computational approach to thermal conductivity. Using this approach, thermal conductivity is predicted by exploring correlations between material properties rather than

direct measurement. This approach is data driven and relies on regression algorithms rather than scientific measurement. In this thesis, I propose to use material dielectric properties to estimate thermal conductivity. Dielectric properties relate to the electrical property of capacitance and quantifies a material's ability to store electric charge. The relative dielectric constant (relative permittivity), denoted by ϵ' refers to a material's ability to store electric charge, while the dielectric loss factor ϵ'' refers to its ability to dissipate energy in the form of heat. The ratio of the two quantities is called the dissipation factor and is also referred to as the tangent of the loss angle, tan δ.

For wood and some wood-derivatives, the correlation of density and moisture with thermal conductivity has enabled the prediction of thermal conductivity rather than direct measurement [13,14]. Sensing of density and moisture content of wood [15] and numerous agricultural products [16–18] has been achieved using their dielectric properties. It is thus hypothesized that the thermal conductivity of wood and wood-based materials may be predicted using their dielectric properties. A study by Venkateswaran in 1974 concluded that wood thermal conductivity and permittivity are more strongly correlated than thermal conductivity is with density and moisture content [19]. Although the study was not completely based on experimental data, it confirms the hypothesis presented in this thesis.

The core of this thesis lies in the extensive experimental work that was conducted to explore the relationship between various material properties. However, before beginning the experiments, a comprehensive data collection was performed from various literature and websites about these material properties. Almost no data was found where thermal conductivity and dielectric properties were measured on the same material. However, data analytic techniques were used to join various sets to form a conceptual dataset and this set was analyzed prior to conducting experiments. The results of the data analysis set forth the precedence for the experimental work.

Substantial experimental work was then conducted to explore the relationship of thermal conductivity with dielectric material properties. A large focus was been placed on materials related to the wood-frame construction. According to the US census bureau, more than 90% new single family and more than 80% percent new multifamily building in the United States were constructed using the wood-frame construction [20]. Solid wood is not only used in construction by itself, but its numerous derivatives form an integral part of wood-frame construction. For this reason, several experiments were dedicated to solid wood and the way its material properties inter-relate. Other materials studied in this category were plywood, OSB, chipboard, MDF and gypsum drywall.

Further experiments were performed on the ceramic family of materials to explore their material properties. Brick construction is the primary form of construction in a large part of the world, and 1,391 billion units of bricks are produced annually [21]. For this reason, clay bricks, poured concrete / mortar and gypsum were included in the study. These materials represent components of brick construction.

In addition to the two material categories described above, further studies were conducted on multilayered materials. For this study, layers of material were stacked together to form a multilayered material representative of a section of a wall. This was done for wood and wood-based materials in a separate study, and for ceramic materials in another one. The

effect of layering materials, like contact resistance was studied. Further, cavity walls and the potential for both thermal conductivity and dielectric constant were explored.

The last study related to moisture content of materials. In this study only wood and wood-based materials were included. After oven-drying the samples to find their dry densities, the samples were conditioned to hold specific moisture levels. The effect of moisture on thermal conductivity and dielectric properties was recorded. Correlations were drawn for various electrical properties with thermal conductivity and the suitability of each metric was explored. Finally, data analytics were applied to effectively predict thermal conductivity of a new set of samples using the collected data.

1.1 Main Results

Results of the experiments indicate that there is enough information encoded in dielectric material properties to effectively predict thermal conductivity. This metric may be used for in-situ energy evaluation efficiently and easily. For the studied construction materials, there is a strong correlation between thermal conductivity and dielectric properties. The tools and gadgets available to measure dielectric properties quickly and easily can be employed to predict thermal conductivity. The study of wood and wood-based materials revealed a straightforward correlation at 100 kHz frequency given that the materials held similar moisture levels. However, higher and lower moisture levels added complication. Thermal conductivity could be predicted within a ±20% accuracy using advanced machine learning. While 100 kHz was found suitable for wood, ceramic materials were found to be better characterized at higher frequencies in the Megahertz and Gigahertz range.

Dielectric properties were found suitable for predicting thermal conductivity not only for the individually tested construction materials, but also in the case where these materials were stacked together in series. Contact resistance seemingly affects both thermal conductivity and dielectric properties in similar ways. The correlation holds for both wood, wood-based materials and materials belonging to the ceramic family. Another significant finding of the study is that cavity walls can be successfully measured using dielectric properties as well.

1.2 Significance of the Work

The correlation explored in this thesis between thermal conductivity and dielectric material properties has several strong implications. If proven, then it would then imply that thermal conductivity can be predicted by measuring the dielectric properties of building envelopes in-situ and the tools developed thus far for measuring dielectric properties can be effectively used to predict thermal conductivity. Such technology to measure dielectric properties of building walls is highly developed in the form of radar systems, GPRs and technology related to structural health monitoring. These technologies can be customized to serve as thermal conductivity meters. It thus has the potential for a bespoke gadget which can be utilized for lay use.

Since the measurement of dielectric properties of a building envelope is independent of environmental conditions, the proposed method would effectively remove such a reliance. For example, both the heat flow meter method and thermography rely on a temperature difference of at least 10°C between indoors and outdoors. At the very least a stable direction of heat flow during measurement time is required. Thermography results are affected by

cloud cover, wind speed etc. which can lead to inaccuracies. The proposed method would be free of such requirements. It would also take a far shorter time for measurement.

This thesis also offers a unique dataset. There is very scarce literature which explores the relationship between thermal conductivity and dielectric properties. Such a relationship has not been systematically explored in the past, and thus this dataset offers unique insights for scientists of various fields.

1.3 Outline

This thesis is divided into two parts. In the first part, the concept of estimating thermal conductivity using other material properties is explored theoretically. The notion that material properties inter-relate and hence one property can be estimated from another is explored using existing data and literature produced by other scientists. The second part of this thesis is about experiments to collect data related to material properties. The methods and tools related to those experiments and the analysis of the collected data.

1.3.1 Part I

Chapter 1: The first chapter introduces the thesis, and the concepts it is built upon. The need for the research is identified, important results are conveyed and the implications of the work are presented.

Chapter 2: The second chapter explores the ways in which thermal conductivity is estimated in-situ. Technology in use today and state of the art techniques are discussed in this chapter. The drawbacks and advantages of each method is presented and the gap in field is identified.

Chapter 3: A brief history of the computational view of material properties is presented. Scientist work to compute the material property of their interest from other properties is explored. The results and success of these studies are investigated.

Chapter 4: Chapter 4 describes the data collected for this thesis from literature, websites and repositories related to thermal conductivity and mechanical properties of materials. Presented in this chapter, are methods used to interrelate this data, and the correlation of various material properties that were uncovered.

1.3.2 Part II: Experiments

Chapter 5: This chapter kick starts the section related to the experiments with a description of fabrication process of hundreds of samples for the experiments. Tools and methods used sample preparation, and the accommodations needed for each experiment type are described here.

Chapter 6: Experimental apparatus and methods are described in this chapter. Experimental methods for the measurement thermal conductivity, dielectric properties and sound are cataloged in this chapter. Tools and gadgets along with make and model number are reported. Associated formulas for calculation of material properties are also narrated.

Chapter 7: Experimental results correlating thermal conductivity and dielectric properties for wood and wood-based materials are detailed. A thorough examination of existing literature

to validate the experimental results is produced. The strength of the correlation and its repercussions are examined.

Chapter 8: Experimental results related to sound are detailed in this chapter. How the speed of sound relates to thermal conductivity and the strength of the correlation is investigated.

Chapter 9: The effect of layering materials together to form composites on both thermal conductivity and dielectric properties is scrutinized and experimental results are illustrated. Contact resistance and the presence of air cavities is considered in the context of material suitable for wood-frame construction.

Chapter 10: The distinctly different behavior of ceramic materials compared to wood and wood-based materials is studied in this chapter. Ceramic thermal conductivity and dielectric properties are explored experimentally. Suitability of frequency range for this measurement is investigated.

Chapter 11: The effect of moisture content on wood thermal conductivity and dielectric properties is described along with important conclusions.

Chapter 12: In the final chapter a summary of conclusions for all experiments is detailed. The potential for unified regression parameters is also explored. The scope for future work is identified and a reflection on the main points of focus is narrated.

2 State of the Art

Based on the nature of the temperature field within a sample, thermal conductivity is measured using either steady state, or transient methods [22]. In the former, a steady temperature field is created or assumed inside the sample, and heat transfer is estimated by subtracting all losses from the delivered heat. Steady state conditions must be created in this case, which means that heat must be flowing at a steady pace through the material during the measurement period. In the case of transient methods, the sample is subjected to time varying temperature field, in which case the losses are negligible due to short measurement times. There is a lot of sophisticated equipment to measure thermal conductivity under lab conditions, using both the steady state and transient means. However, such measurements for in-situ walls are very difficult and mostly limited to steady state methods. A brief description of methods used to estimate thermal properties of in-situ walls that are currently in use are given below.

2.1 Heat Flow Measurements: ISO and ASTM standard practices

Based on the steady state method, calculation of thermal conductivity of existing structures is detailed in international ISO standards (ISO 9869) [23] , and is also defined by the ASTM (C1155-95) [24]. These standards give guidelines on computing the thermal resistance of existing walls using heat flux and temperature measurements, along with the relevant mathematical models. This method requires careful placement of heat flux and temperature sensors on walls, and for measurements of sensor data to be recorded every five to ten minutes over an extended time period. The time series data is analyzed in different ways to calculate the R-value or U-value of the material.

A study carried out in University of Newcastle by Luo et al used heat flow measurements to find thermal conductivity of walls of a test module [25]. Their study and results are indicated by Figure 1 and Figure 2. These figures represent the typical method of finding thermal conductivity of walls based on steady state methods as described in the ASTM and ISO standards. Figure 1 illustrates the sensors used for temperature measurements, and how these are affixed to walls. Figure 2 shows the recorded results over a one-month period. It reveals how the measured thermal conductivity measurements swing wildly over each twenty-four hour time period. These measured values are averaged out to estimate the thermal conductivity.

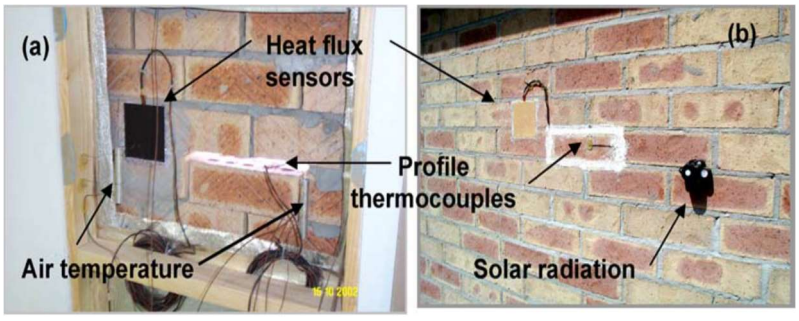

Figure 1 (Left) Sensors embedded in walls during the study by Luo et al [25]. Some of the sensors were painted the same color as the wall in an attempt to match the absorbance and emissivity of the walls.

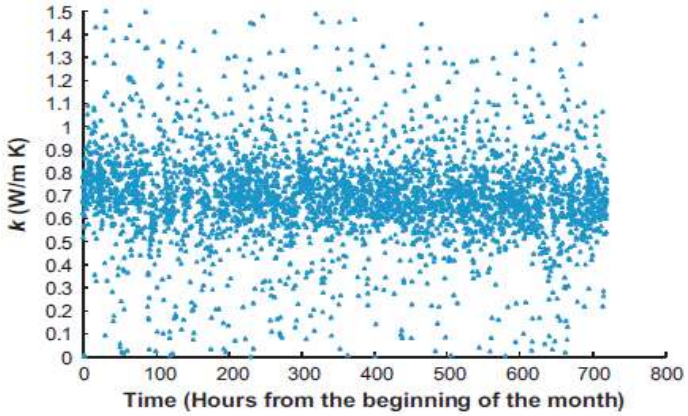

Figure 2 (Left) One data point of measured thermal conductivity for every ten minutes as per the study by Luo et al. Measured values seem to swing between 0 and 1.5 in every 24-hour period

The above study demonstrates that this type of measurement is time intensive. The reason for this is that the time needed to reach steady state conditions is directly proportional to the square of the thickness of the material and inversely proportional to thermal diffusivity of the material [26]. The change in temperature during the day and night ensures that heat is not flowing at a constant rate long enough to attain steady state conditions.

***Drawbacks*:** This method is time extensive and takes several days to collect data [23,24]. The minimum duration for measurement and recording of temperature data is three days, and the accuracy increases with increased number of days [27]. Moreover, it requires a significant temperature difference between indoors and outdoors to yield accurate results, and thus it is seasonally restricted [6]. Appendix A gives the results of a detailed analysis comparing how the number of days required to calculate thermal conductivity changes according to different seasons, and how different mathematical models in use today compare against one another. Furthermore, the accuracy of results increases with an increased temperature gradient. This temperature gradient might not be possible in mild climatic conditions [28]. Additionally, this method also requires training, and according to ASTM standards should only be performed by a skilled individual [24].

2.2 Hot Box Method

This technique is also based on steady state methods, and is described in ASTM C1363 – 11 [29]. This technique designed for testing construction materials under lab conditions and is suitable for materials of a built-up or composite nature. Various scientists have proposed adaptions of the method so that it could be performed in-situ. Figure 3 shows the experimental set up of a hot box as described by Sassin et al [30]. Meng et al [31] presented optimal measurements of a portable hot box and a mathematical model for in-situ measurements of thermal conductivity (See Figure 4). This method has not been tested on multi leaf walls, and is a new technique requiring verification.

Drawbacks: The hot box method is meant for a laboratory setting only. Variations of this technique adapted for on-site calculations have been proposed by various scientists. However, measurement time is very long owing to the need for steady state conditions. Moreover, it requires the transport of cumbersome equipment to the site.

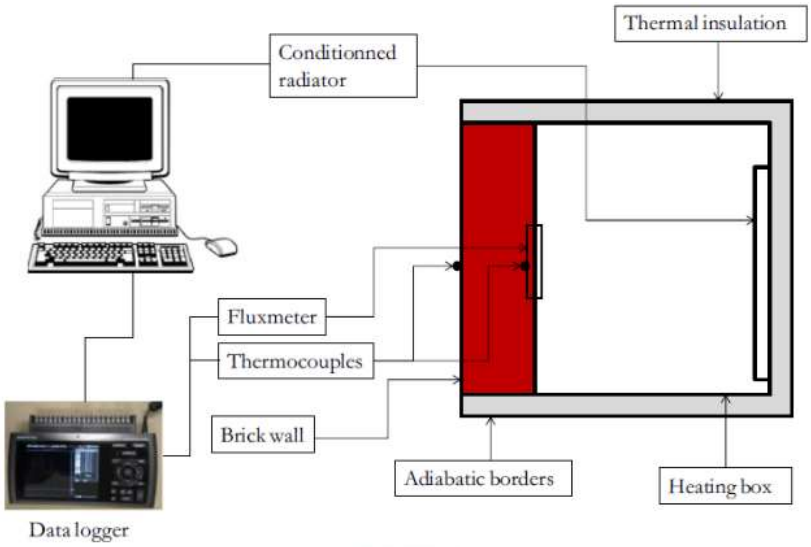

Figure 3 Configuration of a Hot-Box as described by Sassine [30]

Figure 4 Hot box as described by Meng et al [31]

2.3 Infra-red Thermography

Infrared cameras are used to measure surface temperature and emissivity combined with readings for wind speed to calculate thermal conductivity of materials. Calculation time for this technique is within a few hours. Although a lot quicker than heat flow measurements, this method has many boundary conditions as defined by researchers [5,32–35]. These boundary conditions are described as being season and weather bounded requiring specific weather and daylight conditions to work properly. Accurate results can only be obtained in overcast days with best results early in the morning. Required temperature difference between indoors and outdoors must be at least ten degrees, with low wind speed. Moreover, the method works well for heavy structures like bricks, but more research is needed to produce good results for light weight structures like timber etc. Recent research by Tejedor et al (Sept 2017) shows advances in this technology using quantitative internal thermography requiring only a 7 degree temperature difference, workable for single or double leaf walls and doable within 2-3 hours [36]. However, this is a new technique and requires further research to verify and consolidate.

***Drawbacks*:** The technique is weather and hence seasonally bound. While good results can be achieved within a few hours during some seasons, the same may not be true for summers, or for freely ventilated buildings. Moreover, the procedure is very complicated, requiring skilled professionals to take accurate measurements.

2.4 Transient Techniques

Sorensen describes a handheld U-value meter, which is termed as a device for measuring heat loss based on transient methods of calculation. This is illustrated in Figure 5. This device however, only works on single leaf structures in the absence of moisture and the supposition that heat flow is from inside to outside and not vice versa [37,38]. Pilkington et al attempted to determine the thermal conductivity using thermal probes like hot wires, disks, or strips, but reported that the task could not be completed because these sensors need to be inserted into the material, and this is not possible with in-situ walls using non-destructive methods [39]. Rasooli et al proposed a response-factor based approach to calculation of u-values of in-situ walls, and reported accuracy within 2%. However, this technique requires the use of a heater, ice and fan to linearly heat and cool the wall over at least a two hour period and is very cumbersome [40]. This technique is also very new and is yet to be tested by other researchers. Its major drawback is the cumbersome equipment like heater and ice that needs to be transported to the site. The technique is also very sensitive and requires much skill to complete. He built upon this technique and tested it on various types of construction and found that this technique does not work on cavity walls or walls where insulation is very thick [41].

Figure 5 Hand-held u-value meter as described by Sorensen

2.5 Use of Tables

Thermal conductivity values for energy modeling are usually taken out of tables from published data, and many countries have their own standards and practices defined by concerned authorities [6]. It is assessed from the properties of constituent material layers and components.

However, there may be several discrepancies related to the published data used to infer thermal conductivity of building walls. Available thermal properties of materials like concrete may vary up to 80% [42]. A look at ASHRAE's [43] material properties table (chapter 26) reveals that about fifty percent of the sources for the listed data precedes 1989, which means that the statistics are based on materials which may no longer be in use, or their properties changed by new manufacturing methods and materials. Appendix B provides a quick look at such data. It can also be seen that much of the data is established through the work done by a single scientist on a small data set. Furthermore, data from various countries may not be in agreement, and whatever data that does agree is a result of historic 'borrowing' [44] where data is copied from one text to another without correct referencing.

Numerous studies have demonstrated that in-situ measurements of thermal conductivity are significantly different from the calculations based on relevant standards [45,46]. Asdrubali [7] concluded that several factors may be at play. Manufacturers may report an exaggerated performance of their products for marketing reasons, or that installation may not have been carried out correctly. Measurement under controlled lab conditions may also be a factor. Furthermore, environmental conditions, moisture migration, workmanship, and substitution of materials during construction can also affect thermal conductivity in-situ.

***Drawbacks*:** Unreliable and inadequate.

2.6 Conclusion

Of the methods described to estimate the thermal conductivity of in-situ walls, the most commonly used ones are extremely time consuming and bound by weather and seasonal conditions. Some require a lot of equipment to be carried to the site and can only be performed by professionals trained in this practice. All of them are based on a method of measurement of temperature and heat flux. Consequently, there is a need for new tools to estimate the thermal properties of in-situ walls with easier to use methods and devices.

A summary of techniques used for measuring thermal conductivity of in-situ walls, and their related drawbacks are presented below.

Method	Time Taken	Weather / Season Bound	Works for Multi Leaf Walls	Works with moisture content	Accuracy	Equipment	Comment
Heat Flow Method	Min. 3 days Can be more than 20	Yes, highly	Yes	Yes	Only under correct weather conditions	Min. 4 sensors.	Most commonly used method
Infra-Red Thermo-graphy	Few hours	Yes, highly	Not tested for cavity walls	Yes	Only under correct weather conditions	Expensive. Trained operator required	Most commonly used method
Hot box by Meng et al [31]	Min. 3 days	No	Not tested yet	Not tested yet	High for the one wall it was tested.	Cumber-some	New technique not yet verified
U-Value Meter [37,38].	Instant	Yes	No	No	High for dry single leaf walls	Small and handy	Does not work for moisture content
Response Factor Approach [40,41].	Few Hours	No	Not for cavity walls	Yes	High for the walls tested	Heater, ice, fan, and min 4 sensors.	Shows good initial results but needs verification

3 Computational Approach to Material Properties

The ***computational approach*** to material properties is data driven. It is about finding correlations between various properties and using data analytics to make predictions instead of direct measurement. This approach is about mapping one set of numbers onto another in a meaningful and informed way. The crux of this thesis is how material properties are inter-related, and how one property can be used to make predictions about another. Sometimes it can be done by translating one set of numbers onto another using ordinary least squares linear regression, and sometimes by using multidimensional vectors with sophisticated machine learning algorithms to make these predictions.

The concept of a computational approach to material properties is centuries old. One example is that of the measurement of temperature, which was first derived from a measurement of distance in the seventeenth century. Temperature was first measured based on how much a gas expands or contracts in response to environmental conditions [47]. In 1720 a thermometer was invented which determined the temperature based on how much mercury expands or contracts [48]. Thus, a change in volume of mercury provided a yardstick to measure temperature. Modern day thermocouples make use of the thermoelectric effect and map a measurement of voltage difference across two dissimilar electrical conductors to determine the temperature. Here, the computation relates to how the voltage difference across the junction of the two metals is mapped to temperature. In this measurement type, ordinary least squares linear regression is used to map one set of numbers to another.

The exploration in this chapter is intended to lead to an identification of which material properties might be useful in make a prediction of thermal conductivity. It is also meant to explore how this property may be mapped to thermal conductivity. This chapter investigates how scientists in various fields have used a computational approach to measure some material properties of interest.

3.1 Thermal Conductivity: Effect of Density and Moisture Content

By far the most studied link between thermal conductivity and other material properties is that of density and moisture content. This relationship has been extensively studied for wood and wood-based panels used in the construction industry. Some of this work is described in the following sections.

3.1.1 Thermal Conductivity of Solid Wood

There are various models to predict the thermal conductivity of wood based on density, moisture content and porosity. These models assert that thermal conductivity of wood is independent of wood species and depends solely on other properties like density, moisture content and porosity. Thermal conductivity increases linearly with an increase in density or moisture content.

One of the first few studies in this context began in the late nineteen-twenties. Rowley studied these characteristics in detail and published the findings of his work in 1933 [49]. In 1941, MacLean [13] published his model to predict thermal conductivity. The regression

equation on experimental data related to wood samples of various densities and moisture content. It was soon followed by Wangaard in 1943 who produced an alignment chart to predict thermal conductivity based on an experimental data [50]. Following this, various scientists performed experiments and published their findings in various journals. Subsequently other scientists collected data from these scattered publications and compiled them to form a bigger database. One such scientist was Wilkes [51] who calculated and proposed a regression line based on 1094 data points collected from various sources in 1979. His equation is quoted in the current ASHRAE fundamentals handbook [43] as the suggested method for approximating the thermal conductivity of wood. The one suggested by Tenwolde in 1988 [52] is used as a guide to thermal conductivity of various wood species by the US Department of Agriculture's Handbook [53].

As far as raw data is concerned, Cardenas and Bible [54] have perhaps published the biggest dataset for wood. It contains more than 500 unique entries for wood thermal conductivity, and lists the density, moisture content and source of all published readings.

A brief history of such computational approaches to thermal conductivity of wood is summarized in Table 1.

Table 1: A timeline of computational approaches to thermal conductivity of wood

Year	Source	Related info and Equation
1933	Rowley [55]	No published equation, but graph showing straight line relationship between density and thermal conductivity.
1940	Wangaard [50]	Alinement chart representing relationship between thermal conductivity, density and moisture content
1941	MacLean [13]	$\lambda = S (1.39 + 0.028 M) + 0.165$ (for moisture content under 40%) $\lambda = S (1.39 + 0.038M) + 0.169$ (for green wood with more than 40% moisture content) unit of measurement is BTU/(hr·ft·°F)
1954	Maku [56]	$\lambda = 0.02 + 0.0724S_0 + 0.0931S_0^2$ unit of λ in Kcal/mh°
1951	Kollman and Malmquist [57]	$\lambda = 0.219 * (\rho /1000) + 0.0256$ For moisture content of 12%
1979	Wilkes [51]	$\lambda = .02582 + (1.686e\text{-}4 + 5.177e\text{-}6 * M) * \rho / (1 + 0.01*M)$
1984	Siau [14]	$\lambda = 0.510448 – 0.4736288 * a$ where **a** can be calculated as: $a = (1\text{-}0.000667*\rho - 0.00001 * M * \rho)^{½}$ for density range 150-1400 kg/m^3
1988	Tenwolde [52]	$\lambda = (D/1000)*(0.1941 + 0.004064* M) + 0.01864$
1998	Harada [58]	$\lambda = 0.0256 + .000181 \rho$ (for oven dry conditions only)
2011	Yu [59]	$\lambda = 0.04409 + .0001278 \rho$ (for oven dry samples only)
		Where **S** is the specific gravity, $\mathbf{S_0}$ specific gravity at oven dry conditions, **M** is the moisture content in %, **ρ** is density kg/m^3, **a** is porosity and **λ** is thermal conductivity W/m.K. Units used are SI units unless otherwise stated. Given equations are for the direction transverse to the grain.

Of the above summarized equations, all depend on density and moisture content except for Siau. His work presents a model of thermal conductivity based on circuits and explained thermal conductivity in terms of its porosity and moisture content.

Thermal conductivity increases with an increase in temperature. The correction for temperature given by Tenwolde, which falls in close agreement to Wilkes's prediction is given as 0.2 percent per degree Kelvin. That is, there will be an increase of 10% with an increased temperature of 50° C.

3.1.2 Thermal Conductivity of Wood Based Panels

The thermal conductivity of wood-based panels has been linked to density and moisture content, much like solid wood. Lewis studied effect of temperature and density on particle board and fiberboard [60]. Seventeen types of fiberboards and five types of particleboards were studied, and the mean temperatures of 10°, 24°, 38° and 52° C were used for measurements. He found the thermal conductivity of wood-based panels has been found to be lower than that of wood of the same density. He also found the conductivity values for the same density particleboards were higher than the fiberboards. He suggested a design curve as a relationship between thermal conductivity and specific gravity for use by designers. Siau [14] shows the relationship between thermal conductivity of wood and wood-based panels, which is reproduced below in Figure 6.

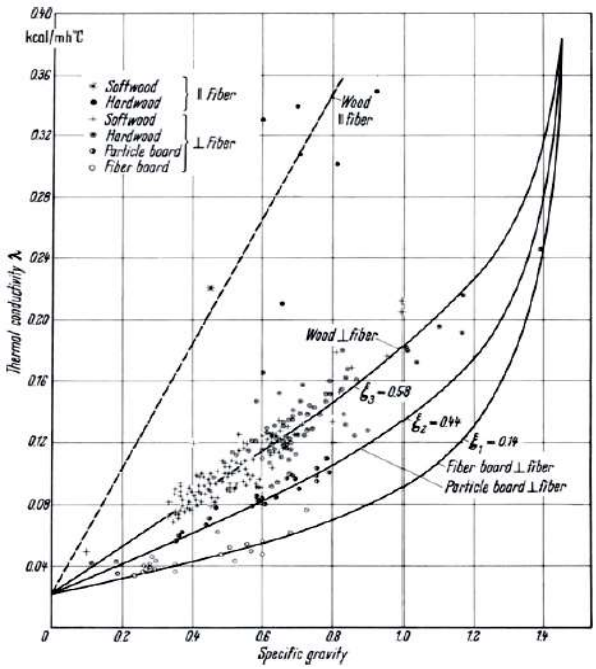

Figure 6 Thermal conductivity vs specific gravity for wood and wood-based panels reproduced from Siau [14]

Tenwolde gives a detailed account of these relationships by using the following equations:

$K_{plywood}$	$= 0.86\ k_{wood}$	Plywood
$K_{particleboard}$	$= 0.75\ k_{wood}$	Particleboard, also chipboard
$K_{fiberboard}$	$= 0.65\ k_{wood}$	Fiberboard, also MDF

Tenwolde also gives corrections for temperature for each wood-based material. These are:

Plywood:	0.0002 for each degree Kelvin
Chipboard:	0.00024 for each degree Kelvin
Fiberboard:	0.00014 for each degree Kelvin

3.2 Electrical Properties of Materials and Thermal Conductivity

Thermal conductivity has been seen as analogous to electrical conductivity, and investigators have sought to find a relationship between the two constants [61]. For materials with freely moving electrons like metal, both thermal and electrical conduction is due to the flow of electrons, and their relationship is explained by the Wiedemann-Franz Law [62]. Scientists have tried to establish the relationship of electrical and thermal resistivity of soil, so that one could be used to estimate the other. Singh et al studied the effect of saturation levels on both electrical and thermal resistivity and presented a generalized relationship between the two [63]. Wang et al showed an inverse linear relationship between electrical and thermal resistivity for 57 soil types having 7 different saturation levels [64]. Erzin et al showed that given the soil type, degree of saturation, and thermal conductivity, artificial neural networks could be used to quickly and efficiently estimate the electrical resistivity of soil [65]. Pia et al represented porous media as a Sierpinski carpet and used the electrical pattern to predict thermal conductivity [66]. Some interesting relationships between dielectric material properties and thermal conductivity are discussed in the following sections

3.2.1 Dielectric Constant: Sensitivity to Density and Moisture Content

Dielectric material properties of solid wood and wood-based materials are highly sensitive to density, moisture content and frequency at which the measurement is made. For solid wood it also depends on the direction of measurement w.r.t the orientation of the wood fibers.

The relationship of wood density and moisture content has been thoroughly investigated by many scientists. Skaar [67] notes that at moisture content below 30%, the dielectric constant is independent of wood species and is affected only by its density and moisture content. Torgovnikov indicates that at moisture content below 30% and room temperature of 20 - 25°C the dielectric constant is proportional to wood density [68]. For transverse direction, she proposes the following equation for the dielectric constant as:

$$\epsilon' \text{ (Transverse)} = a*P_0 + 1$$

where P_0 refers to oven dry density within the range of 300-800 kg/m3 and a is a coefficient based on frequency and moisture content. She further notes that the dielectric constant of fiberboards can be assumed to be the same as wood of the same density. Sahin demonstrated the same rules and showed that dielectric properties increased with increased moisture content for all wood species under study. He determined the dielectric properties in all three directions and found that grain direction had an important part to play [69].

3.2.2 Capacitance

It is very curious how the formulas for heat transfer are very similar to formulas related to electrical charge and capacitance. Heat transfer is often solved in terms of electrical circuits

connected in parallel or series. So, there is similarity in the way heat moves through a material and how electric charge is stored inside a material. Table 2 highlights these similarities and shows the formulas used to calculate electric charge and the rate of heat transfer.

Table 2 Formulas for calculation of capacitance and heat transfer

Geometry	Electrical Charge Equations	Heat Transfer Equations
Rectangular 	$C = \frac{\epsilon_r A}{d}$	$q_x = \frac{kA\,\Delta T}{d}$
Cylindrical 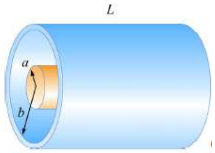	$C = \frac{2\pi\epsilon_r l}{\ln\left(\frac{b}{a}\right)}$	$q_x = \frac{2\pi k l\,\Delta T}{\ln\left(\frac{b}{a}\right)}$
Spherical 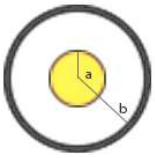	$C = 4\pi\epsilon_r\left(\frac{a\,b}{b-a}\right)$	$q_x = 4\pi k\left(\frac{a\,b}{b-a}\right)\Delta T$
Connected in series 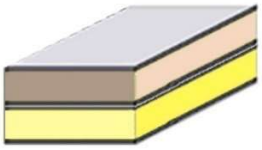	$\frac{1}{C_{eq}} = \frac{1}{C_1} + \frac{1}{C_2}$ $C_{eq} = \frac{1}{(d_1/\epsilon_{r1} A) + (d_2/\epsilon_{r2} A)}$	$\frac{1}{q_x} = \frac{1}{q_{x1}} + \frac{1}{q_{x2}}$ $q_x = \frac{\Delta T}{(d_1/k_1 A) + (d_2/k_2 A)}$
Connected in parallel 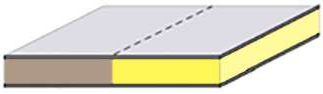	$C_{eq} = C_1 + C_2$	$q_x = q_{x1} + q_{x2}$

The above table shows that the geometry of the object affects its ability to store charge in a way similar to its ability to transfer heat. Moreover, the arrangement of materials, may it be series or parallel, affects electric charge and heat transfer in comparable ways.

3.3 Thermal Conductivity and Speed of Sound

The relationship between thermal conductivity and acoustic wave velocity is based on the phonon conduction theory. This theory asserts that thermal energy propagates in dielectrics through the propagation of acoustic wave packets known as phonons along a thermal gradient. The accepted formula for thermal conductivity is given by:

$$\lambda \propto c\, v \bar{l}$$

where c is the heat capacity of a dielectric that coincides with that of phonon gas, v the mean velocity of phonons approximately equal to the sound velocity, $\bar{l}$ is the mean free path of phonons [70].

If a correlation between thermal conductivity and the speed of sound exists at a molecular level, then perhaps the same would be true on a macroscale, and it might be possible to infer thermal conductivity from the speed of sound through that material.

3.3.1 Thermal Conductivity and Speed of Sound in Geology

Using compressional wave velocity (speed of sound) to estimate thermal conductivity has received a lot of attention in recent times in the field of geology. Scientists want to estimate the thermal properties of a rock bed in-situ. Various studies show a linear relationship between thermal conductivity and compressional wave velocity [71]. Mielke et al found a linear relationship but concluded that this relationship is only true for porous rocks, and the relationship stops for non-porous rocks or rocks with very less porosity [72]. Appendix C provides details. Gegenhuber et al presented two mathematical models to predict the same relationship based on sound velocity, rocks cracks and mineral composition [73]. Pearson's coefficient of correlation between 0.68 and 0.92 was achieved, showing better results for granites with high quartz content and sandstone. The mathematical model presented by Pimienta et al was based on porosity, mineral composition and compressional wave velocity [74]. According to his model, thermal conductivity in rocks with micro-cracks depends mostly on the density and geometry of these micro-cracks. Esteban explored various models presented by scientists and tested these theories on a rock sample collection from two sandstone reservoirs to predict thermal conductivity. The study found a deviation of 10% or less for the predicted values from the measurements found under lab conditions for dry and saturated rocks from one reservoir, and 30% or less deviation from samples collected at a different reservoir [75].

The above discussion highlights how geologists have successfully derived thermal conductivity of rocks by constructing a mathematical model relating speed of sound through that material, porosity and mineralogy. The speed of sound vs thermal conductivity relationship seemed to stop for non-porous rocks, or rocks with low porosity. However, most construction materials are porous, including bricks, concrete, wood, wood derivatives and insulation materials, which works to the advantage of scientists motivated towards finding thermal conductivity of construction materials.

3.3.2 Properties of Construction Material and Speed of Sound

Concu et al investigated the correlation of ultrasonic wave velocity with density, modulus of elasticity and compressional strength on two sets of construction limestone [76]. The samples were completely dry. Coefficient of correlation of 0.82 and 0.72 for density, 0.96 and 0.92 for modulus of elasticity and 0.7 for compressive strength were found.

Vasanelli et al carried out tests on limestone blocks to find that size and geometry of stone does not have any significant impact on ultrasonic wave speed [77]. Vasanelli et al carried out another set of tests on two types of stone commonly used in Italy for construction in historic times [78]. Rebound hammer and ultrasonic pulse velocity were used to show

effectiveness of sound velocity in predicting physical properties of stone. Although one set of stones showed a good correlation between density and speed reporting a coefficient of correlation of 0.8, the other type of stone showed a poor relationship with .4 stated as the coefficient. Vasconcelos et al investigated the physical properties of granites using ultrasonic evaluation [79]. He found a correlation between compressive strength (R^2 = 0.72), Young's Modulus (R^2 = 0.84), porosity (R^2 = 0.74) and Tensile strength (R^2 = 0.89)

3.3.3 Machine learning, Speed of Sound and Material Properties in Civil Engineering

Ultrasonics has been used to study the compressive strength of concrete. Trtnik et al used artificial neural networks to derive the compressive strength of concrete using various material properties [80]. He showed that the speed of sound for predicting compressive strength was not enough to get accurate results. However, by using parameters like aggregate type and ratios as well as the speed of ultrasonic speed yielded high accuracy when processed through ANNs. Amini et al built upon previous work to use UPV along with rebound hammer test to predict compressive strength of concrete [81]. Using advanced statistical analysis, and three-fold cross validation, this method saw a high accuracy of predicted values, without the need for variables related to the history of concrete like water-cement ratios, or aggregate sizes, relying solely on the two numbers produced by the mentioned non-destructive testing techniques. The quoted reason for the success is that the rebound hammer and ultrasonic pulse velocity expose different characteristics of concrete.

3.4 Conclusion

Two material properties have been identified for the study of relationship with thermal conductivity of construction materials. One is the speed of sound through materials, and the other is dielectric properties. Sound speed through a material has been investigated in detail by various scientists and has been successfully used to predict various material properties, including thermal conductivity. Although dielectric material properties have not yet been fully investigated to infer thermal conductivity, its strong relationship to density and moisture content makes it a worthy metric. If density and moisture content affect thermal conductivity similar to dielectric properties, then it could be a useful parameter in making predictions.

4 Analysis of Existing Data

Although there is a lot of available data about various material properties, there is little to no information about how thermal conductivity correlates with dielectric properties or sound speed. As an introductory part of the project, data from various sources: books, journal articles and product websites, was collected, compiled and analyzed. This study attempts to combine the various databases and search for relationships that might exist between thermal conductivity and dielectric properties, and between thermal conductivity and sound properties.

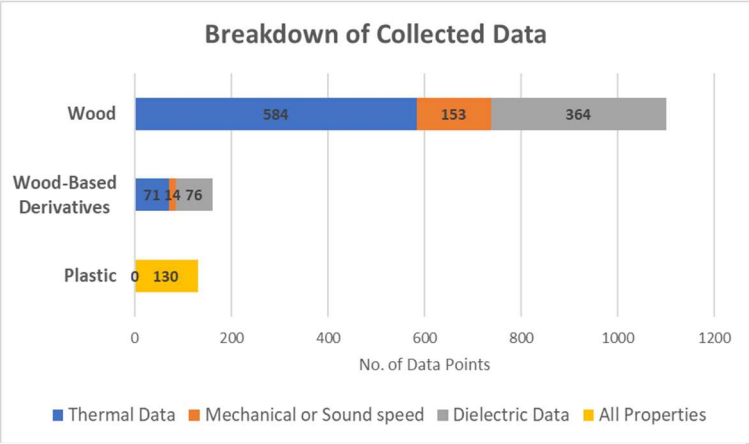

Figure 7 Breakdown of data collected for analysis

A total of 1400 data points were collected for this exercise. Figure 7 gives a breakdown of the type of data that was collected. One of the most researched materials for thermal conductivity has been wood, and a lot of data was available for that. The figure also shows a breakdown of the number of collected data points for each material property. A detailed account the data with referencing is given in Appendix C.

4.1 Solid Wood

The main source of information collected for wood thermal properties was from the database published by Cardenas and Bible with 547 data points. This work consolidates the work of scientists who carried out their work on thermal conductivity prior to 1987 [54]. A large database for dielectric properties of solid wood was published by Torgovinkov [68] in 1993. A full detail of all sources used for this exercise are listed in Appendix D.

4.1.1 Thermal Conductivity of Solid Wood

The collected data related to wood thermal properties consists of over five hundred data points. This data contains measurements where the density and the moisture content were clearly stated, and any data point without this statistic was discarded from the set. Moreover, only the data collected at room temperature was kept, while the data recorded at very high or very low temperatures was excluded from the study.

Figure 8 shows the scatter plot of thermal conductivity vs density and plot of thermal conductivity vs moisture content. Although the density shows some correlation with thermal conductivity, the relationship with moisture content is not at all visible.

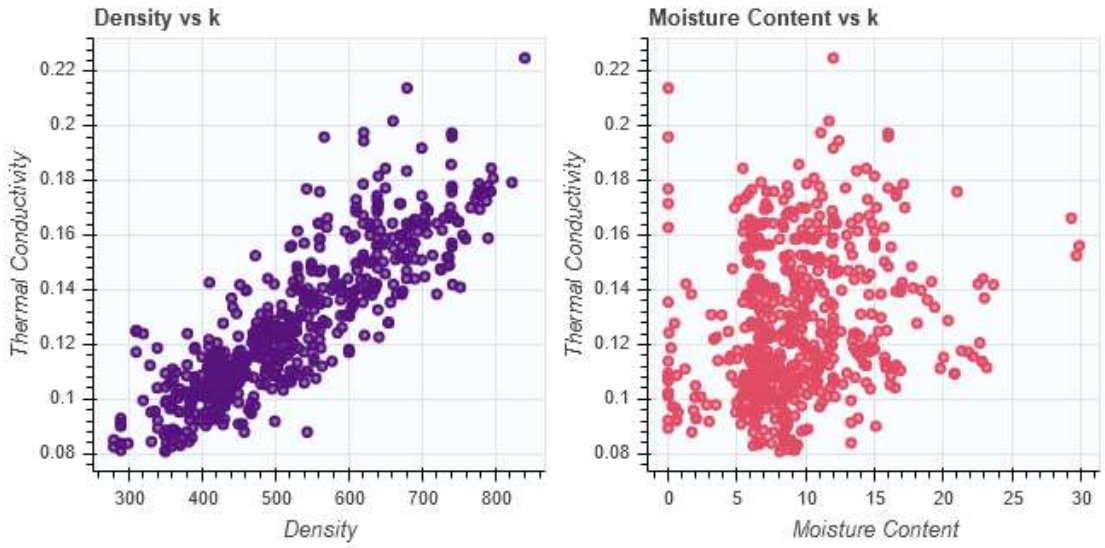

Figure 8 A (left) Scatter plot between thermal conductivity and density. B (right) Scatter plot between moisture content and thermal conductivity

Section 3.1.1 describes the equations by which various scientists predict thermal conductivity from density and moisture content; in this section we follow up with an investigation into how these equations fit with the collected data. A detailed comparison is shown in Figure 9. Figure 9 A shows how Maclean, Wilkes, Tenwolde and Siau's equations for the prediction of thermal conductivity compare to each other on the given dataset. Figure 9 B-D show how the equations of mentioned scientists perform on the entire dataset along with the calculated R^2 scores. Figure 9 E shows my own data analysis on the collected dataset.

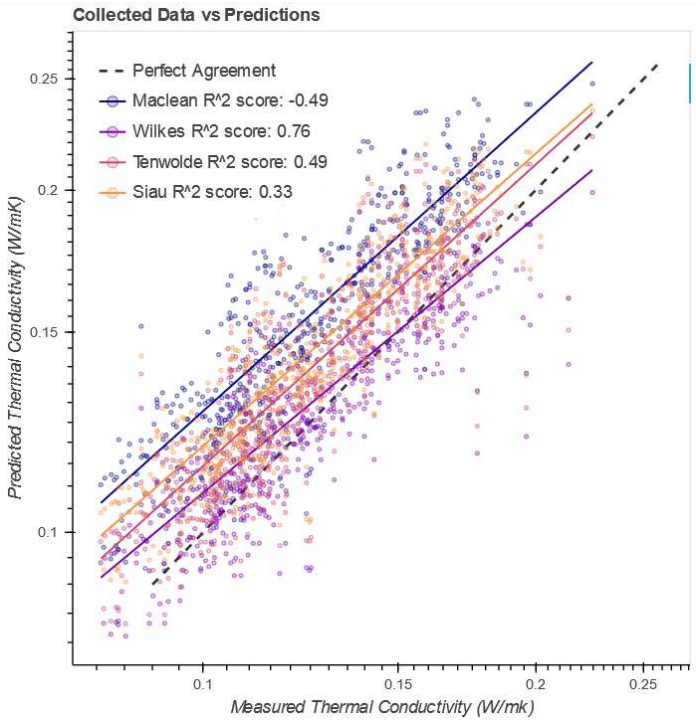

A. Comparison of various equations to predict thermal conductivity through moisture content and density.

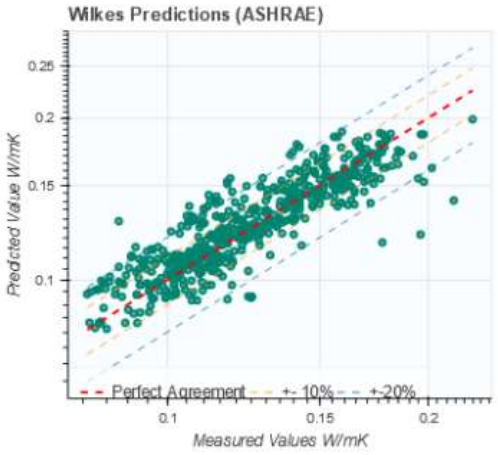

B. Wilkes Prediction (ASHRAE)
R^2 Score: 0.76

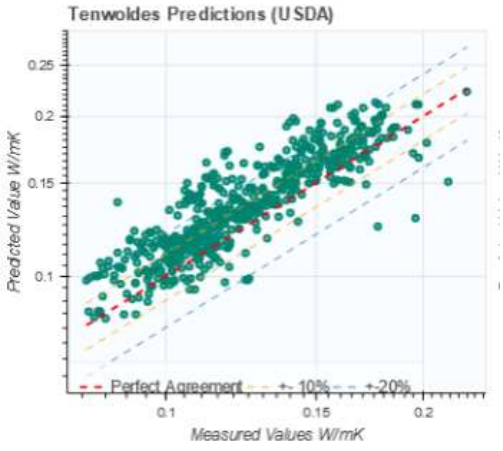

C. Tenwolde's Predictions (USDA)
R^2 Score: 0.49

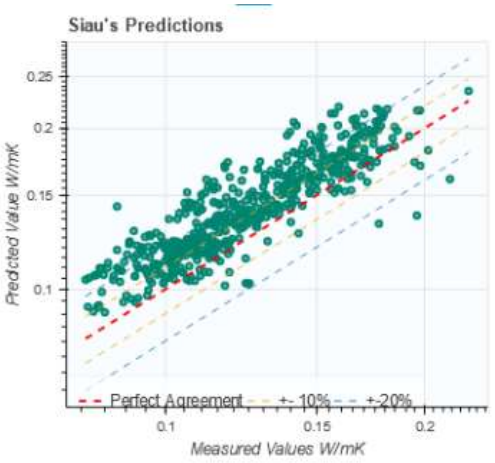

D. Siau's Predictions
R^2 Score: .33

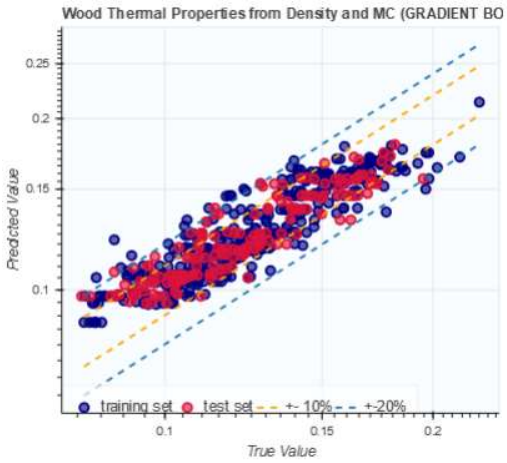

E. Gradient Boost Regression (by author)
R^2 Score test data: .77

Figure 9 A-E: How equations of various scientists performed on the data collected for wood thermal conductivity.

The most curious thing shown by Figure 9A is although the investigated equations all seemingly have the same slope, they have differing intercepts. It is possible that each scientist might have been working with a smaller dataset, and hence obtained different results. The graph suggests that perhaps the experimental data collected by the various scientists have their own bias, which shows up in the form of an elevated reading. Because the biases are perhaps consistent, it results in the same slope, but differing intercepts for the different scientists studying the same problem. The R^2 scores over the dataset as shown in Figure 9B-E indicate that the Wilkes equation seemingly does the best job at making predictions of thermal conductivity. However, this may well be because he had much of the same data as Cardenas and Bible, which form the majority of data for this study.

Figure 9E shows how using modern machine learning might increase the R^2 score of the predictions slightly. However, these are initial test results and lack any method of validation.

4.1.2 Dielectric Properties of Solid Wood

Figure 10 shows an analysis of data collected for wood dielectric properties at different frequencies. It shows how a high moisture content results in more variation of the dielectric constant across different frequencies and vice versa. The same is also true for density and is reflected in the graph shown in Figure 10.

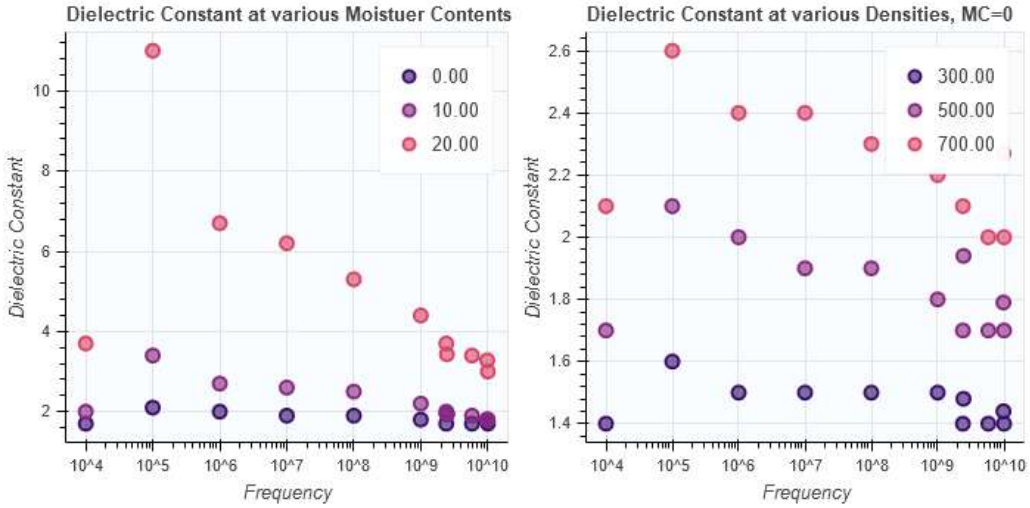

Figure 10 Dielectric constant as a function of frequency. A (left) varying moisture content %. B (right) varying density (unit kg/m^3)

There is no dataset which gives both the thermal properties of wood as well as its dielectric properties. Although there is much information in literature that addresses the thermal properties and dielectric properties separately, the correlation between the two has not been systematically studied. Both properties are heavily dependent on moisture content as well as density. Thus, it makes sense to explore this correlation.

For the next part of the study, data related to thermal conductivity was generated against the data relating to dielectric properties found in existing literature. The data related to dielectric properties found in literature typically also contains information on density and moisture content of wood. This information was used to generate values for thermal conductivity based on Tenwolde's [52] formula as well as Wilke's [51] formula for predicting thermal conductivity from density and moisture content.

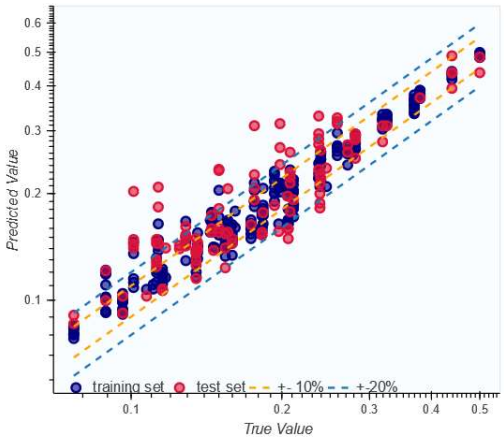

[0.97, 0.81, 42.2, 70.64]

A: Dielectric Properties predict thermal conductivity data generated by Tenwolde's equation (all frequencies)

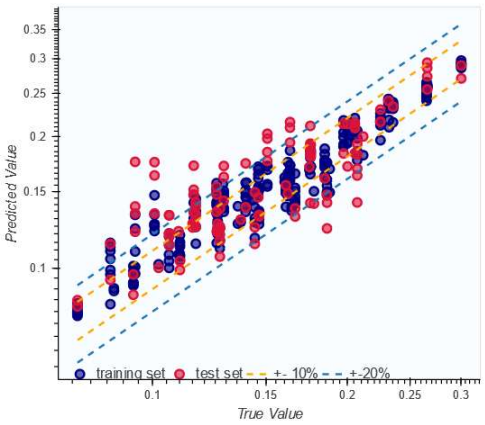

[0.93, 0.69, 50.46, 70.64]

B: Dielectric Properties predict thermal conductivity data generated by Wilke's equation (all frequencies)

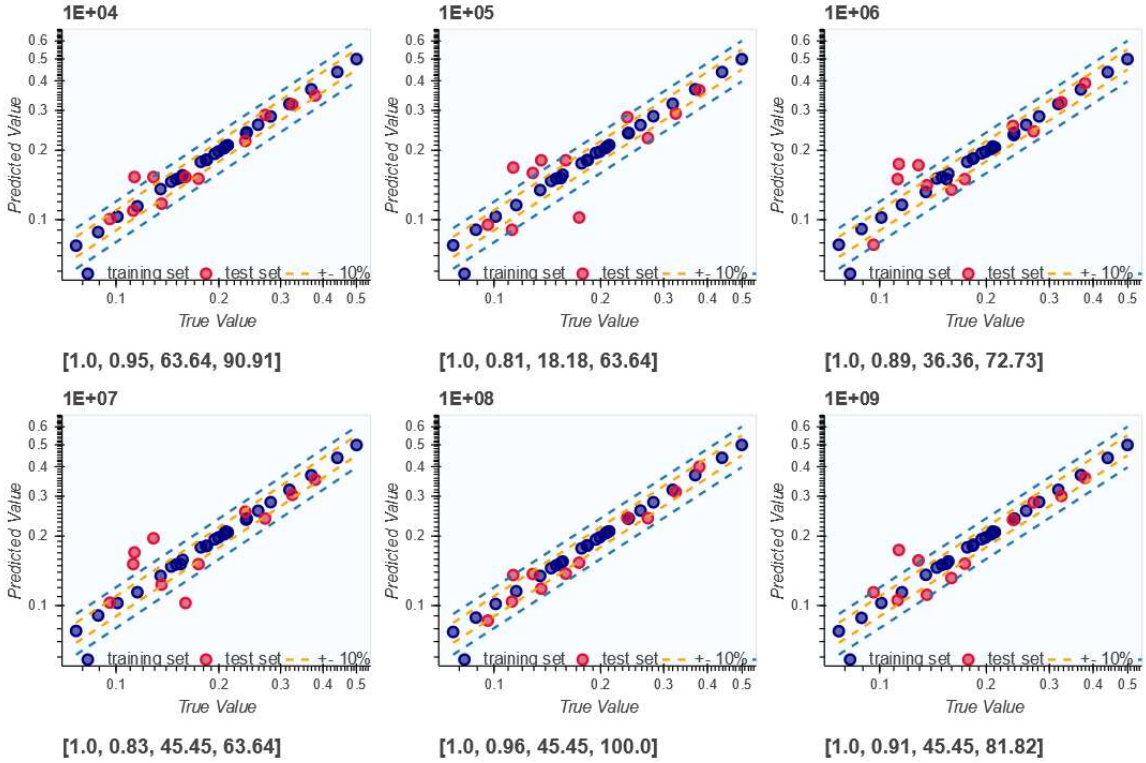

[1.0, 0.95, 63.64, 90.91] [1.0, 0.81, 18.18, 63.64] [1.0, 0.89, 36.36, 72.73]

[1.0, 0.83, 45.45, 63.64] [1.0, 0.96, 45.45, 100.0] [1.0, 0.91, 45.45, 81.82]

C Thermal conductivity (generated by Tenwolde's equation) as predicted by dielectric properties at different frequencies

Figure 11 Predictions of thermal conductivity from dielectric material properties.
Numbers in parenthesis denote: [Training Score, Test Score, % of test Set within +-10%, % of test Set within +-20%]

Figure 11 shows that dielectric material properties can predict thermal conductivity accurately. However, it must be noted that the predicted thermal conductivity is not based on experimental data, and was calculated based on a regression equation. The equation can predict thermal conductivity with an error of ±20% according to the Tenwolde.

Although in the previous section, it was shown that the Wilkes equation was the most effective in predicting thermal conductivity, this figure shows a stronger relationship between dielectric properties and the way thermal conductivity is affected by density and moisture content as given by Tenwolde. Figure 11C shows how the dielectric constant changes with different frequencies, and how the relationship continues to hold across the spectrum. The dielectric constant at 10kHz seems to be as good at making predictions of thermal conductivity as at 1Ghz. This figure shows that no single frequency is better at predicting dielectric properties, and the minor variations shown in the graph might be a random chance.

Various algorithms were also explored to make the predictions of the assumed thermal conductivity. Linear models as well as some ensemble methods were tested for the simulation. Linear models work with the assumption that the target value is a linear combination of the given set of predictors. These work to minimize a predefined loss function. Ensemble methods are distinguishable in that these use several weak models to build one strong predictive model. Results of the analysis showed that any of the ensemble methods were superior to the linear models. The algorithm with the best R^2 scores was Gradient Boost Regression, which works to reduce bias in the predictive model.

4.1.3 Combined Properties of Solid Wood

A dataset was generated to compare how each of the dielectric and sound properties correlate with thermal conductivity. The data related to mechanical properties and sound speed was used as the base, and properties relating to thermal conductivity and dielectric properties were attached based on the given sample's density and moisture content. Reaching into the database for thermal properties, the density which was closest to a given sound speed data point was selected, and the corresponding thermal conductivity was recorded. Since density is so closely related to the dielectric properties, the gradient boost algorithm was used to generate and attach this data with the sound and mechanical properties data.

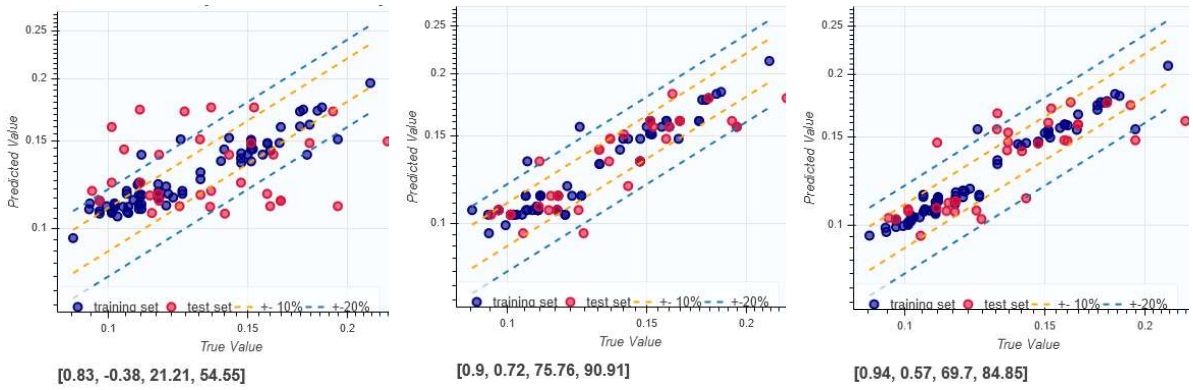

A. Prediction of thermal conductivity from sound speed

B. Prediction of thermal conductivity from dielectric properties

C. Prediction of thermal conductivity from sound speed and dielectric properties

Figure 12 Predictions of thermal conductivity from Dielectric and Mechanical properties

Numbers in parenthesis denote: [Training Score, Test Score, % of test Set within +-10%, % of test Set within +-20%]

Figure 12 shows the analyzed data and the cross correlations found. This figure shows that while dielectric constant may be a strong predictor of thermal conductivity, sound speed may be a weak predictor. Extending the feature space so that both dielectric constant and sound speed are used as the predictors only weakens the overall predictive power of the algorithm.

4.2 Plastics: Dielectric, thermal and sound speed

Data was collected from various websites of manufacturers of plastic material products. Plastic manufacturers websites were explored and those were shortlisted which gave substantial information related to their product's thermal, dielectric and mechanical properties. Most websites were found to have omitted at least one material property. These were excluded from the study and data collection. Only data points were recorded that contained a complete set of information were recorded.

No data was found on these websites relating to sound speed. This data had to be generated based on the material's mechanical properties. The speed of sound is roughly estimated through its Young's Modulus and density. Shear modulus is approximately equal to Young's modulus, thus this value was substituted whenever the correct information wasn't available. The formula for the sound speed through mechanical properties is:

$$c = \sqrt{\frac{E}{\rho}}$$

where c is the speed of sound, E is Young's modulus and ρ is density.

Another drawback to this study is how the dielectric properties were reported using different frequencies by different manufacturers. The most commonly reported frequency was 1 MHz. Figure 13 to Figure 15 show the result of the analysis. Once again, gradient boost was found to be the best performing algorithm. The figure shows that although there is a strong correlation between dielectric and thermal properties, there are some very strong outliers which drastically reduce the R^2 score of the analysis. The same is the case for mechanical

properties. Figure 13 and Figure 14 show somewhat scattered results. However, Figure 15 shows more accurate predictions.

While dielectric properties alone were found to be a good predictor of solid wood's thermal conductivity, the analysis of plastic reveals that extending the feature space to include sound speed as well improves the R^2 score of the prediction.

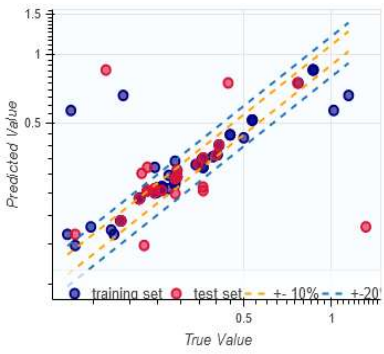

[0.68, -0.39, 53.57, 67.86]

Figure 13 Predictions of thermal conductivity from dielectric properties

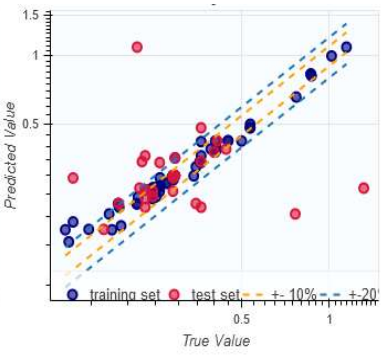

[0.98, -0.67, 42.86, 57.14]

Figure 14 Predictions of thermal conductivity from mechanical properties

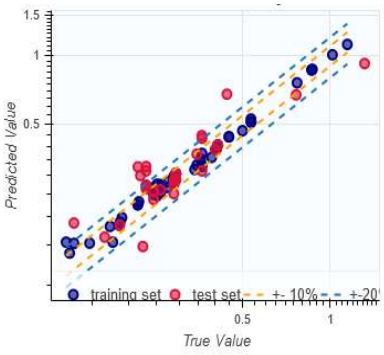

[1.0, 0.79, 46.43, 64.29]

Figure 15 Predictions of thermal conductivity from both dielectric and mechanical properties.

The numbers in the parenthesis indicate [training score, test score, % readings within 10% accuracy, % readings within 20% accuracy]

4.3 Wood and Plastic Combined: Can Wood Learn from Plastic?

194 Sample Points (91 Plastic 103 Wood)

While all the analysis described so far pertains to only one material type, in this part of the analysis, work was done on a mixed set. Data points for wood and plastic were mixed, and the material type was not a part of the predictors. The aim of this exercise was to find out if the pattern exhibited by wood continues onto other material types. In short, this part of the exercise had a focus on whether wood could learn from plastic or vice versa.

A four-fold cross validation was performed to interpret the predictive power of the algorithm. The results of this prediction are shown in Figure 16 below. The red color refers to datapoints relating to wood, and the blue color refers to plastics. Larger circles indicate the test set, whereas the small squares refer to the training set.

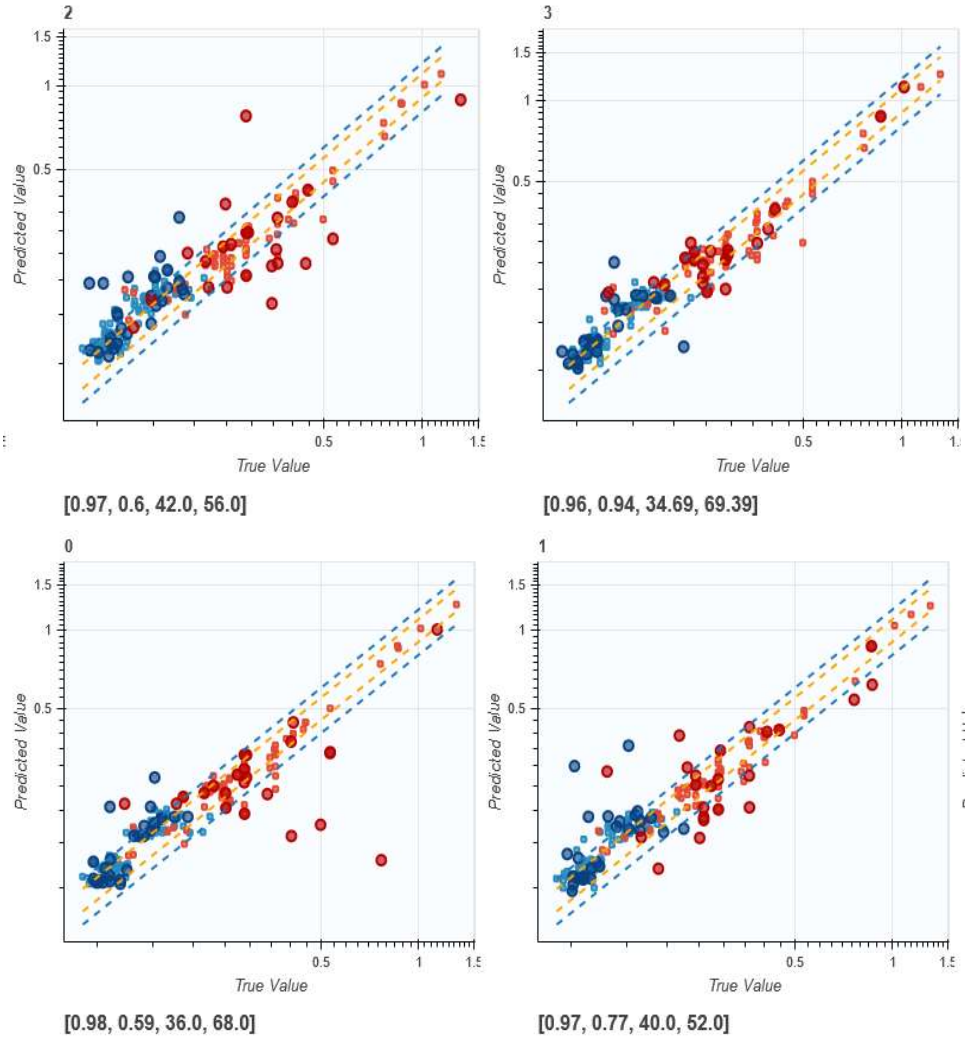

Figure 16 Four-fold cross validation results from wood and plastic combined. Red dots relate to wood, and the blue dots relate to the plastics data. The small squares represent training data, while the larger round symbols represent the test data

As shown in Figure 16, the R^2 scores range from 0.49 to 0.95 and have an average of 0.72. This means that given enough data, patterns of correlation found in one material type might be translatable into another material type.

4.4 Masonry

There is not much data available on materials such as brick or stone masonry. A small amount of data was found in the BRE BEPAC study using figures reported by the Belgium CSTC [82]. The found data was plotted, and the result can be seen in Figure 17. It shows a clear correlation between density, moisture content and thermal conductivity. Data related to the same specimen's dielectric or sound properties could not be found, so no such analysis could be performed.

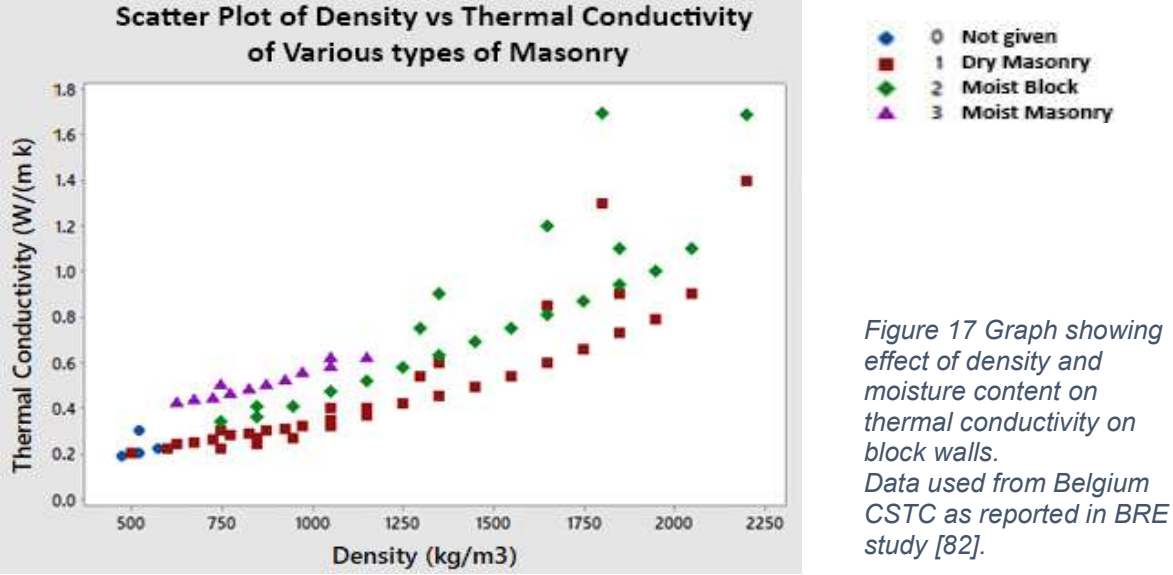

Figure 17 Graph showing effect of density and moisture content on thermal conductivity on block walls.
Data used from Belgium CSTC as reported in BRE study [82].

4.5 Conclusion

Despite the incomplete information, the analysis showed some interesting results. This exercise served as a precursor to the results of experiments that were yet to be performed. It showed that:

1. Dielectric properties may be a stronger predictor of thermal conductivity than the combination of density and moisture content.
2. Mechanical properties or sound speed have a weak correlation with thermal conductivity.
3. Adding sound speed or mechanical properties to the feature space with other predictors may or may not improve prediction scores based on the material type being studied.

PART II

Experiments

Part II: Experiments

A series of experiments are described in this part of the thesis. Hundreds of experiments were conducted to explore the relationship of thermal conductivity with other material properties. The collected data, analysis and implications of these results are discussed in these chapters.

Over ***four hundred samples*** were fabricated for various experiments. The included materials were *wood, plywood, chipboard, MDF, OSB, XPS insulation, clay bricks, concrete, gypsum drywall and acrylic*. The work begins by describing the fabrication process of these materials. Material samples were fabricated differently for thermal conductivity measurements and differently for measuring electrical properties. This chapter is followed by a description of the apparatus and methods used for the experiments. A detailed description of each experiment type as well as its error analysis are included in this chapter.

Results of experiments are described in the chapters following those of sample preparation and methods. Each chapter describes a different material category. All but one of these chapters deal with the relationship of materials thermal conductivity with their dielectric constant. In the chapter that does not deal with dielectric properties, the relationship of thermal conductivity with properties of sound moving through material are explored. This chapter deals with the collected data on sound prediction of thermal conductivity based on the collected data related to sound.

The chapter on wood and wood-based materials describes experiments related to materials suitable for the wood-frame construction. The multilayered materials chapter also describes the same category of materials, but its focus is on the effect of layering materials together. The chapter on ceramic materials deals with materials related to brick construction. Finally, the chapter on moisture studies explores how moisture affects wood and wood-based materials, their dielectric properties and their thermal conductivity.

The final chapter summarizes important conclusions of all experimental work. It represents the key take-aways of this thesis and outlines the potential for future work.

5 Sample Preparation

Fabrication of material samples was a major part of the thesis and over 400 samples were prepared for the study. Samples in wood, plywood, OSB, chipboard, MDF, XPS foam insulation, acrylic, clay bricks and concrete were prepared for the experiments. These were cut into 25 mm x 50 mm pieces, with thickness varying between 20 and 25 mm. Each material's fabrication presented its own challenges and had to be cut and prepared using suitable equipment. The figures below show the plethora of machines used for cutting and grinding of the material samples.

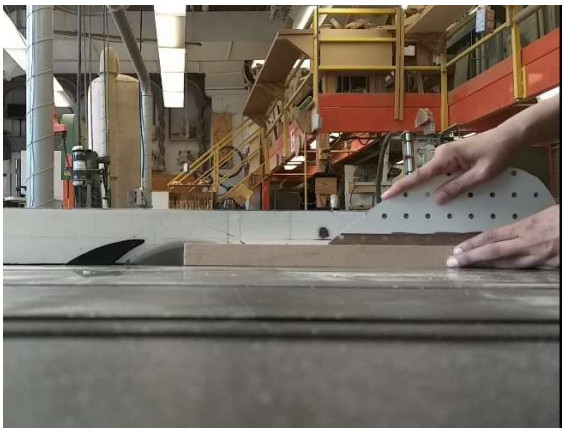

Figure 18 Table Saw (wood and derivatives)

Figure 19 Drill press (wood and derivatives)

Figure 20 Grinder (wood)

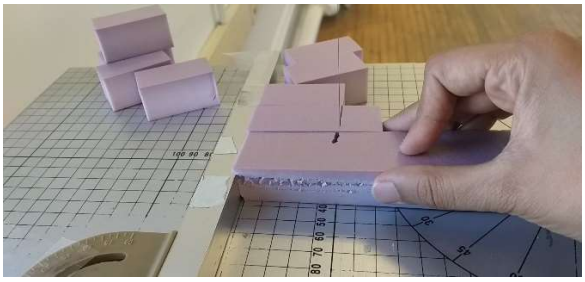

Figure 21 Foam Cutter (foam insulation)

Figure 22 Wet saw (ceramics, cutting)

Figure 23 Knee mill (ceramics, drilling)

Figure 24 Angle grinder (ceramics, cutting)

Figure 25 Dremmel tool (ceramics, grinding)

5.1 Thermal Conductivity

After cutting and trimming of the samples, they were measured, weighed and recorded under a unique ID. Half-inch deep holes with diameter matching that of the thermocouple were drilled into each of the samples. The temperature sensors could thus be placed at the core of the material under test.

5.2 Dielectric Properties

Preparation for these samples began in much the same way as the thermal conductivity experiments, i.e., by documenting the physical properties of each sample under a unique ID. The top and bottom of the samples were then covered with copper conductive paint which would act as electrodes. The edges of the paintwork had to be sharp in order to get a good reading. For this, the sides were covered with a protective tape before the application of the paint.

Fixing the wires to the samples was a bit tricky. It was noted that incorrect fixing of the wires resulted in unstable readings. For example, using copper tape made for a shaky connection. Using an acrylic holder to keep the wires in place resulted in a poor connection of the wire with the painted electrode, where full contact was not achieved. After much experimentation, it was found that silver conductive epoxy is best to hold the wires in place. Epoxy by Atom Adhesives, product number aa-duct 902 was used for these experiments. Pictures of the prepared samples are shown in Figure 26.

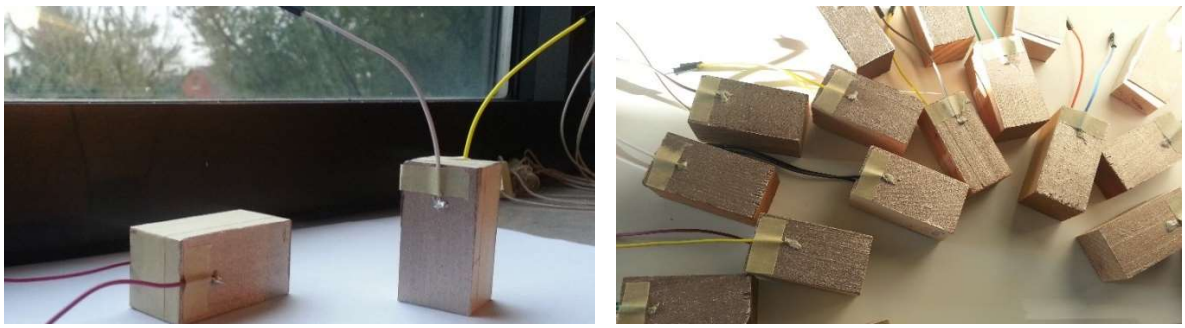

Figure 26 Prepared samples for dielectric measurements

5.3 Sound

Figure 27 and Figure 28 show the prepared samples for the sound experiments. The samples for the sound experiments varied in length from just three inches to twelve inches in length. In the case of sound impact a piezo was attached to the sample, and conductive paint applied to the opposite side. For the experiments relating to the resonance method, the samples had to be cut to equal lengths and cross sections. After the samples were cut to equal lengths, a second piezo was attached opposite the first.

Figure 27 Prepared samples for the sound impact method (sound speed)

Figure 28 Prepared samples for the resonance method with signal generator

5.4 Moisture Studies

To prepare the samples for the moisture studies, they were first oven dried to find their oven dry weight. Samples were placed inside a convection oven for over 24 hours at approximately 104°C. It was noted that there was no appreciable change in weight at 4-hour

intervals after the first 24 hours were over. A picture of the oven and solid wood samples are shown in Figure 29. After all moisture was removed, the samples which were to be tested at 0% moisture levels were placed inside vacuum bags as shown in Figure 30.

Figure 29 Oven Drying

Figure 30 Samples inside vacuum bags meant to retain oven dry condition of samples

A humidity box was constructed to condition the samples for the moisture study. This consisted of a plastic box, a stand to hold the samples, humidity sensors and a humidifier as shown in Figure 31. The humidifier was controlled by an Arduino and relay switches based on the readings of the humidity sensor. It was programmed to spray water droplets inside the box at regular intervals. When the humidity sensors inside the box registered humidity levels above a certain level, the humidifier was switched off. The readings from the humidity sensors were programmed to show on an LCD screen (see Figure 32). The LCD screen was used to monitor the humidity levels inside the tanks, as well as keep track of any loose connections in the system.

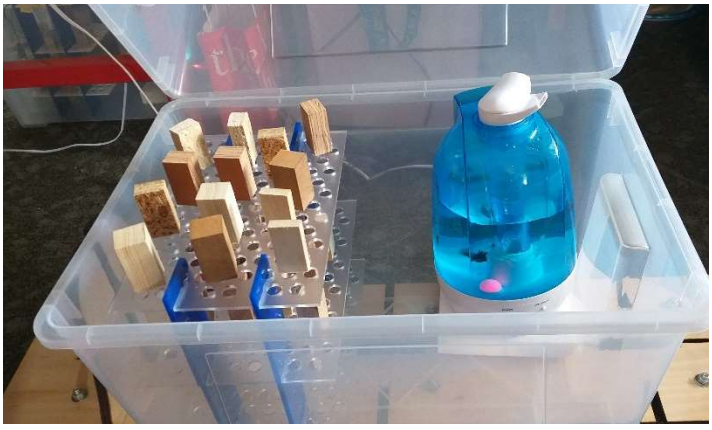

Figure 31 Humidity box containing humidifier, samples and humidity sensor.

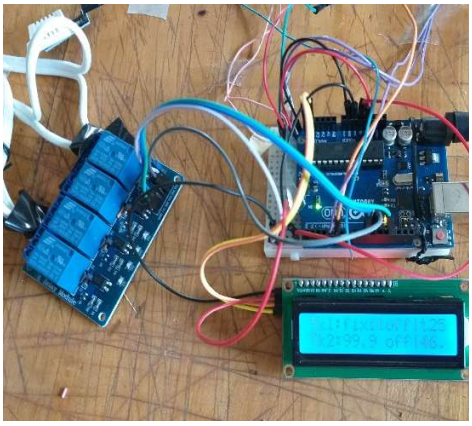

Figure 32 Arduino, relay switch and LCD screen

The samples remained inside the humidity box for a month at a time while the moisture levels in each sample were constantly monitored by weighing the sample. The same levels of humidity inside the box produced higher moisture content in softwood as compared to the higher density hardwoods.

All woods did not require the same number of days inside the humidity tank to reach the same moisture levels. It was seen that softwoods absorbed moisture a lot more quickly than hardwoods. Moisture dissipated inside the softwoods a lot more easily as well.

5.5 Pouring Concrete

Mixtures of cement, sand and aggregate were prepared and poured into molds to form concrete. The molds were prepared out of foam, with cavities of 25 mm x 50 mm each. The poured samples were regularly sprayed with water during the first thirty days of curing. These are shown in Figure 33.

Figure 33 Molds for casting concrete samples

6 Apparatus and Methods

Contains material for reports by Saeed et al in [83–85]

Each of the three experiment types were designed and developed through a continuous learning process. Several iterations were run until a successful result close to theoretical values was achieved. All three experimental setups and procedures are described in detail in the following sections.

6.1 Thermal Conductivity: Measurement Apparatus and Method

The method to measure thermal conductivity was developed over time. Two main methods were used for this measurement. These differ in the equipment used for the measurement. These are discussed in detail in the following sections.

6.1.1 Measuring Thermal Conductivity: Method A

The goal of these experiments was to measure the thermal conductivity of materials as accurately as possible. It took several iterations to design a setup which gave satisfactory results close to theoretical results. The configuration that was finally used, was chosen from layouts suggested by the ASTM Standard C518 [86] for calculating thermal transmission properties under steady state conditions.

The schematic for the experiment is shown in Figure 34. The setup involves creating a temperature gradient across the material to be tested by placing it between a heater and a cooling plate. A heat-flux sensor (Flux Teq Model PHFS-01) measured heat flow through the material, and thermocouples were used to measure the temperature along the temperature gradient at two points of the sample. The heat flux sensor was calibrated using NIST tracible materials by manufacturer and is sold with a certificate of calibration. The heat flux was monitored using a multimeter (Aneng AN8008), while the thermocouples readings were observed using a temperature reader by PerfectPrime TC-41. A 12V heater which maintained its temperature at 80°C was used for the experiments, and 12V Peltier modules for the cooling plates. A heat sink and fan were used so that the cooling plates would produce a lower temperature. The thermocouples were inserted into a small cavity drilled into the material to monitor the temperature at the core of the sample. Fourier's Law was then used to calculate the thermal conductivity. The equation is:

$$q_x = \lambda \frac{\Delta T}{x}$$

q_x is the heat flux in W/m^2, ΔT is change in temperature in °K, x is the distance between the two thermocouples in meters and λ refers to thermal conductivity in W/m.K. The distance was obtained by a Vernier caliper by measuring the distance between the two incisions where the thermocouples were inserted. q_x was given by the heat flux sensor and ΔT was calculated as the recorded temperature difference between the two thermocouples.

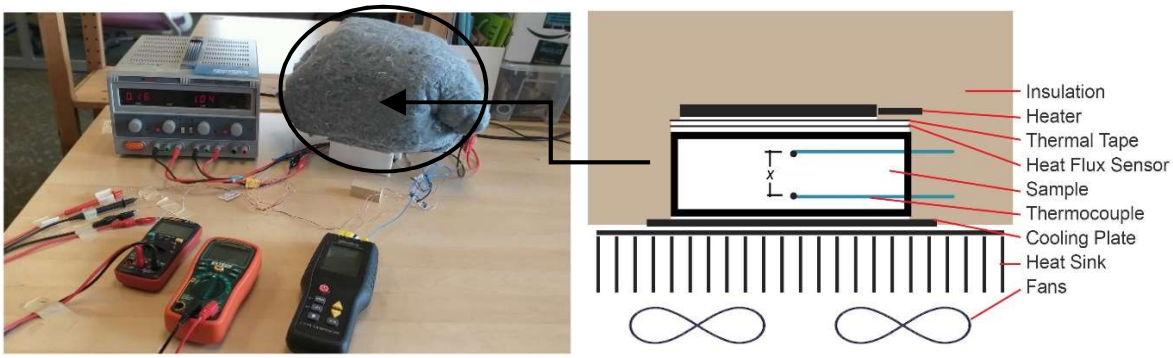

Figure 34: (Left) The instruments used for measuring thermal conductivity. Right: Schematic for the measurement.

For each experiment, the samples along with the heater were carefully placed inside layers of foam insulation. Care had to be taken that the cooling plates were in full contact with the material under test so that the heat can be vented out through the heat sink. Once everything was packed inside, another layer of cotton insulation was wrapped around the apparatus.

With the insulation, heater, sample and sensors in place the apparatus became ready for the measurement. Two power supplies were used to provide DC current to the heater, cooling plates and fan. Three readers were used to take measurements from the thermocouples and heat flux sensor. These readers were manually turned on, and the readings on each was recorded, and the relevant formula applied to calculate the thermal conductivity value of each sample.

Measurements were recorded at ten-minute intervals. The condition for meeting steady state conditions was that a new measurement was not to deviate from the average of previous five readings by more than half a percent (Figure 35). This rule has been taken from the ASTM standard C518 [86] for steady state measurement of thermal transmission properties.

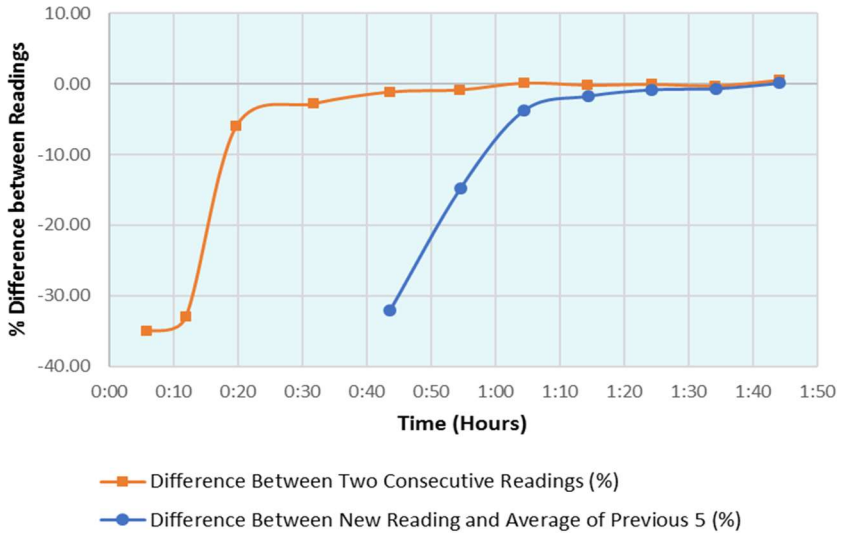

Figure 35 Reaching steady state conditions for sample # 131 of Redwood.

It was seen that steady state conditions were achieved in less than two and half hours for wood, and the measurement process was stopped in three hours or less in these cases.

6.1.2 Measuring Thermal Conductivity: Method B

The difference between measurement method A and B, is that a single heat flux sensor was used in method A, while two were used in method B. A second difference was the use of different readers for thermocouples and heat flux sensors. In method A, digital multimeters were used, and readings were recorded manually every ten minutes. For method B, a datalogger was acquired, which recorded the readings every half a minute or so.

Figure 36 and Figure 37 show the equipment used for the thermal conductivity measurements and a schematic of the testing assembly. Thermal conductivity was measured by creating a temperature gradient across the layers of the material until steady state conditions were met. The temperature gradient was created by placing the material between a heater and cooling plate. The temperature was regulated through the power supply. Two heat flux sensors (Fluxteq, model PHFS-01) were placed to measure the heat flux through the sample. One between the heater and material, the other between the cooling plate and the material. The average of the two readings was taken for the calculation. Two thermocouples (Perfectprime 0.13mm) were placed well into the core of the material by drilling halfway into it. A data logger (Windaq, model DI-2008i) connected to a CPU was used to collect data from two heat flux sensors and thermocouples. Both the heat flux sensor and datalogger are calibrated with NIST traceable materials from the manufacturer.

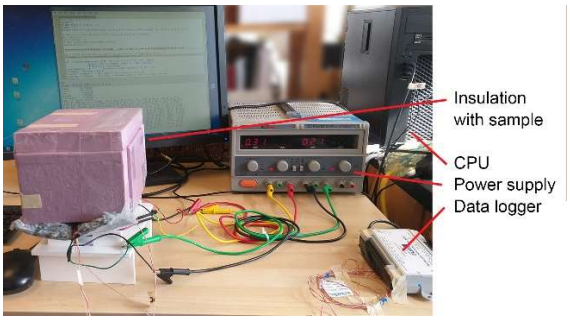

Figure 36. Apparatus to measure thermal conductivity. This consisted of Data-logger connected to CPU, to monitor the readings and the power supply to control temperature on the hot and cold side of material under test.

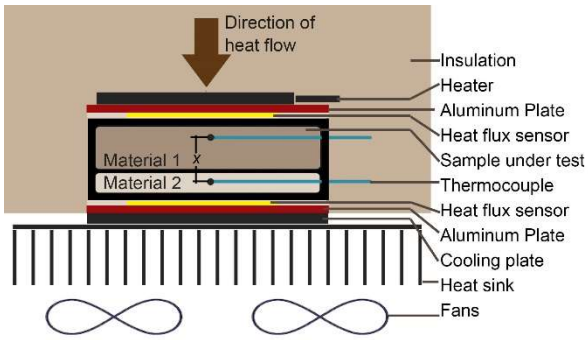

Figure 37. Schematic for measurement of thermal conductivity. The apparatus consisted of two heat flux sensors, two thermocouples, heater, cooling plate and heat sink with fans.

Since two heat-flux sensors were used, the average of the two readings was used to make calculations of thermal conductivity. For the sake of uniformity, if one heat flux sensor's readings were significantly higher than the other, then the voltage of the heater or cooling plate was adjusted. The voltage was adjusted precisely, so that the heat flux at both the sensors became similar.

The rule establishing steady state conditions was that a new reading of thermal conductivity should not deviate from the average of previous five readings by more than 0.5% (same as method A). This rule is suggested in ASTM C518 [87] for steady state measurement of

thermal transmission properties. Fourier's law was used to calculate thermal conductivity, (same as Method A).

6.1.3 Development Process for Thermal Experimental Setup: Lessons Learned

The experimental setup and procedure were developed over several iterations. A number of interesting observations were made along the way, which prompted more refinements to the apparatus. These are noted below:

1. **Upside Down Apparatus**: In earlier iterations of the development of the setup, the fan, heatsink and cooling plates were placed at the top, while the heater was placed at the bottom. The arrangement was purely based on convenience. Figure 38 illustrates this layout. However, since hot air rises, and cool air tends to settle down, it was felt that this arrangement might cause the minute amounts of air inside the apparatus to move around. Theoretically speaking, the small amount of air trapped inside the apparatus could transport heat, causing an interference in the readings. In the middle of a measurement process, the apparatus was turned upside down, so that the heater was now at the top, while the cooling plates along with heatsink and fan were at the bottom. In theory, the temperature gradient inside the material would be replicated by the air adjacent to it causing less air movement. As expected, doing this caused the numbers on the reader to move differently, and a difference in the accuracy was immediately noted.

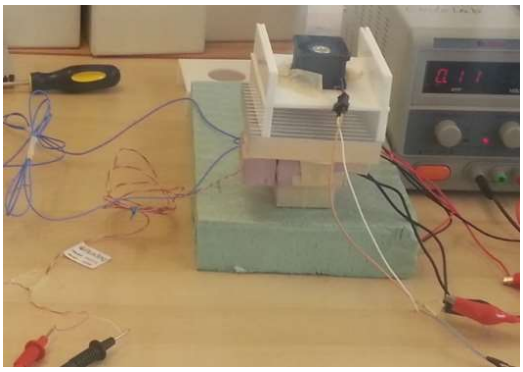

Figure 38 Upside down Apparatus

2. **Thermocouples Inside vs on the Surface**: Drilling the samples so that the thermocouples measured the temperature at the core of the sample rather than the surface made a huge difference in the readings. This was a very important detail in the experiments.

3. **Moisture Migration:** Although a steady reading was reached within two or three hours from the beginning of the experiment, it was noted that the reading for the calculated thermal conductivity continued to fall. The change was miniscule, but it was an unmistakable downward trend. Figure 39 shows the readings of the Cherry wood sample number 105 and shows how the thermal conductivity decreased from 0.148 to 0.145 in four hours. That is a difference of 2% in five hours. Experimentation has shown that this downward trend does not stop even when the wood is heated for fourteen hours.

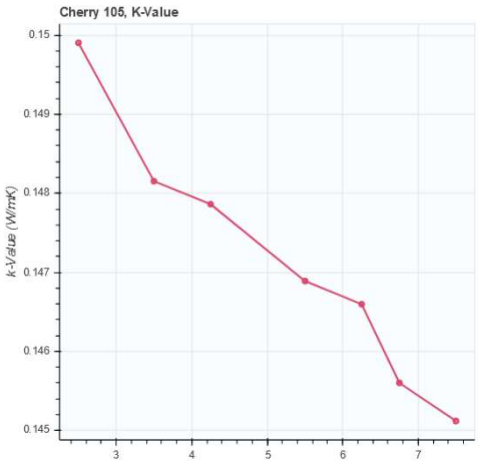

Figure 39 Readings of thermal conductivity for wood sample No 105.

Theoretically, the material should reach steady state conditions within one hour. However, the reason for the continued downward trend might be moisture migration. As soon as heat is applied to one side of the test specimen, moisture begins to move from the heated side to the cool side [55]. This creates a gradient of moisture inside the material and influences the measurement. For some samples, the prolonged exposure to heat resulted in a thin layer of moisture condensation on the cooling plates. In the case of one piece of MDF (Sample no. 316) two droplets of water were noted at the end of a three-hour long measurement period.

4. Temperature Corrections: The temperature varied from sample to sample during the measurements owing to the performance of the heater. The heater created a slightly higher temperature for samples which are more insulating and vice versa. Moreover, the average temperature that the heater was kept at the beginning of the experiments to around 80°C. It was later brought down to 60°C to reduce moisture migration. For this reason, a correction was applied for the temperature. The applied corrections are given in sections 3.1.1 and 3.1.2 of this work.

6.2 Dielectric Properties: Measurement Method and Apparatus

Relative Dielectric constant was calculated based on capacitance from an unshielded, two-electrode system. The samples reserved for the measurement of dielectric properties were covered on two sides with copper conductive paint 843WB by MG Chemicals, which has an advertised resistivity of 5.3 x 10-4 Ω·cm. The wires were fixed using a conductive silver epoxy by Atom Adhesives. These samples were sized 50 mm x 25 mm with a typical distance between the plates of 25 mm. The capacitance and dissipation factor readings from an LCR meter (DE 5000 by DER EE) were recorded at 10 kHz and 100 kHz.

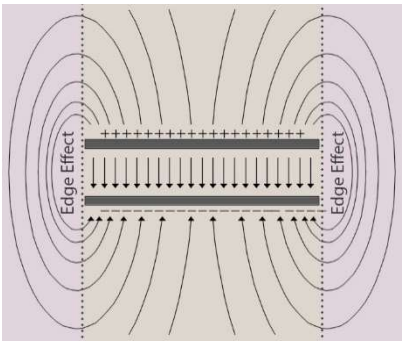

Figure 40 Edge effect between two plates of a capacitor is shown in pink

Since the relative dielectric constant was measured from capacitance using an unshielded system, a correction for edge capacitance had to be applied. When electric voltage is applied to two electrodes, the resulting electric field does not just exist between the two plates but extends a little bit beyond them. This is known as the fringing effect or the edge effect shown in Figure 40. As the distance between the two plates increases, so does the edge effect. The edge effect is therefore the part of the capacitance, which is a result of the geometry of the material. Numerous studies have proposed formulas to remove the edge effect from the readings. The formula used in this study to remove the edge effect is the one presented in the Journal of National Bureau of Standards, 1939 [88] by Scott and Curtis. The ASTM standard D150 [89] for calculations related to the dielectric constant are derived from the document by Scott and Curtis. Although ASTM D150 contains formulas for edge correction for several configurations of electrodes, it does not contain information for rectangular electrodes.

The formulas presented by Scott and Curtis [88] for rectangular electrodes of size equal to samples was used for this work and are given as:

$$Ce + Cg = \left(1.113\ \frac{l}{(4\pi^2)}\right)\left\{1 + \ln\left[1 + \frac{\pi w}{d} + \ln\left(1 + \frac{\pi w}{d}\right)\right]\right\} + \left(1.113\frac{w}{(4\pi^2)}\right)\left\{1 + \ln\left[1 + \pi\ \frac{l}{d} + \ln\left(1 + \frac{\pi l}{d}\right)\right]\right\}\mu\mu F$$

$$Cn = 1.113\frac{l\,w}{(4\pi D)}\mu\mu F$$

$$k = \frac{(Cp - Ce)}{Cn}$$

Ce is edge capacitance, Cn is normal capacitance, k is the relative dielectric constant w, l refers to the dimensions of the electrode in cm and d is the distance between the two plates in cm. As no formula exists for separating Ce and Cg, Scott and Curtis [88] rate the method of using rectangular electrodes inferior to using circular electrodes and estimate an error of at least 2.3% in measurements.

6.2.1 Practical Measures for Dielectric Measurement

Average measured capacitance for wood and wood-based materials was 2.7 pF. Such a small capacitance can easily be influenced by environmental conditions. Some measures taken to minimize errors were:

- Wires were kept as short as possible.
- All samples were fitted with the same gauge, quality and size of wires.
- Instrument was calibrated using open and short method specified by manufacturer before the measurements.
- Material under test was kept clear of other objects to avoid their field of capacitance. Special care was taken to remove any electronic gadgets from the surroundings which might interfere with the readings.
- Wires not to cross each other to avoid interference.
- As many items as possible were measured in a single cycle. This ensured that environmental conditions like temperature, humidity etc. acted on all the samples in a similar way
- During measurement, the surface that the sample rests on can influence the reading. Surface with a very small capacitance was chosen for this work.

6.3 Other Electrical Properties

While measuring the capacitance and dissipation factor using the method described in the previous section, the series resistance (ESR) was also noted for some experiments. The following formulas were then used:

$$Xc = \frac{ESR}{\tan\delta}$$

$$|Z| = \sqrt{ESR^2 + X^2}$$

$$Z = ESR + jX$$

$$pf = \frac{Df}{\sqrt{1 + Df^2}}$$

Where Xc is reactance, ESR is series resistance, |Z| is magnitude of impedance in ohms, and Z is the complex impedance, pf is the power factor and Df is the dissipation factor. The uncertainty for impedance was higher than that for capacitance. The readings for ESR often shifted on the meter.

6.4 Sound: Measurement Method and Apparatus

Two methods were used to record the behavior of sound through the materials. These are described in detail in the following sections.

6.4.1 Sound Impact Method to Measure Sound Speed

A unique technique was developed to record the velocity of sound through the material. A pictorial view of this method is presented in Figure 41. The time required for sound waves to travel through a material was recorded using an oscilloscope (Owon, model number VDS1022i). The top side of the sample was struck to produce a noise, which was recorded by the piezo at the bottom of the sample. The time delay between when the wood was struck and when the sound was recorded by the piezo was recorded using the oscilloscope. See Figure 42 for a typical reading from the oscilloscope. The thickness of the material was measured using a Vernier caliper which gave a resolution in millimeters down to two decimal places. The formula used was

$$v = d / t$$

Figure 41 Apparatus for the sound impact method to record sound speed

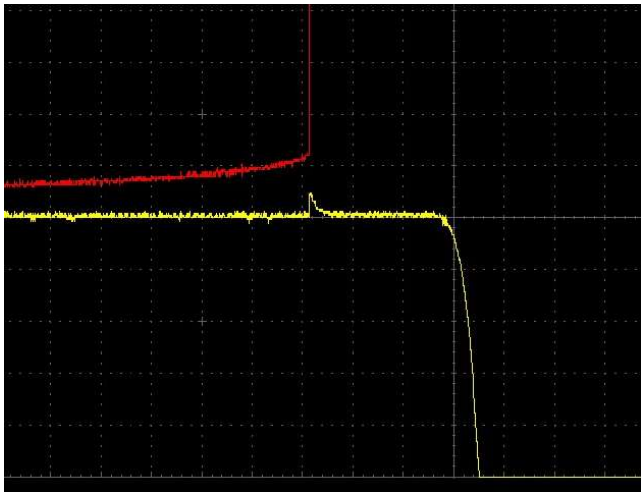

Figure 42 Typical reading from the oscilloscope from the sound impact method

To produce a signal at the top of the sample, a small voltage was applied. This voltage was produced by static electricity. A 3/8” ball bearing was channeled through a paper tube, and as the ball bearing fell through the tube, it collected static charge. This charge was discharged as the ball bearing struck on the sample, creating both a sound as well as a small applied voltage of approximately 5 to 10 mV. The coin sized conductive paint that was applied to the top of the sample then conveyed the signal to the wire, which was connected to the oscilloscope. The conductive paint was applied directly opposite to where the piezo was attached and served two purposes. One was to channel the signal from the ball

bearing to the oscilloscope, and the second was to make sure that if the ball bearing strayed it would not come in contact with the paint, and so that signal would not be detected, and such a reading discarded.

At least five readings were taken for each sample using this method. However, samples which showed a high variation in readings were given ten trials. The average time delay was recorded, and then divided by the thickness of the material to find the sound speed.

6.4.2 Resonance Method with Signal Generator

All wood and wood-derivatives were cut to the same length for this set of experiments. The setup is shown in Figure 43. A signal gen was connected to a piezo fixed to the top side of the wood, and the oscilloscope to the piezo attached to the bottom side of the wood. This way, one piezo became the speaking device, and the other became the listening device. A sweep of frequency from 1 Hz to approximately 500 Hz was done. The oscilloscope's response was recorded in terms of which frequencies showed a distinct peak, and what amplitude these peaks occurred. It was also noted at which frequency the signal was completely attenuated. A complete list of variables recorded is given in Table 3.

Figure 43 Apparatus for resonance method with signal generator

Table 3 Variables recorded for the resonance method

Thickness	F1	F1 Amp	F2	F2 Amp	F3	F3 Amp	F4
Thickness of Sample	First Peak	Amplitude of First Peak	Highest Peak	Amplitude of Highest Peak	Last Peak	Amplitude of Last Peak	Frequency where the signal was lost

6.5 Density

Density was measured by recording the sample weight and dimensions. Formula used was:

$$D = \frac{M}{V}$$

where D is density, M is mass and V is volume.

6.6 Moisture Content

Samples were oven dried in a convection oven at 105°C for about 24 hours. The oven drying process continued until no significant change in weight was found at four-hour intervals. This method is compliant with ASTM's standard test method for direct moisture

content measurement of wood and wood-based materials D4442 [90]. The formula used to measure moisture content was:

$$Mc = \frac{M - M_{dry}}{M_{dry}}$$

where Mc is moisture content, M is weight of the sample, and M_{dry} is oven dry weight

6.7 Error Propagation

Calculated uncertainty for each sample measurement is presented in the results section. Uncertainty is calculated based on Taylor's [91] formula for uncertainty in a function of several variables. For *x, …,z* measured independent and random variables with uncertainties *δx, …,δz* used to compute a function *q(x, …,z)* then the uncertainty in *q* is given as:

$$\delta q = \sqrt{\left(\frac{dq}{dx}\delta x\right)^2 + \ldots\ldots + \left(\frac{dq}{dz}\delta z\right)^2}$$

The uncertainty calculated for the thermal conductivity experiment is determined by the derivatives of Fourier's law. The rate of the error for each variable is assumed according to the specifications of the instrument manufacturer.

6.7.1 Other Sources of Error

While the previous section accounts for errors caused by instruments and measurements, a few other sources of errors need to be taken into consideration. One source of error may be from the use of a different piece of wood for thermal and a different one for dielectric measurements. Although both the pieces were removed from the same block of wood, the natural variation in grain could imply that both pieces were dissimilar to some extent. A second source of error may be from the hygroscopic properties of wood which causes its moisture content to change with a change in relative humidity of surrounding air. The measurements were carried out over a few months, so changes in weather may have caused changes in the moisture levels of samples, which went undocumented.

6.8 Repeatability

Additional experiments were performed on acrylic samples to test the repeatability of the experiments. A set of acrylic samples in four thicknesses were obtained from the same manufacturer. The manufacturer provided brochure about material properties was also obtained. The results of these experiments are described in the following sections.

6.8.1 Repeatability of Thermal Conductivity Measurements (Method B)

Three acrylic samples (seen in Figure 44) were tested using the data logger and two heat flux sensors method B described in Section 6.1.2. The recorded thermal conductivity was 0.187, 0.188, 0.179. W/m.K. The coefficient of variation was 2.6% and standard error was 0.003 W/m.K, which shows that the experiments are highly repeatable. Manufacturer provided value for thermal conductivity is 0.187 W/m.K.

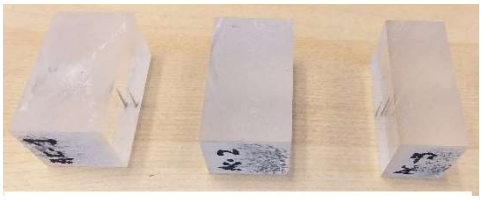

Figure 44 Acrylic samples that were measured for thermal conductivity

6.8.2 Repeatability of Dielectric Measurements

Sixteen acrylic pieces of various sizes and thicknesses were tested for repeatability in dielectric measurements. The sample thicknesses were 9.5, 11.7, 17, 22.9 mm. The average recorded relative dielectric constant at 1 kHz was 3.1 with a coefficient of variation of 6.3%. The manufacturer provided value for relative dielectric constant was 3.3.

Average dissipation factor for this set of experiments was found to be 0.0343 while the manufacturer provided value was 0.039. The coefficient of variation for the sixteen measurements for the dissipation factor was found to be 6.3% and standard error was found to be .05.

7 Wood and Wood-Based Materials

This chapter is based on a paper by Saeed et al [85]

7.1 Materials

Experiments were performed to determine the correlation between dielectric properties and thermal conductivity for solid wood and wood-based materials as seen in Figure 45. The sample types, number of samples for each type and their range of densities are highlighted in Figure 46. Materials representative of frame construction were chosen for this study and included 30 solid woods and 17 wood-based materials samples. The wood-based materials included flakeboard (OSB), plywood, chipboard and fiberboard (MDF) samples. A higher number of wood samples were chosen because several construction materials like insulation, OSB, plywood etc., are derived from wood. Samples for wood were also available in a large density range, and an even spread of densities was desirable in establishing correlation. The selected samples were cut into at least two pieces of size 50 mm x 25 mm x 25 mm each. One of the pieces was reserved for determining its thermal conductivity and the other to measure its dielectric properties.

Figure 45 Material samples for solid wood (above) and wood-based materials (below)

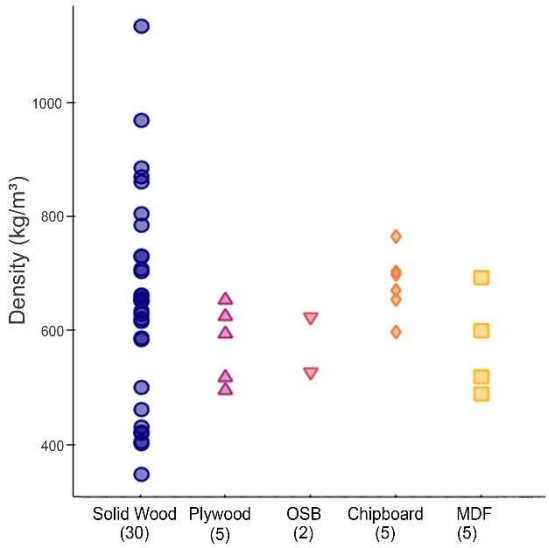

Figure 46 Density distribution and number of samples and types studied

7.2 Methods

For solid wood, all measurements were made perpendicular to the direction of the grain. All dielectric measurements were made at room temperature of 20°C to 25°C prior to the oven drying process. The experimental apparatus and method are described in Section 6.1.1 of this dissertation detailing Method A. Dielectric properties were measured using the method

described in Section 6.2 of this dissertation while the density and moisture content were measured as described in Section 6.5 and Section 6.6 respectively.

7.3 Results and Discussion

Results obtained for the measured thermal conductivity and dielectric properties are in agreement with the values reported in literature. Thermal conductivities of wood perpendicular to the grain were found to be between 0.11 W/m.K (softwood) and 0.28 W/m.K (hardwood). Wood-based materials were found to have thermal conductivities between 0.09 W/m.K (MDF) and 0.15 W/m.K (plywood). The relative dielectric constant of wood perpendicular to the grain was measured to be between 2.0 and 6.0, while the oven dry density of the samples was in the range of 325 kg/m^3 to 1050 kg/m^3. Raw data for these measurements can be found in the article by Saeed [83].

7.3.1 Correlation with Oven-Dry Density and Moisture Content: Equations Predicting Thermal Conductivity

Scientists have constructed empirical equations to predict the thermal conductivity of wood using their oven dry density and moisture content. The oven dry density is the density of materials once all moisture has been removed from them and is lower than the density of the material in its original state. To compare the results of this study with past literature, the samples used in this study were oven dried, and their moisture content was calculated. It was found that the moisture content of most samples was between 5% and 8% at the time of measurement. Less than 20% of the samples had higher moisture content of up to 13%. Samples were only measured for thermal conductivity and dielectric properties in their original state and were not measured for these properties in their oven dry condition. Further, a temperature correction of 0.2% per degree Kelvin was applied to the measured thermal conductivity for solid wood to match the average temperature of 25°C for which much of the literature related to thermal conductivity exists [52].

The first equation for wood thermal conductivity, based on oven dry density and moisture content was given by Maclean [13] in 1941. This was subsequently followed by Wilkes [51] 1979, Siau [14] in 1985, and Tenwolde [52] in 1988. These equations are given below modified to express λ in SI units.

$$\lambda = \rho\,(0.200342 + 0.00547699\,mc)\,/\,1000 + 0.024358 \qquad \textit{Eq 1 Maclean}$$

$$\lambda = 0.02582 + (1.686e^{-4} + 5.177e^{-6}\,mc)\rho\,/\,(1 + 0.01mc) \qquad \textit{Eq 2 Wilkes}$$

$$\lambda = 0.510448 - 0.4736288\,a \qquad \textit{Eq 3 Siau}$$

where $a = \sqrt{1 - 0.000667\,\rho - 0.00001\,mc\,\rho}$ *Eq 4*

$$\lambda = \left(\frac{\rho}{1000}\right)(0.1941 + 0.004064mc) + 0.01864$$ *Eq 5 Tenwolde*

Where ρ is the oven dry density in kg/m3, *mc* is moisture content in %, and *a* in Eq 9 is porosity of wood.

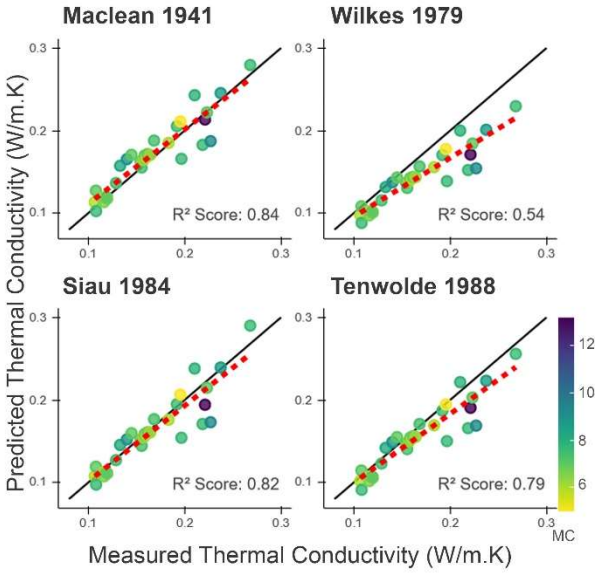

Figure 47 Comparison of measured data with predicted data from equations 5 to 9. The color of the dots indicates the moisture content, black line represents the line of perfect agreement, and dotted line represents regression line of data as per suggestion of scientist equation.

The comparison of measured experimental readings with predictions made from equations 5 to 9 are shown in Figure 47. The calculated regression line between measured data and predicted data from above mentioned equations are shown in the above graph. It is seen that the measured data closely follows the equation for predicting thermal conductivity as given by Maclean and Siau with only minor discrepancy. Although Wilkes equation is seen to have the least similarity to the true measurements, it is interesting to note that it is still accurate up to 0.2 W/m.K thermal conductivity. Moreover, it seemingly has the same slope as that of Maclean, but with a different intercept. The Wilkes equation is based on 1094 data points and is quoted in the ASHRAE (2013) fundamentals handbook [43] as the suggested method for approximating the thermal conductivity of wood. Tenwolde's equation is used to derive and display thermal conductivity for solid wood materials by the US Department of Agriculture's wood handbook [53].

7.3.2 Correlation with Density Independent of Moisture Content

The measured thermal conductivities are shown as a function of density in Figure 48. The thermal conductivity of solid wood is proportional to its density and is independent of wood species, as shown in this graph. For wood-based materials of the same density as solid wood the thermal conductivity is typically lower. The presence of moisture elevates thermal conductivity. These observations are manifest in Figure 48 and are consistent with literature in Tenwolde [52], Kollman [92], Kollman and Cote [93], Lewis [60] etc. According to Lewis, fiberboards have lesser thermal conductivity than particleboards and our data is consistent with his findings.

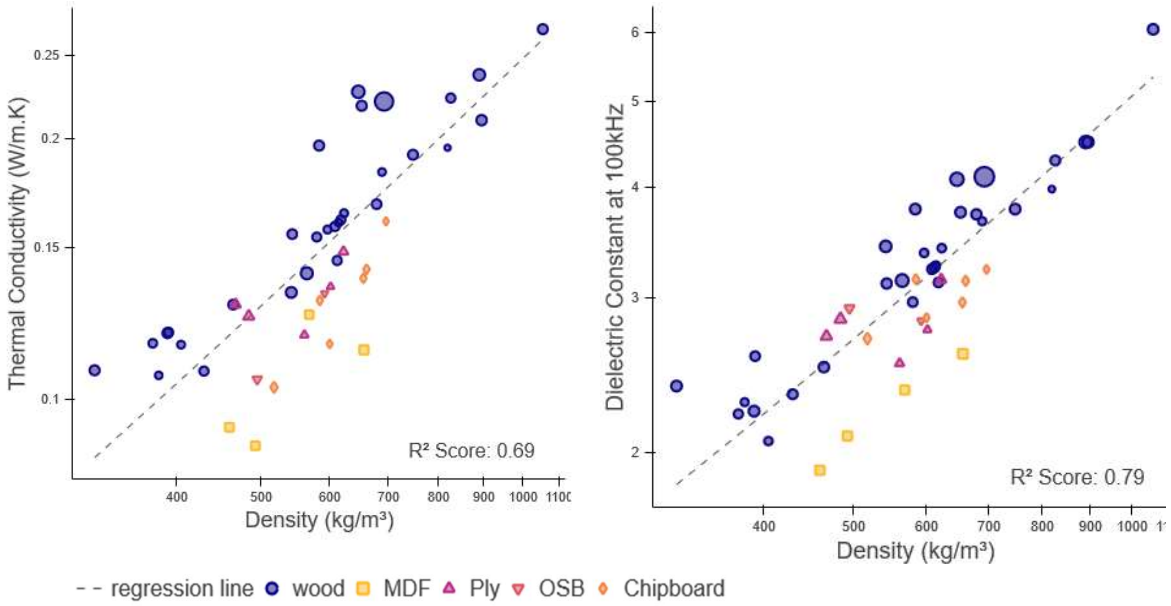

Figure 48 Correlation of density and thermal conductivity for wood and wood-based materials. Density is based on moist weight of samples. Size of data-points suggests moisture content between 5% and 13%

Figure 49 Correlation of density and relative dielectric constant for wood and wood-based materials. Density is based on moist weight of samples. Size of data-point suggests moisture content between 5% and 13%

The strong correlation between relative dielectric constant and density of wood and wood-based materials is demonstrated in Figure 49. The relationship of wood density and relative dielectric constant has been extensively studied in the past, with the earliest being in 1948 by Skaar [94]. He showed that if frequency, temperature, direction of measurement and moisture content was constant, then wood density had a strongly linear correlation with its relative dielectric constant. Torgovnikov [68] estimates that the coefficient of correlation between oven dry density and relative dielectric constant for moisture levels up to 30% and frequencies above one kHz, is above 0.95 in most cases. For measurements perpendicular to the grain, she finds a linear relationship between oven dry wood density and its relative dielectric constant.

7.3.3 Correlation of Dielectric Properties and Thermal Conductivity

Thermal conductivity as a function of relative dielectric constant is shown in Figure 50. The coefficient of determination (R^2 of the regression) between the two material properties was found to be 0.87, which indicates a strong correlation. 72% of the data points were found to be within 10% of the regression line, whereas all but one reading was within 20% of the regression line revealing the strength of the correlation.

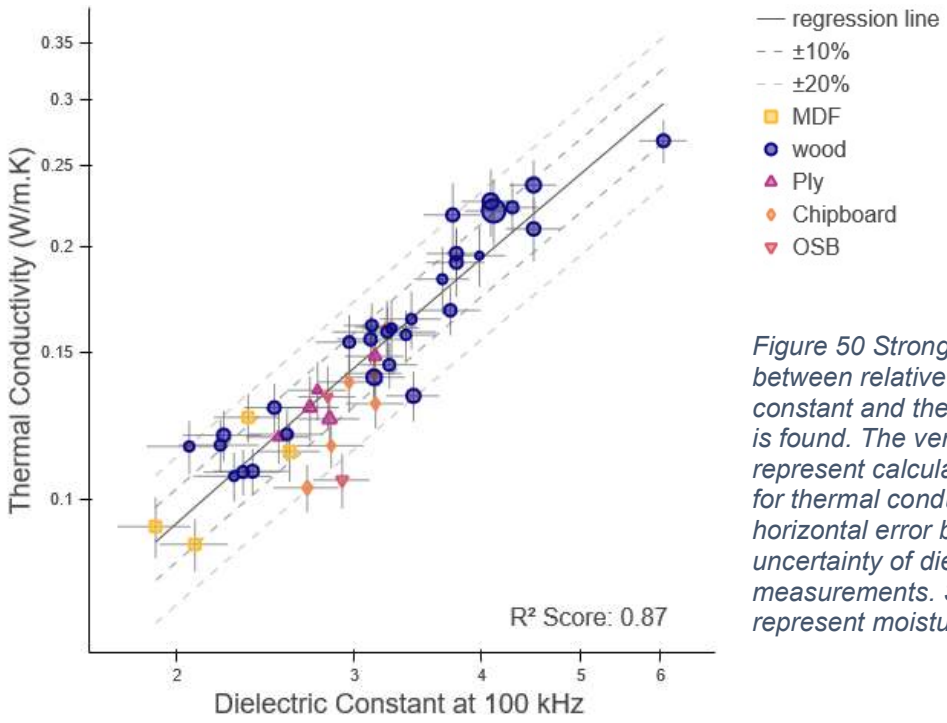

Figure 50 Strong correlation between relative dielectric constant and thermal conductivity is found. The vertical error bars represent calculated uncertainty for thermal conductivity, while the horizontal error bars indicate uncertainty of dielectric measurements. Size of data points represent moisture content.

Based on this strong correlation, we conclude that the measurement of relative dielectric constant could be used as a robust metric for predicting of thermal conductivity of wood and wood-based material. The correlation between thermal conductivity and relative dielectric constant seen in Figure 50 is stronger than their respective correlation with density seen in Figure 48. While many equations to predict thermal conductivity using oven dry density and moisture content are listed in section 7.3.1, the R^2 score of this method is superior. Moreover, in most cases density and moisture content are unknown and, in many situations, not measurable in-situ.

Although the datapoints in Figure 50 do not line up in a perfect agreement with the regression line, it must be noted that there is no perfect method or tool to measure thermal conductivity of in-situ walls. In the case of measurement using steady state conditions, ASTM's C1155 [24] standard for determining thermal resistance of building envelope components from in-situ data allows uncertainty of measurements to be within 10%. Ficco et al [95] found the uncertainty of in-situ thermal transmittance measurements are dependent on operative conditions. Their study estimates the uncertainty to be 8% under optimal operative measurements, and 50% under non-optimal measurement conditions. Atsonios reports the expected error for the four different methods of calculating thermal resistance based on steady state conditions in-situ to be between 11% and 28% [27]. Moreover, depending on the season and whether the building is freely ventilated, it can take 20-30 days to reach steady state conditions and meet the criteria for convergence [6]. In contrast, the advantage of the proposed method of measurement is that it can be done within minutes. As an alternative to steady state methods, thermography for determining in-situ thermal conductivity also has high uncertainty. Depending on testing conditions, and method of measurement for thermography, scientists have reported a deviation between 5% and 200% [4,96–98] from actual values. A higher error is associated with unfavorable environmental conditions for measurement.

The R^2 score of the shown relationship can be further improved by collecting dielectric data of specific materials at higher frequencies and applying machine learning techniques. Studies show that measuring dielectric properties at higher frequencies can reveal some material behaviors that are not apparent at lower frequencies [99]. This additional information from higher frequencies would expand the feature space for machine learning, leaving the algorithm more information to draw from, hence improving the prediction quality. Additionally, more data can be collected for the materials relevant to the construction industry to improve the score. While testing many wood species was central to establishing the regression line, only a select few are used in building construction. Targeting specific materials, relevant to construction for machine learning would remove some of the error seen in the predictions in Figure 50.

Wood and wood-based materials are seen to fall closely within the same regression line in Figure 50. All previous models to predict thermal conductivity rely on a different equation for wood, and an added correction for each of plywood, fiberboards and particleboards. But using dielectric properties, the same equation and instrumentation may be used to predict thermal conductivity of all the above materials. Having all these materials fall close to the same regression line gives rise to the question as to whether the correlation could continue to hold if these materials were to be connected in series, much like an architectural wall. The author speculates that if enough construction materials are similarly correlated, then there is a likelihood that their combined thermal conductivity and relative dielectric constant may have a similar relationship as shown in Figure 50. This question deserves future research.

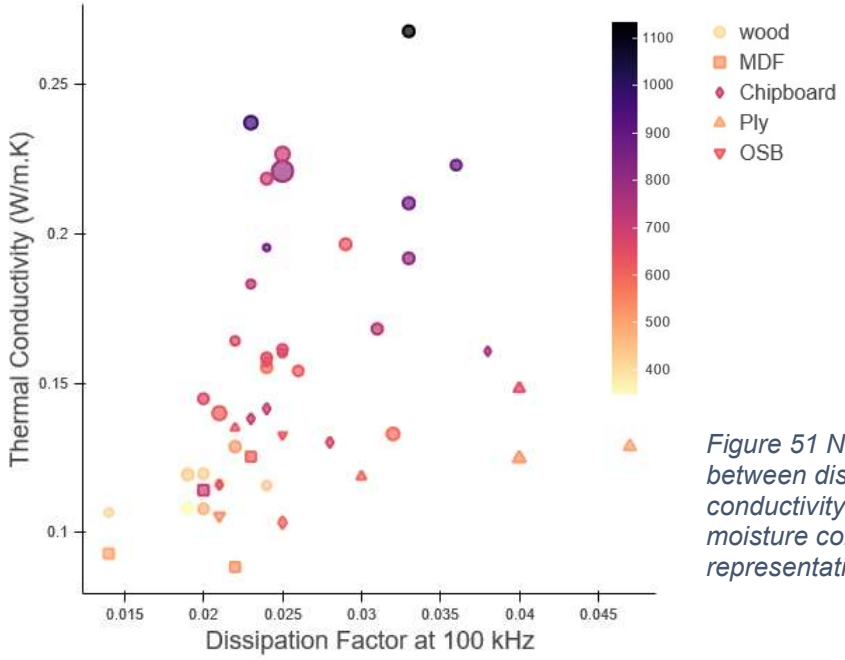

Figure 51 No correlation was found between dissipation factor and thermal conductivity. The size denotes the moisture content and the colors are representative of the density in kg/m³.

No correlation was found between thermal conductivity and dissipation factor in Figure 51, but it may be useful in future work to involve materials with a broader range of moisture content. Torgovnikov reports that at frequencies between 10kHz and 10GHz wood dissipation factor is mainly influenced by its density and moisture content [68]. Many moisture meters rely on the relationship between moisture content and the dielectric loss factor of materials to detect moisture in wood. The power factor, which is a direct function of

the dissipation factor is described as a nonlinear function of moisture, temperature and frequency, exhibiting minimum and maximum values at various combinations of these variables [15,67] . Various reports have shown the increase in the dielectric loss factor as linear or curvilinear with increased moisture content [69,100–103] for a given frequency in the microwave range. Given the strong relationship of thermal conductivity with moisture levels, information related to the dissipation or loss factor may yet be beneficial in predicting thermal conductivity in materials with unknown amounts of moisture.

7.4 Conclusions and Future Work

The results of the experiments show a strong correlation between thermal conductivity and the relative dielectric constant. In other words, the potential for predicting thermal conductivity using dielectric material properties has been demonstrated. But much work remains in order to address composite walls. Once implemented, this method would eliminate the need to create steady state thermal conditions for the measurement. This will result in a faster measurement process, perhaps making the measurement possible within minutes rather than in days. It will also be independent of weather conditions, like requiring a large temperature difference between indoors and outdoors. A third advantage is the potential development of a gadget for lay use.

While no correlation was found between the dissipation factor and thermal conductivity in this study, it might be a useful metric for future work involving moisture content. The dissipation factor is known for its strong sensitivity to moisture in materials and is used in many applications to detect and quantify moisture. One limitation of the conducted study is that it was not examined in the context of moisture content which has a secondary impact on thermal conductivity. Except for a few samples, all had moisture levels between 5% and 8%. The study of construction materials in the context of water content is important because the thermal properties of a building envelope can change over time due to water seepage and deterioration. While both thermal conductivity and dielectric properties increase with increased moisture levels, it is unknown if moisture effects both properties in a similar way. This may be a point of interest in future work.

8 Sound

8.1 Sound

Data related to sound was collected using two different methods. These methods are described in Section 6.4.1 and Section 6.4.2. The preparation of samples for the two methods is described in Section 5.3 of this dissertation.

8.2 Sound Impact Method

Results obtained using the sound impact method are shown in Figure 52. The figure shows no strong correlation between density and sound speed through a material. The regression line looks more like a line of classification separating the two types of wood and wood-based materials. The only thing highlighted by the results is how sound moves very differently through solid wood, and wood-based materials. The structure of solid wood with its vessels, fibers and rays effects the propagation of sound differently, while the wood-based materials, which are compressed with resin and glues using heat treatments seemingly are less conductive to sound.

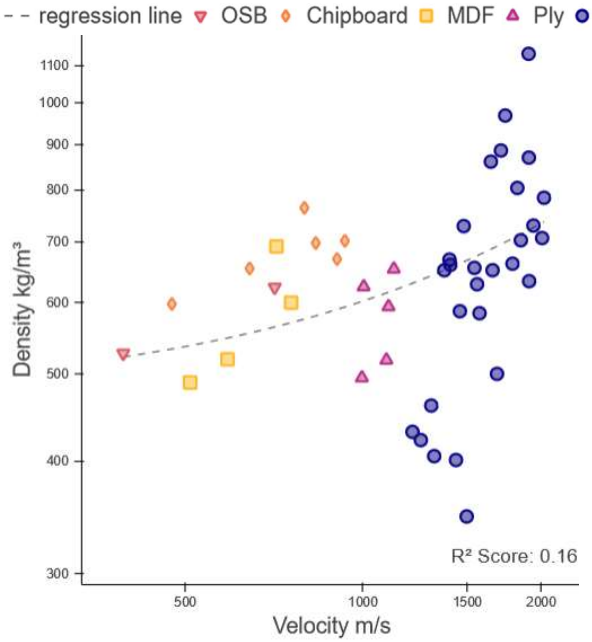

Figure 52 Scatter plot of sound speed vs density:

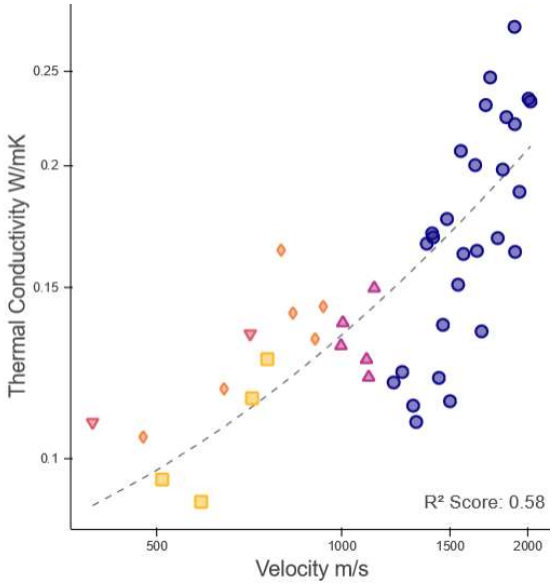

Figure 53 Scatter plot of sound speed vs Thermal Conductivity.

Figure 53 shows show the results for the sound speed found through the sound impact method. The displayed scoring function is the R^2 coefficient of determination. The score is not robust towards outliers, and so some scores may have been heavily affected by the lone outlier (yellow triangle) seen within the data.

8.3 Results from Signal Gen Method

The scatter plots of thermal conductivity to various documented sound properties is found in Figure 54. It shows the results of work done for wood and wood-based materials. No seeming correlation can be observed between amplitude and density. However, there is some correlation between when the signal seemingly begins to die out, and the density of the material. Less dense materials seem to carry signals less effectively. The best correlation with density seems to exist between the product of the thickness of the material and the frequency which displays the highest amplitude.

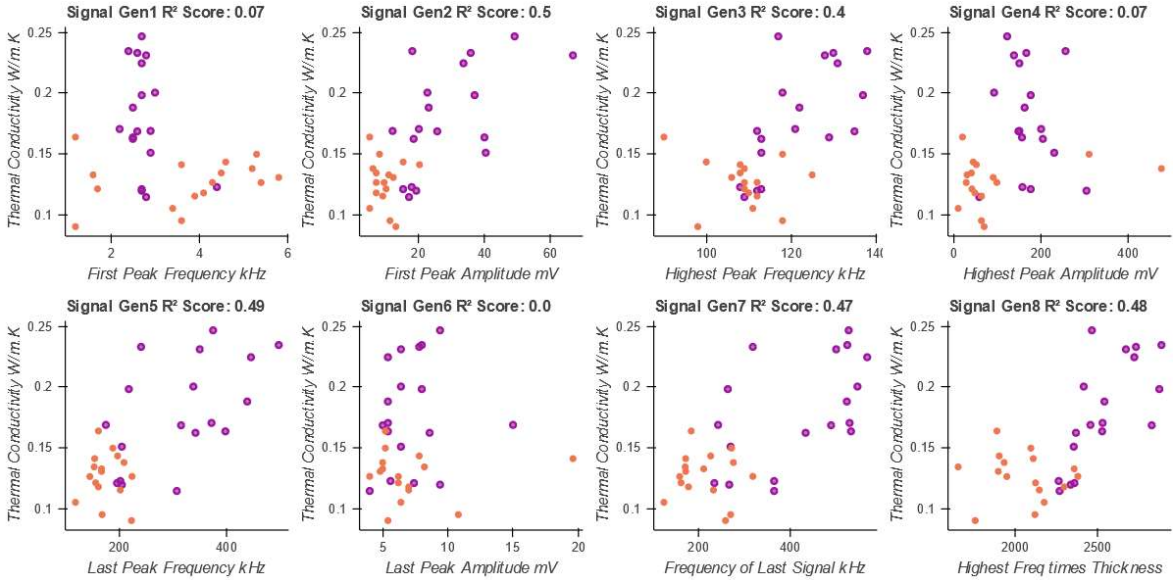

Figure 54 Results from signal gen: Thermal conductivity vs sound properties

8.4 Machine Learning Results

Numerous studies indicate that several weak classifiers can be combined to make accurate predictions. To this end, thermal conductivity was predicted using results of the sound speed experiment combined with the signal generator experiment. The columns were first projected into a third-degree polynomial. Then ordinary least squares regression was performed to obtain the results. These results are shown in Figure 55.

The three features selected for regression were velocity from the sound impact method (which has the strongest correlation for all sound related data), the frequency with the highest amplitude, and the amplitude of the first peak. These features were chosen based on their individual strength of relationship with thermal conductivity. Each of these parameters were multiplied with their thickness to account for sample thickness.

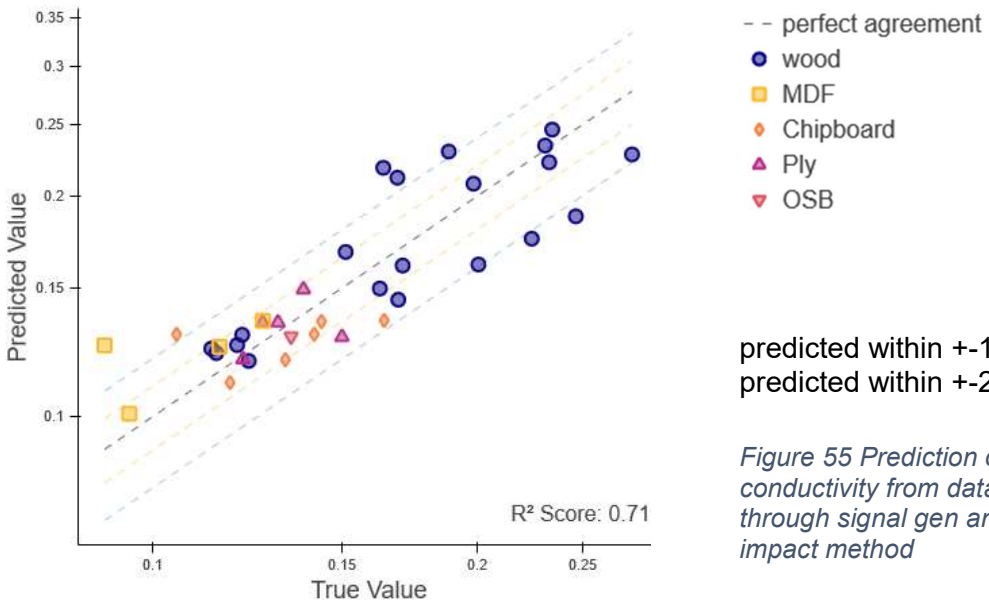

predicted within +-10%: 64%
predicted within +-20%: 81%

Figure 55 Prediction of thermal conductivity from data collected through signal gen and the sound impact method

8.5 Conclusion

Data collection for any of the methods related to sound are tedious and time consuming. Moreover, the uncertainty of this method is very high, and the readings are unstable. Although several weak classifiers were used successfully to predict thermal conductivity, the result is not as reliable as the one obtained from the dielectric properties. For this reason, it is concluded that using sound may not be a good metric to predict thermal conductivity.

9 Multilayered Materials: Wood Frame Construction

This chapter is based on report by Saeed et al [84]

9.1 Properties of Multilayered (Composite) Materials and Contact Resistance

When two materials of different properties are stacked together, then the resulting multilayer system's properties depend on the constituent layers. A multilayered material is illustrated in Figure 56. The following formulae give the thermal conductivity and dielectric properties of a multilayered material based on its constituent layers:

Thermal conductivity:

$$\lambda = \frac{L}{\sum_{i=1}^{n} \frac{L_n}{\lambda_n}} \qquad \textit{Eq 6}$$

Relative dielectric constant:

$$\epsilon_r = \frac{L}{\sum_{i=1}^{n} \frac{L_n}{\epsilon_n}} \qquad \textit{Eq 7}$$

Where λ, ϵ_r, L are thermal conductivity, relative dielectric constant and total length of material of the composite material respectively. λ_n, ϵ_{rn}, L_n refer to the thermal conductivity, relative dielectric constant and length of a constituent layer.

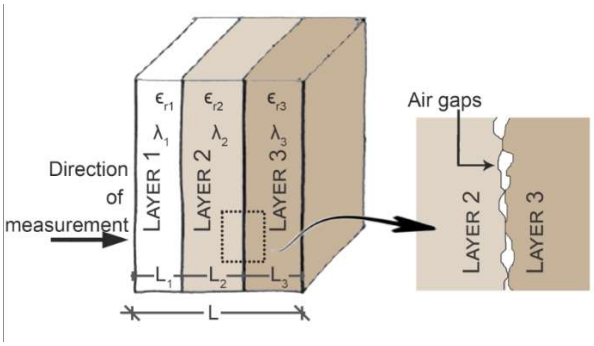

Figure 56 Multilayered material: Layers connected in series. Contact resistance occurs at the interface of two layers because of the roughness of the two surfaces.

Contact resistance causes the theoretically calculated properties of multilayered materials to deviate from measured values. The roughness of surfaces causes spots of contact as well as tiny gaps at the interface of the two materials. These pockets are usually filled with air (see Figure 56). Although several theories predict the value of thermal contact resistance, the results from practical experiments are considered to be more reliable and accurate [26]. In the case of dielectric measurements, a lack of electrical contact between the two surfaces causes the deviations from theoretical values. As more individual slabs of materials are used to form a composite, the disagreement between measured and theoretical values becomes greater [104]. For these reasons, the thermal conductivity and dielectric properties of the multilayered materials must be practically measured rather than estimated theoretically from its constituent layers.

9.2 Measurement of Multilayered and Cavity Walls

9.2.1 Thermal Conductivity

In addition to conduction and radiation, heat transfer in cavity walls also occurs through convection. An air cavity is often used in wood-frame and masonry construction, as well as in construction materials like cinder blocks etc. When a temperature gradient is formed across these walls, a convective current arises. This convection depends on the size and geometry of the cavity, as well as the size of the openings into the cavity [105]. The effects of convection and radiation are accounted for by calculating the wall thermal transmittance value. A distinction is made between thermal transmittance value and thermal conductivity value. While thermal conductivity (lambda value) is a measure of how easily heat can flow through a material via conduction, thermal transmittance (u-value) accounts for the effect of conduction, convection and radiation in heat transfer. The former is independent of thickness with SI units of W/m.K, while the latter is dependent on thickness and has SI units of W/m^2K. Thermal properties of cavity walls can be measured under lab conditions using ASTM's hot box method for building envelope assemblies [29].

For the purpose of heat transfer calculations, cavity walls are considered a multilayered material, where air is treated as an opaque solid [106]. The thermal transmittance properties are estimated by assigning a convective and radiative heat transfer coefficient to the air gap. These coefficients are estimated based on studies which correlate aspect ratio of cavity, orientation and direction of heat flow with heat transfer [107]. However, some studies have found large discrepancies between theoretical calculations and ground reality [108].

There is no quick or easy way to measure thermal conductivity of cavity walls. Literature related to thermography has not addressed walls with an air gap or convective heat flow [4]. The more recent transient technique developed by Rasooli [41] is effective in measuring multilayered walls, but not for cavity walls or heavily insulated walls. Sorensen's u-value meter [37,38] only works for single leaf walls without moisture and its effectiveness is yet to be tested. The hot box method for lab measurements [29] requires dimensioning of the meter chamber to be equivalent to the effective height of the assembly with the air cavity and detailed CFD analysis, making for a very cumbersome process.

9.2.2 Dielectric Properties

One method of measuring dielectric properties is by directing electromagnetic waves toward the material under test. The reflected signal or the reflected and transmitted signal are measured and recorded by a sensor. Since the phase and attenuation of the reflected and transmitted wave depend on the materials properties, a mathematical derivation can be used to interpret its dielectric properties [109]. This measurement of dielectric properties can be done on a single layer as well as multilayered materials. The reflection and transmission of electromagnetic waves through multilayered materials was presented by Richmond [110] in 1965.

Several researchers have extended the theory of the measurement of multilayered materials to architectural walls of various compositions like cinder blocks, rebar concrete, drywall construction etc., and the theory surrounding such measurements is well developed [111]. The measurement of dielectric properties of composite materials is typically done using free

space methods [112]. It has been found that if the thickness of a multilayered material is small compared to the wavelength, then the multilayers can be considered as an equivalent homogenous material [113,114]. Moreover, reflections at the boundaries of internal structures can give useful information like the presence of cavities, width of the cavity or blockages in cavities, thickness of the leaves etc. [115–117].

9.3 Materials

A building wall typically consists of many component layers which represent a multilayered system. According to the United States Census Bureau, since 2009, more than 90% new single family and more than 80% percent new multifamily building in the United States were constructed using the wood-frame construction [20]. The wall assembly of this type of construction generally consist of sheathing material like plywood or OSBs, followed by a layer of insulation and or air gap and finished on the interior side with gypsum drywall [118]. For this reason, the materials chosen for the study were OSB, plywood, gypsum drywall, insulation and solid wood. An emphasis was placed on solid wood as a material of study because several construction materials are derived from solid wood and exhibit similar behaviors. Of the twenty-six samples tested, 6 were constructed by leaving an air gap between two layers of solid materials.

Figure 57 shows some of the samples that were tested and the types of materials that were combined to construct these samples. Solid wood samples were placed to be measured perpendicular to the grain. The layer surfaces were not glued together, but rather held in place with tape on the outer side. The dimensions of the samples were 50mm x 25mm width and height, but the thickness was variable. The thickness of each layer ranged between 5mm and 20mm, whereas the total thicknesses of the samples ranged between 19mm to 30mm. Using a thicker layer of insulation material resulted in a material with overall low density. The layer thicknesses were thus varied to produce a good density range between 150 and 700 kg/m^3.

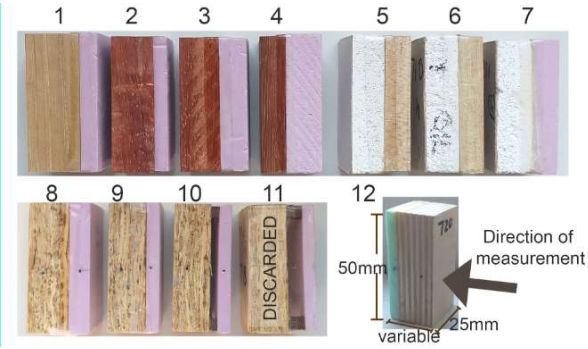

Figure 57 Samples 1-4: Hardwood-insulation. 5-7: gypsum drywall with insulation or solid wood. 8-11 OSB samples, first without air, then with layer of air. 12: Typical sample with dimensions.

Of the twenty-six samples tested, 6 were constructed by leaving an air gap between the two layers of materials. Figure 57 samples numbered 10-11 are two such examples.

9.4 Apparatus and Method

Apparatus and method used to measure thermal conductivity is described in Section 6.1.2 and for dielectric properties in Section 6.2 of this dissertation.

9.5 Results and Discussion

Measured thermal conductivity was found to be between 0.05 and 0.15 ± 0.01 W/m.K and the relative dielectric constant at 100kHz was found to be between 1.5 and 2.7 ± 0.2. The results for thermal conductivity were compared with theoretical calculations using the properties of constituent layers. The measured results agree with theoretical values for all samples except for the ones with a large air gap. Elevated readings were observed in these, indicating that additional heat exchange took place due to convection. The air inside the sample could not sealed and heated air was replaced by surrounding cooler air. For this reason, three samples with an air gap larger than 3.5mm were discarded from the dataset.

9.5.1 Correlation with Density

Thermal conductivity, relative dielectric constant and dissipation factor are all strongly sensitive to density and moisture content. This is evident in Figure 59, Figure 58 and Figure 60, where the density of the materials is plotted against their thermal conductivity, relative dielectric constant and dissipation factor respectively. Comparing the data in these figures with the images of the samples reveals how varying the thickness of the primary material or insulation effects density and other material properties. For example, hardwood + insulation samples 1-4 show decreasing thickness of hardwood, which is reflected in the figures with decreasing density, thermal conductivity and relative dielectric constant. Samples numbered 5 and 6 may look similar, but the difference in densities is achieved by pairing gypsum in sample 5 with hardwood (high density material) and in sample 6 with softwood (low density material). Samples number 8 and 9 do not differ much in density, but the thicker layer of insulation in 8 has produced a higher thermal conductivity and a higher dielectric constant. Samples 8 and 10 have the same volume, but a part of the insulation is replaced by an air gap. Doing so has not caused much change in either dielectric or thermal conductivity measurements, but the density is affected.

Solid wood, plywood and OSB: These materials demonstrate a linear increase in thermal conductivity with an increase in density, given that moisture and temperature are constant [13,14,52]. Similar to thermal conductivity, the relative dielectric constant also increases linearly given that the frequency, moisture and temperature are constant [68,119]. The dissipation factor for these materials is mostly influenced by density and moisture content [15,68,100]. The presence of insulation material has reduced the over-all moisture levels in the composite materials made with solid wood, plywood and OSB. With the effect of moisture content greatly reduced from these materials, we therefore see a strong correlation of these materials' density with their dissipation factors. See Figure 60.

Insulation materials: The relationship of thermal conductivity with density is more complex for insulation materials. For most insulation materials, thermal conductivity first increases and then decreases with increased density [120][121]. In the described experiments only extruded polystyrene insulation (XPS) was used. According to literature thermal conductivity of XPS insulation is not affected by density in the range of 35 to 65 kg/m^3 [122] and can remain constant. The insulation materials used in this study have thermal conductivity and relative dielectric constant (information as provided by manufacturer) that are not appreciably higher than those for air. Their dissipation factor is very low because of the low density and absence of moisture.

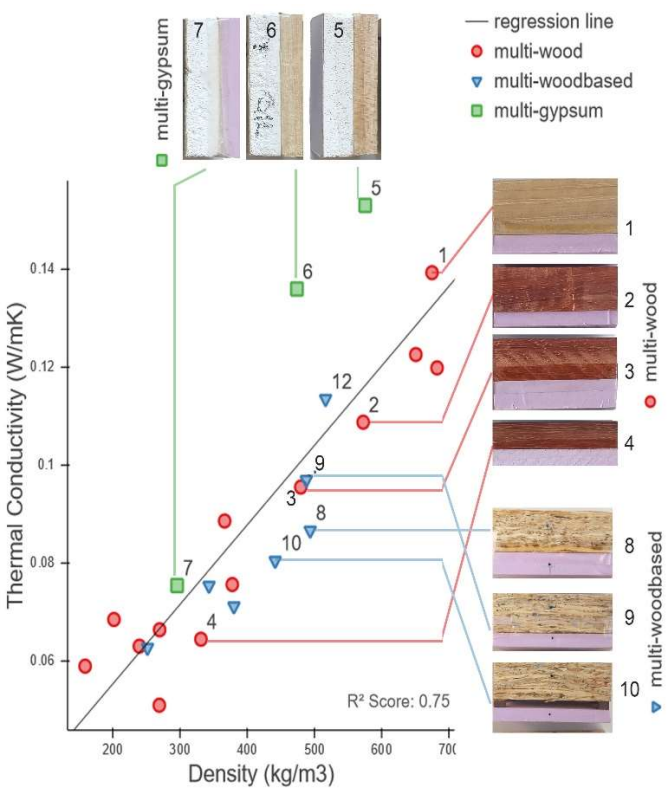

Figure 59. Scatter plot for density and thermal conductivity. Variation in insulation thickness affects both density and thermal conductivity.

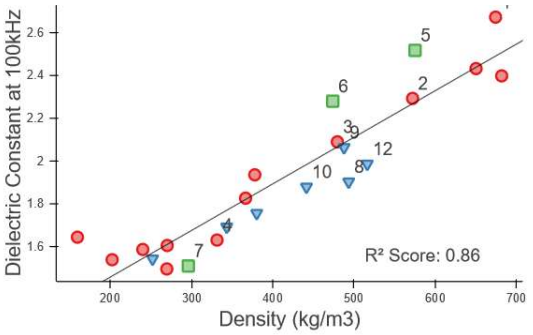

Figure 58. Scatter plot between density and relative dielectric constant.

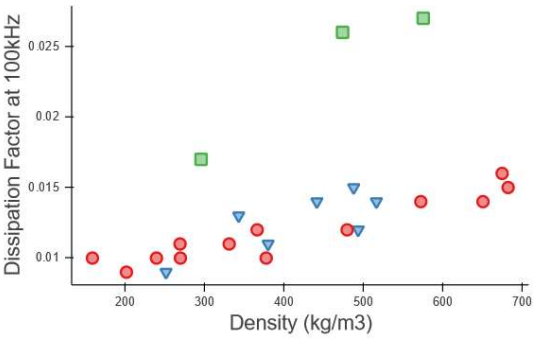

Figure 60. Scatter plot between density and dissipation factor

Gypsum Drywall: 21% of gypsum rock is made up of water molecules [123]. This accounts for its high dissipation factor as seen in Figure 60. The added moisture content raises its thermal conductivity as well as its relative dielectric constant. Samples made with gypsum are titled 5-7 in these figures. The thermal conductivity for the gypsum material is higher by 36% of the values from the regression line, whereas the dielectric constant is higher by about 10% from the regression line.

9.5.2 Correlation of Thermal Conductivity and Dielectric Constant

The strong correlation of relative dielectric constant with thermal conductivity for the tested multilayered materials is seen in Figure 62. It is shown that the dielectric constant is a stronger predictor for thermal conductivity than the more commonly used metric of density. It is seen that contact resistance does not change the linear, positive correlation between thermal conductivity and relative dielectric constant.

The found regression line seems to pass through the datapoint which represents the theoretical values of air. Datapoints 5 and 6 are made of a layer of drywall and a layer of wood and these samples fall distinctly above the regression line. Since the gypsum drywall layer accounts for more than 50% of the total thickness of these two samples, its properties have a stronger influence on the properties of the composite material.

The results of this study were compared with the results of a study on single layers by Saeed et al [83] consisting of solid wood, plywood, chipboards etc. The single layered materials are shown in grey, and ones from this study are shown in color in Figure 61. The regression line of both studies seems to be in general agreement, indicating that contact resistance did not alter the correlation of the materials.

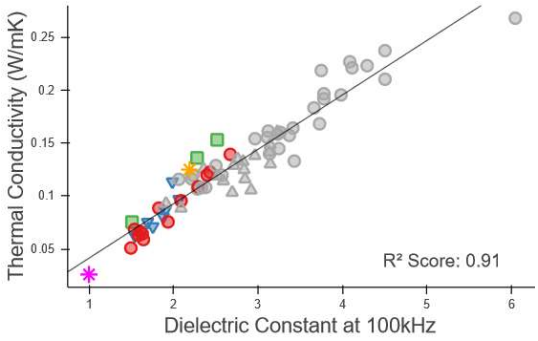

Figure 61. Multi-layered materials (red, blue, green) and single layered (grey) from Saeed et al [83] for solid wood and wood-based materials.

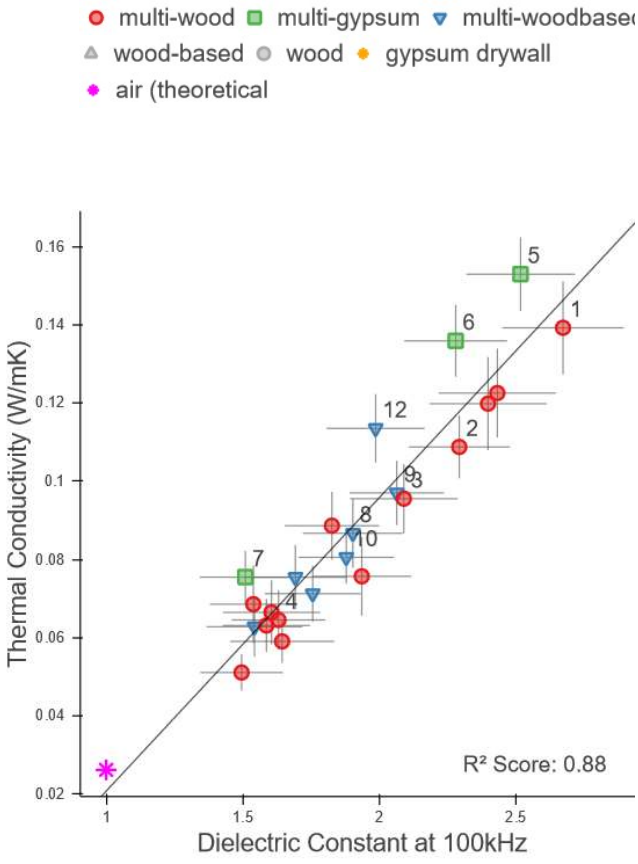

Figure 62. Thermal conductivity shows a strong correlation with relative dielectric constant at given frequency. Horizontal and vertical error bars indicate the uncertainty associated with each measurement.

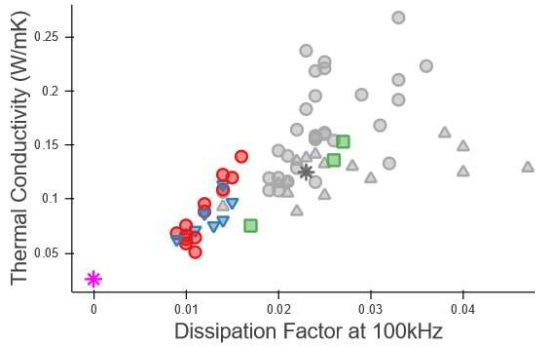

Figure 63. Scatter plot of dissipation factor and thermal conductivity for multilayered materials (shown in red, blue and green) and for solid wood and wood-derivatives (shown in grey) as found by Saeed et al [83].

While the dissipation factor does not have a strong correlation with thermal conductivity, it is seen to be strongly affected by moisture content and density. Both density and moisture content affect thermal conductivity directly. The scatter plot of the dissipation factor and thermal conductivity is shown in Figure 63. The coefficient of determination between dissipation factor and thermal conductivity for the multilayered materials of this study was found to be 0.64. This figure makes a comparison with data for solid wood taken from a previous study by Saeed et al [83]. The datapoint representative of theoretical value for air has also been marked on the plot for reference. It is clear from Figure 63 that multilayered materials of this study (shown in red and blue) have a lower dissipation factor as compared to solid wood. By coupling wood and insulation, the moisture content percent of the resulting

material was reduced and consequently the dissipation factor as well. The reverse can be observed for the multilayered materials made with gypsum drywall samples (datapoints 5-7).

9.5.3 Multivariate Linear Regression

Multivariate linear regression analysis was performed using the relative dielectric constant and dissipation factor at 100 kHz. The regression algorithm draws into the strong correlation of relative dielectric constant with thermal conductivity, as well as the sensitivity of the dissipation factor to moisture content and density. Thermal conductivity prediction as a function of these two variables compared to experimentally measured values can be seen in Figure 64. The found regression equation is:

$$\hat{y} = 2.0563\,(\epsilon_r) + 75.6334(Df) - 4.9842$$

Where $\hat{y}$ is the predicted thermal conductivity, Df is the dissipation factor. Both dielectric constant and dissipation factor were recorded at 100 kHz.

It is demonstrated through Figure 64 that thermal conductivity can be predicted using dielectric properties accurately. A high R^2 score of 0.95 is obtained for the tested materials using this regression equation. All the predicted values lie within ±20% of the experimentally found values, and about 80% lie within ±10% of the true values. The addition of more data would serve to refine the equation and improve results further.

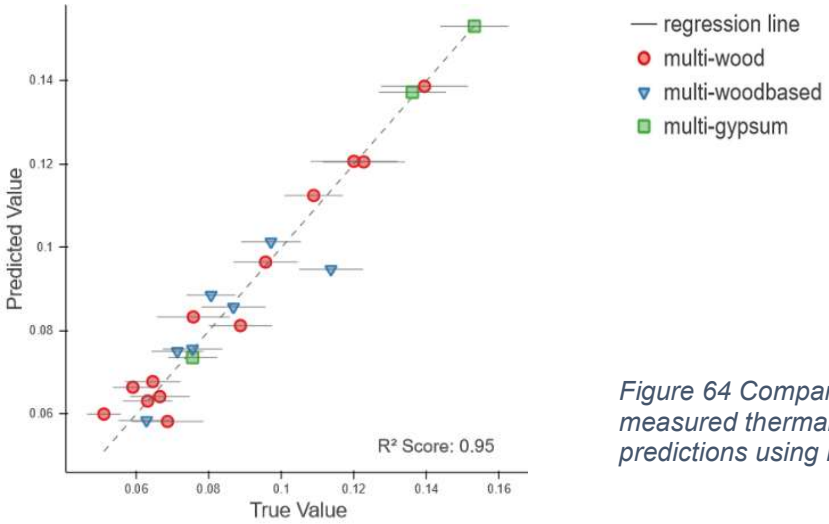

Figure 64 Comparison of experimentally measured thermal conductivity with predictions using multivariate linear regression

9.6 Conclusion

Given enough quality data, thermal conductivity of a building walls can be predicted using dielectric properties in a quick and efficient manner. Using this method would eliminate the dependency on environmental conditions required for steady state conditions. It would also eliminate the lengthy measurement periods that can stretch into days or even a month using conventional techniques. Additionally, the theory of the dielectric measurement of a building walls as a multilayered system has already been well studied. Advanced technology for

measuring dielectric properties is available for multi-leaf walls, cavity walls as well as for non-homogenous materials like concrete walls with rebar. Moreover, these measurements are non-destructive, requiring no advanced preparation of surfaces. This technology can thus be utilized to predict thermal conductivity of walls non-invasively.

Although using dielectric properties to make predictions of thermal conductivity for cavity walls cannot account for thermal transmission properties resulting from convective heat flow, this disadvantage can be offset by accompanying it with CFD analysis. The thickness of each leaf of the wall and the cavity can be measured using the same instruments that measure dielectric properties of the building walls.

Before the proposed technique is ready for real life application, more data related to various construction materials and construction techniques needs to be collected. It needs to be collected not only for the materials used in construction, but also with in the ratio of thickness which each material represents inside a building wall. The quality of the prediction of thermal conductivity depends on the quality and quantity of the collected data.

10 Moisture Study: Wood and Wood-Based Materials

While previous chapters describe experiments in the context of density, this chapter describes experiments related to moisture content and its effect on both dielectric properties and thermal conductivity. Two sets of experimental studies were performed. In the first study, six solid wood samples were studied at very small intervals of changing moisture levels. This generated about 180 datapoints of high-resolution data, which was used as the training set for a machine learning model. In the second study, fifteen additional materials were studied, at select moisture levels. This generated 45 more data points, which were used as the test set for the machine learning model.

Through the first set of experiments, it is demonstrated how dielectric properties respond to a change in moisture content, given that the density is constant. It is meant as a very fine-grained study of the behavior of materials as a function of moisture levels. Solid wood at moisture contents from 0 to 20%, at 0.5% to 1% intervals was recorded, and the corresponding change in dielectric properties was documented. 30 datapoints were collected for each of the six sample's dielectric properties, totaling 180 datapoints in all. On the other hand, thermal conductivity was measured for only three datapoints for each piece of wood, and the rest of the values for thermal conductivity were interpolated.

While the first set of experiments was meant as a set of data to learn from, the second set of experiments was meant to generate data for testing. This set was used to test how accurately the machine learning algorithms can predict thermal conductivity. This set of experiments were performed on 10 solid wood, 2 plywood, 2 OSB and 1 MDF pieces. The dielectric properties and thermal conductivity of these pieces were recorded at 0%, 10% and 20%.

10.1 Experiments to Generate Training Data: Materials and Methods

Six pieces of solid wood were used for this study. The wood species used were Basswood, Cherry, Fir/Pine, Wenge, Purple Heart and Red Oak. The density range for these wood pieces was between 460 kg/m^3 and 860 kg/m^3. Each piece of solid wood was cut into at least five pieces, and thus five sets of solid wood were produced; each set containing the six unique wood species. Each of these sets of wood was first oven-dried to find its oven-dry density, and then conditioned to a different moisture level. A description of how each set was conditioned and used for is given below.

- Sets # 1, 2 and 3 (each set containing six unique wood species) were reserved for measuring thermal conductivity. While set # 1 was left in its oven-dry state at 0% moisture level, set # 2, and set # 3 were conditioned to approximate 10% and 20% moisture levels respectively. This was achieved by placing them inside humidity tanks. The details of the humidity tank and related procedures are outlined in Section 5.4 of this dissertation, which deals with sample preparation.
- Sets # 4 and 5 were reserved for dielectric measurement. Set # 4 was left in its oven dry state. These wood pieces were placed inside vacuum bags to preserve their oven dry state until a suitable time to conduct the tests. Set # 5 was conditioned to >20% by placing them inside a humidity tank.

Subsequently, wood of sets # 4 and 5 were removed from their controlled environment and placed in normal indoor conditions. While the weight of wood from set # 4 began to increase as the pieces absorbed moisture from the environment, the pieces of set # 5 began to decrease in weight as they lost moisture to the environment. Both the sets eventually stabilized to approximately 3% – 5% moisture levels in the indoor environment. Minor fluctuations in weight continued with natural changes in humidity levels in the environment.

While the moisture levels of wood from sets # 4 and 5 changed, their dielectric properties were continuously monitored. Their parallel capacitance, dissipation factor and ESR were recorded using an LCR meter at approximately every 1/2% to 1% change in moisture content. The change in moisture content was measured by recording the change in the sample weight. By recording such measurements, a dense sent of datapoints points was built, between 0% and 20% for each wood species and patterns of change began to emerge.

While a fine-grained set of datapoints related to dielectric properties was meticulously tabulated, thermal conductivity of solid wood belonging to Set # 1, 2, and 3 was only measured at 0%, 10% and 20% respectively. The rest of the datapoints for thermal conductivity were interpolated and joined to the dataset for dielectric properties using moisture content as the point of intersection. The increase in thermal conductivity was assumed to be linear based on extensive literature. Some equations related to this are given in Section 7.3.1. A dataset containing over 180 data points was thus constructed.

The process to determine moisture level in any sample began with oven-drying it. Once each sample was oven-dried and devoid of all moisture, its weight was recorded. Subsequently when placed inside a moist environment, its weight increased with time. The difference between the current weight and weight in its oven dried state yielded the amount of moisture in the sample. This difference divided by its oven-dried weight is the sample's moisture content as a percent.

10.1.1 Results: Correlation of Moisture Content with Electrical Properties

Correlation of electrical properties of the studied wood is shown in Figure 65. Very distinct patterns of change in the electrical properties can be seen with a change in moisture content.

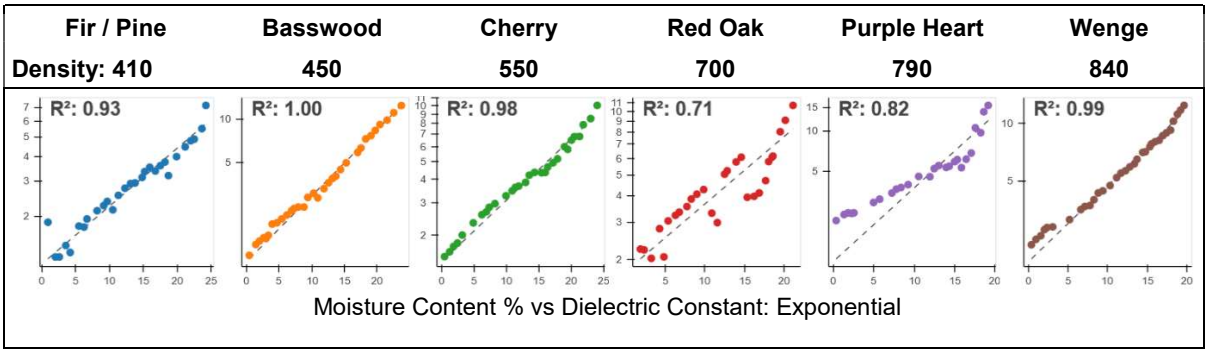

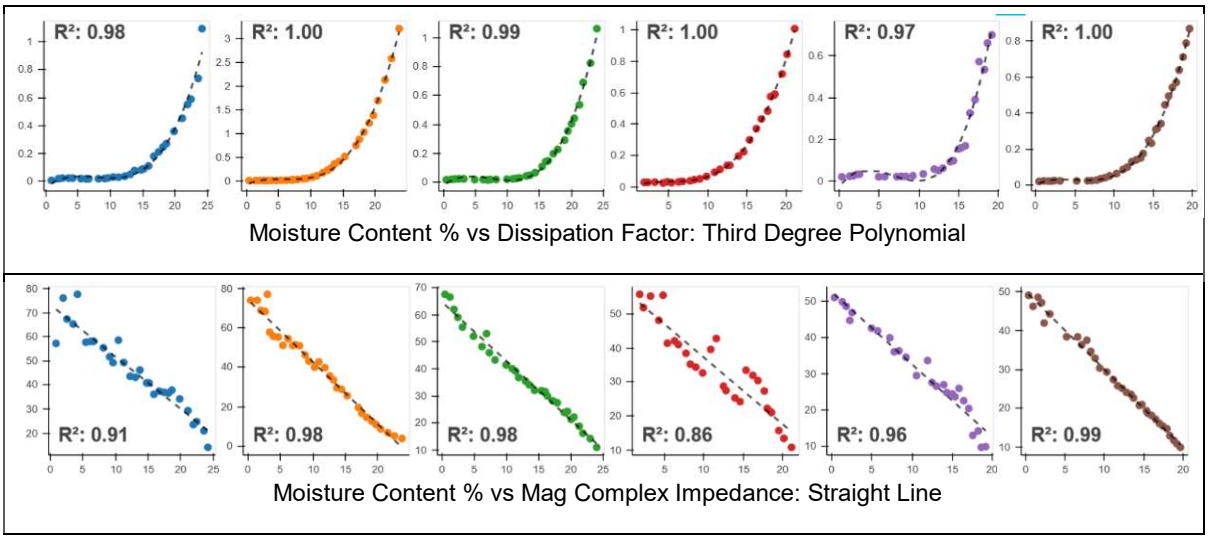

Figure 65 Scatter plots showing change in electrical properties with a change in moisture content. Moisture content is shown on the x-axis as percent, and corresponding dielectric constant (top), dissipation factor (middle) and magnitude of complex impedance (bottom) are shown on the y-axis.

Dielectric Constant: The dielectric constant is seen to rise exponentially with an increase in moisture content for all the samples studied. The shown curve's y-axis is in log scale, and the obtained curve looks a straight line. An increase in dielectric constant by up to 700% is observed when moisture content is increased from 0 to 20%

Dissipation Factor: The change of dissipation factor with changing moisture level is described as a third-degree polynomial. Although resembling an exponential curve, it has a better fit using a polynomial. The highest increase in dissipation factor was observed in the Basswood, where an increase of 7300% was recorded with a 20% increase in moisture levels.

Complex Impedance: Impedance changes linearly with a change in moisture content. Up to an 86% decrease in the magnitude of the complex impedance was observed with an increase in moisture levels from 0% to 20%

The Basswood and Red Oak represent some differences in the quality of data that was collected. For Basswood, a very smooth curve, without much noise can be observed. It is a low-density softwood, with very less variation in its grain. On the other hand, the Red Oak shows a lot of noise, with two distinct trends. Two independent streams of data can be seen. The discrepancy in the curves can be explainable by a loose wire connection at the point of attachment. At higher moisture levels, it was seen that the epoxy used to attach the wires to the samples did not hold well. Wires fell out easily at 25% or higher moisture levels.

10.1.2 Correlation of Thermal Conductivity with Electrical Properties

Thermal conductivity is shown as a function of electrical properties in Figure 66. The nature of the material properties interrelationships is highlighted in this figure. A clear understanding of these patterns can lead to precise predictions for untested materials.

Dielectric Constant: The natural log of the dielectric constant is plotted against thermal conductivity in the figure. The straight line indicates that the rate of growth of the dielectric constant with increased thermal conductivity is exponential.

Dissipation Factor: The log of the dissipation factor plotted against thermal conductivity is seen in the graph. A third-degree polynomial can be observed here.

Complex Impedance: Impedance is seen to decrease linearly with an increase in thermal conductivity.

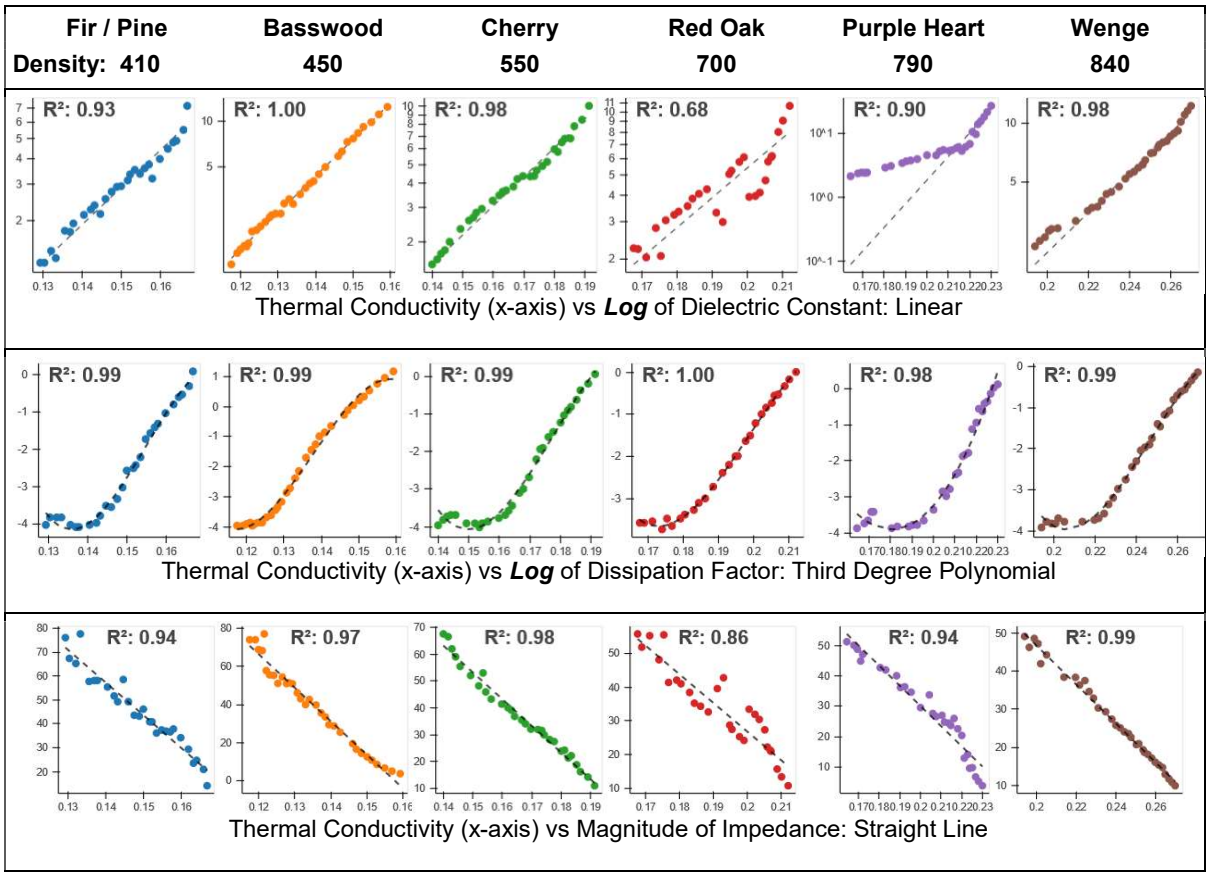

Figure 66 Change in thermal conductivity as a function of change in relative dielectric constant

The summary of the above figure can be seen in Figure 67 and Figure 68. The comparison of all six woods is shown here, along with their average oven dry densities. The dashed line in Figure 67 shows how the dielectric constant at oven-dry moisture level increases with increased density. Comparing Figure 67 and Figure 68 one can see how an increased dielectric constant is also accompanied by an increased dissipation factor and thermal conductivity. However, the only anomalous reading is that of the Basswood. Although having a lower thermal conductivity than the Fir/Pine, it has a higher density in comparison. For the same moisture levels, it has higher dissipation factor and dielectric constant than the other woods.

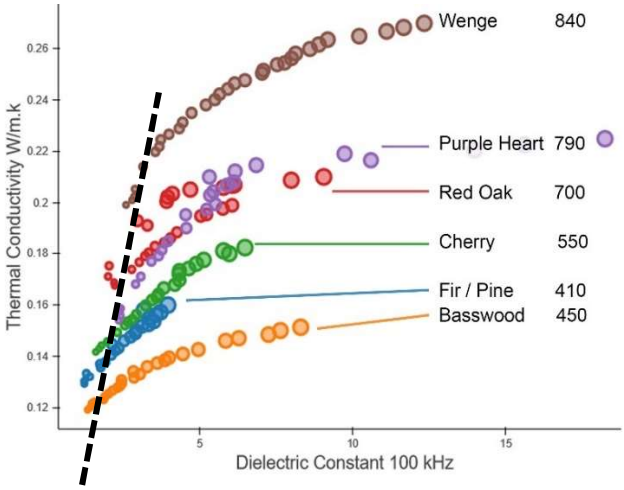

Figure 67 Thermal conductivity as a function of dielectric constant for all the woods measured for study 1. Size indicates moisture levels

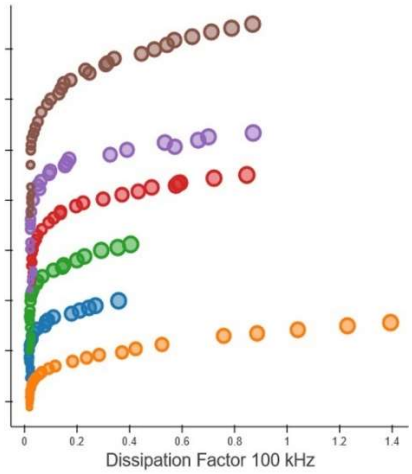

Figure 68 Thermal conductivity as a function of dissipation factor for all the woods measured for study 1. Size indicates moisture levels

10.2 Experiments to Generate Test Data: Materials and Methods

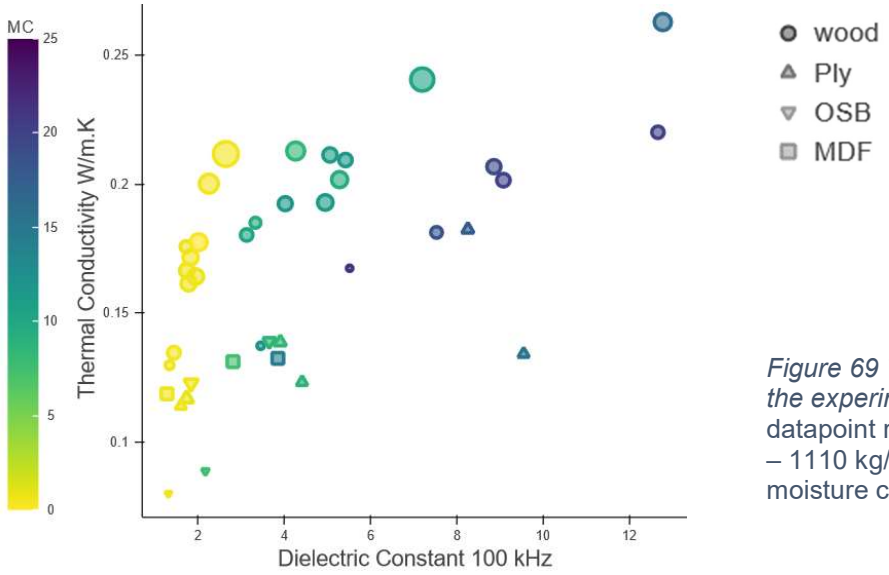

Figure 69 Test data collected for the experiments. Size of datapoint represents density (450 – 1110 kg/m^3). Color represents moisture content % (MC)

As seen in Figure 69, the test set represented a large range of oven dry densities, and moisture levels. The test set consisted of ten wood, two OSB, 2 plywood and 1 MDF samples, totalling15 materials in all. Their density ranged between 450 to 1110 kg/m^3. Each material was experimentally measured to find its thermal conductivity and dielectric properties at approximately 0%, 10% and 20%.

Much like the previous described study, different samples cut off from the same block of material were used to measure thermal conductivity and dielectric properties at different

moisture levels. Six samples were cut off from a single block of material. Three of these were reserved for the thermal conductivity measurement at 0%, 10%, and 20%, and three were kept for the dielectric measurement at matching moisture levels.

10.3 Results: Predictions of Test Set Using Generated Training Data

Once data collection was complete, some data cleaning was performed, and predictions were made. As seen in Figure 65 and Figure 66, the datapoints for the red oak do not display a regular pattern. The wire may have been loose and may not have transmitted the full signal each time. The readings from this set were discarded from the training set. Some readings from the test set also had to be discarded because of deterioration caused by excess moisture.

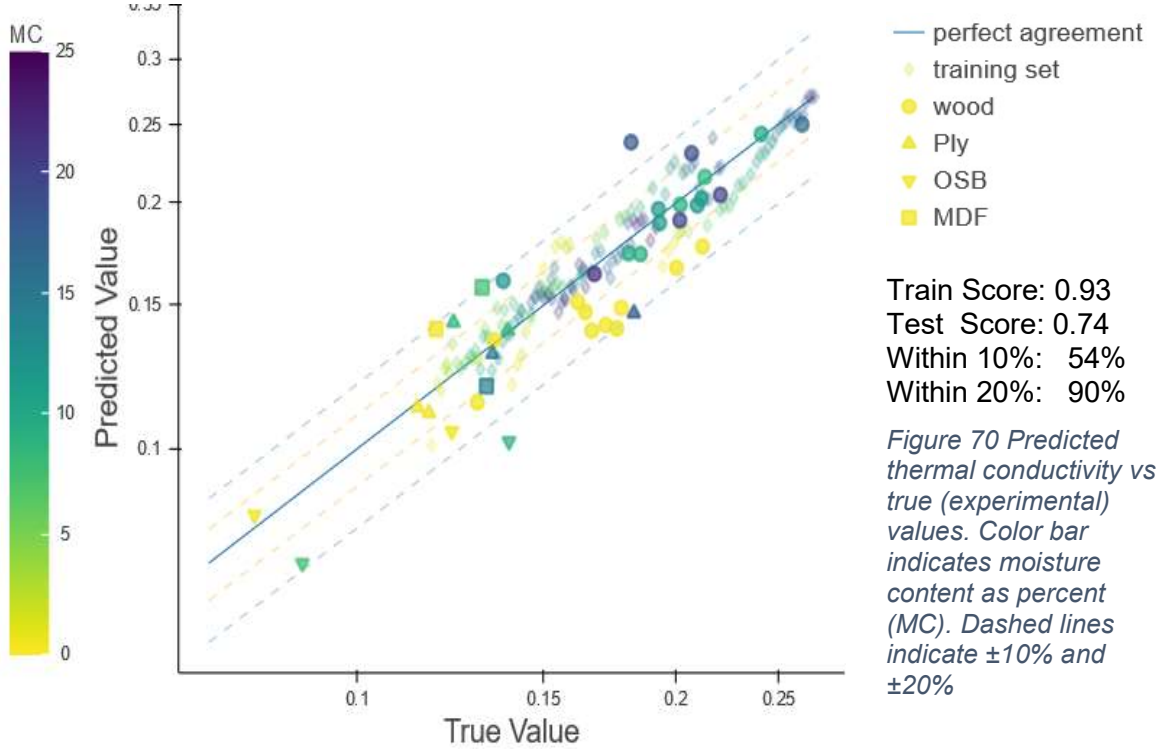

Figure 70 Predicted thermal conductivity vs true (experimental) values. Color bar indicates moisture content as percent (MC). Dashed lines indicate ±10% and ±20%

The results for machine learning to predict thermal conductivity are shown in Figure 70. It is clear from this graph that wood and wood-based material's thermal conductivity can be predicted using electrical properties even if varying levels of moisture is present within the materials. By using the first set of experimental results as a training set, a set of predictions were generated for predicting the thermal conductivity of the second set of collected data. An R^2 score of 0.74 was obtained between predicted values and experimentally measured values. About half of the predicted values fall within ±10% of the regression line (shown as yellow dashed line) and about 90% fall within ±20% (shown as blue dashed line). Material properties that were used in the feature space are the dielectric constant, dissipation factor, impedance and reactance at 100 kHz and dielectric constant and dissipation factor at 10 kHz.

The algorithm used for the prediction was Kernel Ridge Regression, using a third-degree polynomial. The first difference between this algorithm and ordinary least squares regression in how it penalizes the size of the coefficient, as well as minimizes the residual. By adding a penalty to the size of the coefficients, it introduces a bias such that some features get more importance than the others. The second difference is the use of a kernel. It projects the feature space based on the defined kernel before performing the regression. In this case, a third-degree polynomial kernel was used.

10.4 Dielectric Properties of Water: Feasibility of Measuring at Higher Frequencies.

The frequency and temperature dependent behavior of water is shown in Figure 71 and Figure 72 as shown by Rusiniak [124] and Andryieuski et al [125] et al.

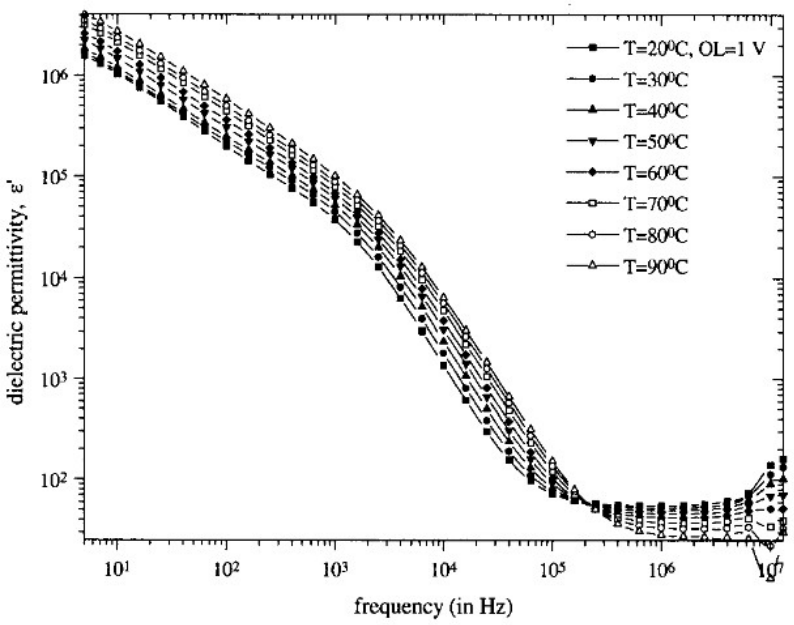

Figure 71 Change in dielectric constant of water with increased frequency below 10 megahertz as shown by Rusiniak [124]

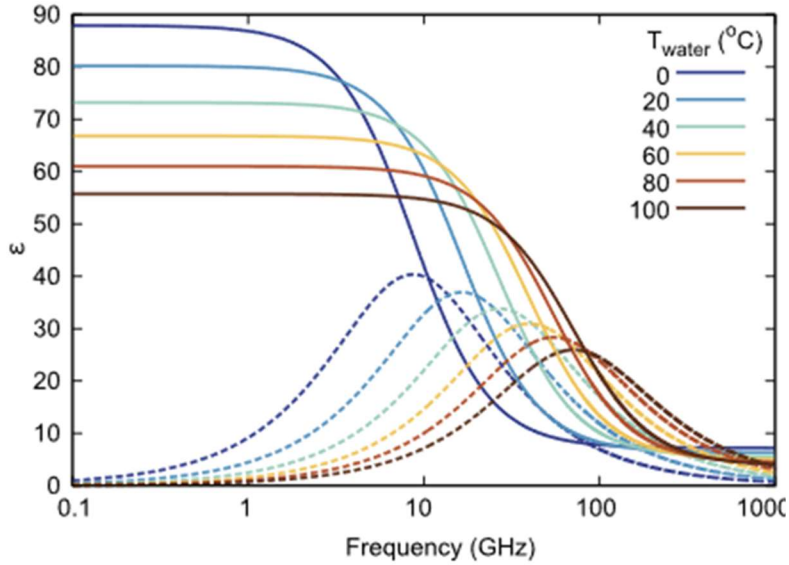

Figure 72 Change in dielectric constant of water at room temperature with increased frequency in gigahertz range as shown by Andryieuski et al [125]

The figures show that the dielectric constant of water decreases with increased frequency, but the behavior is more complex when temperature is varied. Increased temperature may result increase or decrease the dielectric constant of water depending on the frequency range. A sharp decrease in the dielectric constant is seen up to frequency of about 100 kHz at room temperature, but changes slowly between 100 kHz and 10 MHz. It is considered to be approximately 78 in this frequency range [126]. It is seen to decrease considerably in the frequency range of 10 GHz and 100 GHz.

The decreased value of the dielectric constant of water at frequencies in the gigahertz range indicates that the overall effect of moisture on the dielectric properties of materials would decrease with increased frequency. Since the presence of moisture elevates the dielectric properties of water significantly in the lower frequencies, it might be more feasible to measure at higher frequencies.

10.5 Challenges and Sources of Errors

Several challenges were faced while creating the test set. As soon as the samples were removed from the oven, they began to absorb moisture from the environment. This could be observed from their increasing weight. Consequently, these samples had to be placed inside vacuum bags to maintain their oven-dry state until ready for measurement. Similarly, samples with high moisture levels started to lose their moisture as soon as they were removed from humidity tanks. Since the process of measuring thermal conductivity takes more than two hours, the sample weight was recorded before and after the measurement. The recorded weight and moisture level at the end of the measurement was kept and shown as the moisture level of the sample.

Some ways the moisture content adversely affected the material samples is shown in Figure 73. The first image (Picture A) shows the formation of cracks in the MDF sample. Permanent damage to the structure of the material was seen due to the presence of moisture inside the material.

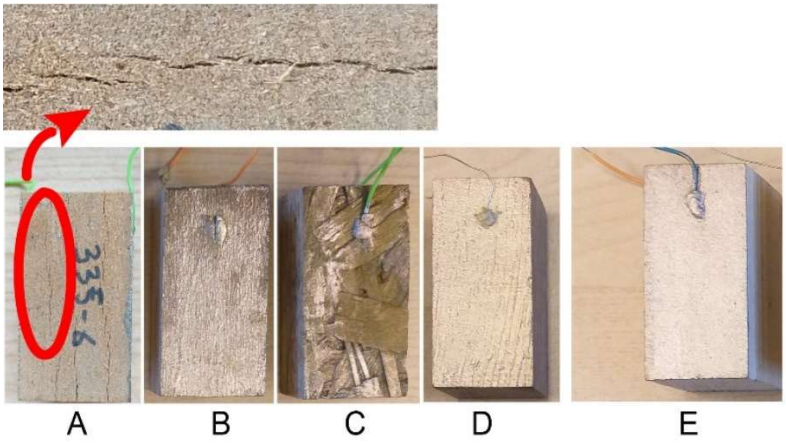

Figure 73 Adverse effects of the moisture content on the samples.

Sample A: Deterioration of material. B: Wires falling off. C: Severe discoloration. D: Slight discoloration and different wires. E: What the sample should look like.

The second picture in the same figure shows how the epoxy was rendered ineffective at fixing the wire to the sample. The wires of several samples kept falling off, and had to be reattached. Picture C shows the effect of moisture on the copper conductive coating meant to act as an electrode for the dielectric measurements. Samples with moisture levels higher

than 20-25% could not be tested, because the electrodes deteriorated, and the wires fell out. A batch of 15 samples had to be thrown out of the sample set because of this issue.

Picture labelled D represents the typical oven-dried sample. The predicament for the measurement of the sample in its oven-dry state was that painting on the electrode would introduce moisture into the sample because the paint is water-based. Moreover, the sample would absorb more moisture from the environment when placed outside, (instead of vacuum bags) as the paint required some time to dry. For this reason, some samples were oven-dried with the wire and electrode in place. This way, the weight of the wire and paint could be differentiated from the weight of the moisture. However, this resulted in a discoloration of the paint. Compared to Picture E, which represents a normal electrode, Picture D shows a lot of color difference. This indicated that the electrode may have reacted with the water as it evaporated from the sample. The quality of the electrode is thus compromised, and its resistance may increase, affecting the capacitance readings. Moreover, the jacket of the wire had to be removed before placing it in the oven, so it wouldn't melt. This wire has a different capacitance than other wires, and it introduced a bias into the readings.

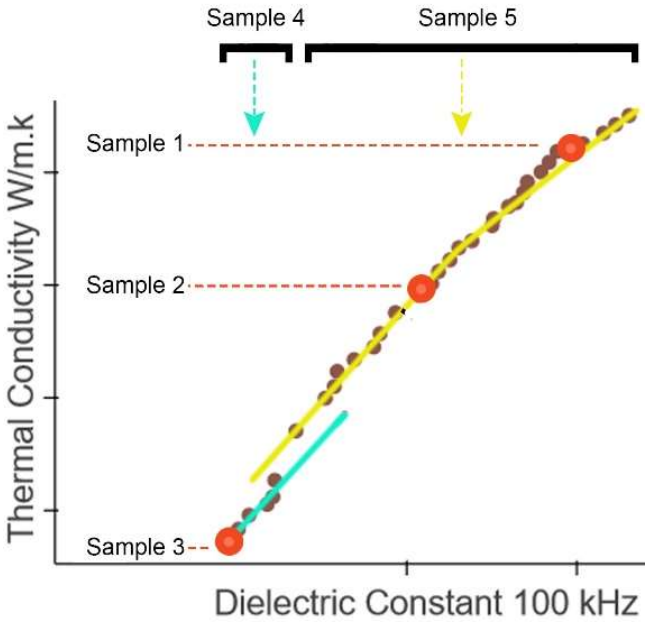

Figure 74 Use of two different blocks to collect data for dielectric properties and thermal conductivity resulted in some errors in the dataset.

In this study, a single block of wood was cut up into at least five or six pieces, and each piece was used to measure the thermal conductivity or dielectric properties at various moisture levels. It was assumed that since each block came from the same bigger block, then their densities and hence properties would be similar. However, that is not the case. Each sample cut off from the bigger block varied in density because of the natural grain of the wood. The maximums standard deviation of the densities of individual blocks cut from the same bigger block was 60 kg/m^3.

As seen in Figure 74, the use of different pieces of wood introduced errors into the results. The two samples used to collect data related to dielectric properties had a minor difference in density, and so two regression lines can be seen (labelled sample 4 & 5). Moreover, three separate samples were used to collect data related to thermal conductivity (labelled sample

1, 2, 3). These differences had to be ironed out manually in the interpolation process. In conclusion, the result would have been more accurate if a single piece of wood had been conditioned to different moisture levels and measured for various material properties, instead of using several blocks.

10.6 Conclusions

Presence of moisture inside materials complicates thermal conductivity prediction. However, using machine learning algorithms, and including impedance in the feature space enables the prediction of thermal conductivity for wood and wood-based materials effectively.

Although it felt intuitive to have separate humidity tanks, each conditioning wood at different moisture levels simultaneously, in the end it caused errors instead of saving time. Conditioning wood cut from the same block to different moisture levels saved time because it enabled the preparation of several samples simultaneously. However, because wood is an anisotropic material, each block had a slightly different density. This introduced bias into the test as well as training data.

11 Ceramics: Single and Multiple Layers

Materials representative of brick construction and belonging to the ceramic family are discussed in this chapter. Brick-construction is prevalent in a large part of the world with an annual production of approximately 1,391 billion units of bricks [21]. Clay bricks, poured concrete, gypsum drywall and naturally occurring stone samples were included in this study.

11.1 Materials

Thirty-three material samples were included in this study. These consisted of five categories i.e. stone, clay bricks, concrete, gypsum drywall and multilayered materials. The four stone samples acquired for the study are granite, sandstone, marble and Taxila stone as shown in Figure 75. Seven concrete samples were poured into molds with different ratios of cement, sand and aggregate (see Figure 76). Some represented mortar mixes, some were made from high strength concrete mix, while others were poured using cement sand and aggregate procured from the market. Six clay bricks baked in kilns from Lahore, Pakistan were acquired as shown in Figure 77. Three of these represented the A, B and C class brick construction. Roof tile, over burnt brick and handmade yellow brick from soft clay were also included. Three samples of gypsum drywall were also studied. Furthermore, fourteen samples were constructed by layering together brick or concrete samples with foam as seen in Figure 78. These represented the category of multilayered materials.

Figure 75 Stones: granite, sandstone, marble and taxila stone (from left to right).

Figure 76 Poured concrete samples

Figure 77 Clay brick samples

Figure 78 Fourteen multi-layered ceramics samples included in the study: brick+foam, concrete+foam, brick+concrete

11.2 Methods

Sample preparation is discussed in detail in Chapter 5. The experimental apparatus and method for measuring thermal conductivity are described in Section 6.1.2 of this dissertation detailing Method B. Dielectric properties were measured using the method described in Section 6.2. Pouring of concrete and related details are described in Section 5.5.

11.3 Additional Uncertainty

Fabrication errors caused uncertainty in measurements in additional to the factors described in Section 6.7 of this dissertation. While the wooden samples were fabricated with much precision, the same could not be done for the ceramic's samples. The ceramic fabrication requires shaping and cutting tools which are different from wood fabrication. While the tools for wood are widely available at wood shops across Carnegie Mellon, the same is not true for ceramic materials. Cutting, grinding and smoothing of these samples presented a huge challenge. Hand tools like angular grinder and rotary tools were utilized for this purpose. Examples of fabrication errors are shown in Figure 79.

Figure 79 Errors in fabrication: presence of voids, irregular geometry and larger cavities to house thermocouples.

The errors caused by fabrication of the ceramic family are:

- Uneven surface and edges resulted in some inconsistencies in the measurement of the size of the sample. Since the dielectric properties are calculated based on the size of the sample, this caused additional uncertainty.
- Ceramic is a hard material, difficult to drill into. The holes drilled into the ceramic samples to house the thermocouples had bigger diameters than the ones for the wood sample. Since there was a bigger void in which the thermocouple was placed, the distance between the two thermocouples could be measured with less certainty. The thermal conductivity measurement had additional uncertainty due to this imprecision.
- Each datapoint was created by two material samples. One to measure thermal conductivity and one to measure dielectric properties. It was assumed that both pieces are identical, so that the thermal conductivity of one corresponds to the other. However, this assumption is incorrect. Some concrete pieces have voids, which may be unevenly distributed. These voids would cause both material samples to have different properties, and so an error was introduced into the system.

11.4 Results: Bricks, Concrete, Gypsum and Multilayered Materials

The density of the samples was found to be between 470 and 2100 kg/m^3 for the single layered ceramic materials, and 700 and 1900 kg/m^3 for the multi-layered ceramic materials. The thermal conductivity ranged from .075 to 2.16 W/m.K and the dielectric constant was measured to be between 1.4 and 14.1 at 100 kHz.

11.4.1 Correlation with Density

The correlation of density to thermal conductivity, dielectric constant and dissipation factor of ceramic materials was found to exponential. Whilst this relationship is best described as a

straight line for the wood and related products, for ceramic materials it is shown to be an exponential curve. Another distinguishing factor is that the correlation of density with thermal conductivity is seemingly stronger than that of density and dielectric constant.

11.4.1.1 Density – Thermal Conductivity

The R^2 score for density and thermal conductivity of the studied ceramic materials was found to be 0.92. This correlation can be seen in the scatter plot in Figure 80. It can be described by the equation:

$$\lambda = 0.0069435 \; exp(0.00262506\,\rho)$$

While the density to thermal conductivity relationship was seen to be a straight line for wood materials, it is seen as a curve for the ceramics. However, this may be due to a difference in the density range of the two studies. The range for the studied wooden materials was 700 kg/m^3, while it is 1600 kg/m^3 for the ceramics study. The curve may not have been evident in the study related to wood, because it represented a small portion of the curve that can be perceived as a straight line.

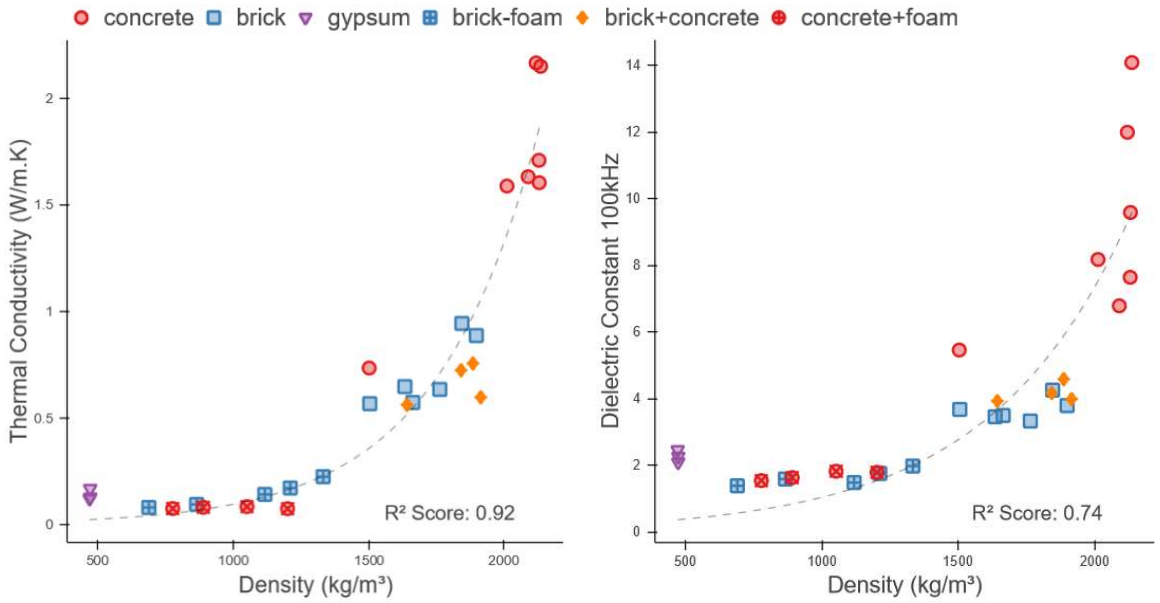

Figure 80 Scatter plot of density and dielectric constant at 100 kHz of the ceramics studied

Figure 81 Scatter plot of density and dielectric constant of the ceramics studied

Studies indicate that thermal conductivity of concrete is not as simple to predict from density, as it is for the wood and wood-based materials. In addition to density, the thermal conductivity of concrete depends on the mineralogical content of the aggregate, moisture content and conditions of compacting [127] etc. Several scientists [128–131] collected data related to concrete and showed an exponential relationship between density and thermal conductivity of concrete. These studies found the coefficient of determination for the data to be between 0.87 and 0.99. However, various studies present their own equations to predict thermal conductivity from density, which are vastly different from one another. The equations

are different based on whether the concrete is lightweight, admixtures used, moisture content and minerology. Two examples of such work are presented in Appendix E.

Much like concrete, bricks also present a scenario where thermal conductivity is not easy to predict based on density. While thermal conductivity is strongly influenced by its bulk density, it is also dependent on firing temperature [132], pore size and distribution [133] mineralogical composition and microstructure [134], and additives used in the clay mixture [135]. Dondi et al [136] collected data related to thermal conductivity and density of clay bricks from literature, and conducted measurements of his own. He obtained an R^2 score of 0.42 for the correlation between density and thermal conductivity in his study. Lassinantti [134] showed a score of 0.54 on his collected data. The graphs from these authors are presented in Appendix F.

11.4.1.2 Density – Dielectric Constant

The R^2 score for the density-dielectric constant for this study was found to be 0.74, which is lower than the score for density-thermal conductivity. This correlation can be seen in Figure 81. This correlation contrasts with the wood and wood-based materials study, where dielectric constant had a stronger correlation with density.

The dielectric properties of concrete is influenced by density, curing time, water / cement ratio, compressive strength and moisture content [137], much like thermal conductivity. It decreases with an increased curing time [138], and increases with an increased moisture content or water / cement ratio [139]. The dielectric constant of concrete is also known to decrease with increased frequency [140]. Dielectric properties of clay bricks have not been well studied. The few studies conducted on the subject matter indicate that the dielectric constant of clay bricks increases with increased moisture content and decreases with increased frequency [141,142]. It also increases with an increase in temperature at which the bricks are fired [143].

11.4.1.3 Density - Dissipation Factor

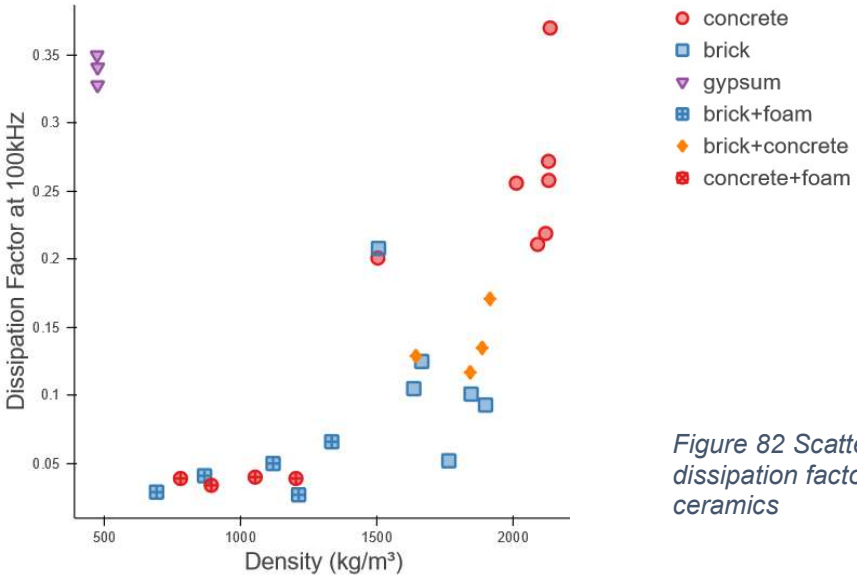

Figure 82 Scatter plot of density and dissipation factor at 100 kHz for the ceramics

The correlation of density with dissipation factor of ceramic materials can be seen in Figure 82. While most datapoints fall easily into the regression curve, a few exceptions are easily identifiable. The samples made of gypsum drywall material and plaster of paris show a high dissipation factor, which may be attributed to their high moisture content. The sample of mortar mix and handmade yellow brick also exhibit higher dissipation factor, distinguishing them from the rest of the samples. On the other hand, the multilayered samples with a layer of insulation material can be observed to have a very low dissipation factor. Since insulation material has no moisture content, the overall dissipation factor for these materials is lower.

11.4.2 Correlation of Thermal Conductivity with Dielectric Properties

Correlation of thermal conductivity of the studied samples, with their dielectric constant and dissipation factor is shown in Figure 83 and Figure 84 respectively. The R^2 score is 0.92 and 0.27 is obtained. Although the graph between thermal conductivity and dissipation factor does not show a strong correlation, material properties like moisture level and density are evident from the graph.

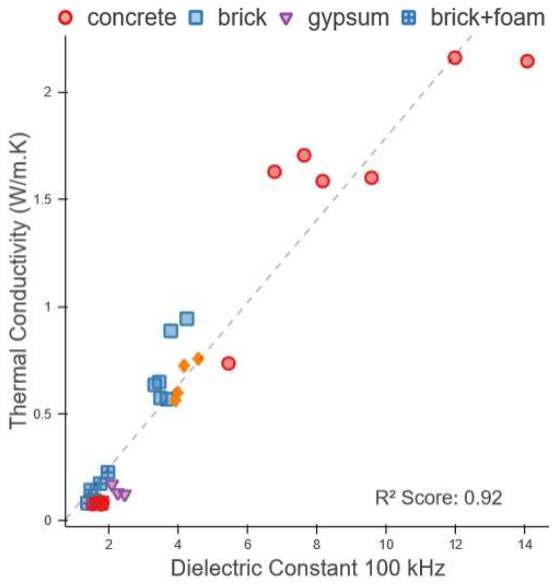

Figure 83 Correlation of thermal conductivity and dielectric constant at 100 kHz

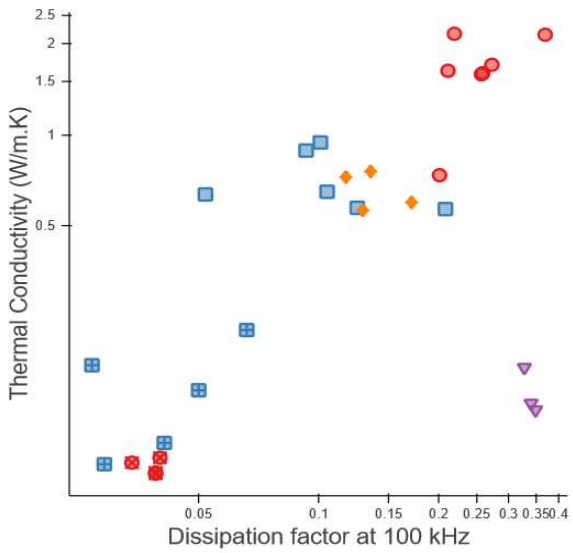

Figure 84 Correlation of thermal conductivity and dissipation factor at 100 kHz

Thermal conductivity was predicted using dielectric constant and dissipation factor at 100 kHz with a gradient boosting algorithm. These predictions are shown in Figure 85. The shown graph represents a leave one out validation, where the shown data points are the result of the held-out set. The predicted value of the held-out set is plotted against the true value found by experimentation. An R^2 score of 0.98 is achieved, where half of the samples fall within ±10% of the regression line, and 80% fall within the ±20% of the regression line. Fewer of the multi-layered materials are predictable because the uncertainty in measurement is higher in the lower range of thermal conductivity. Prediction quality may be improved with more data.

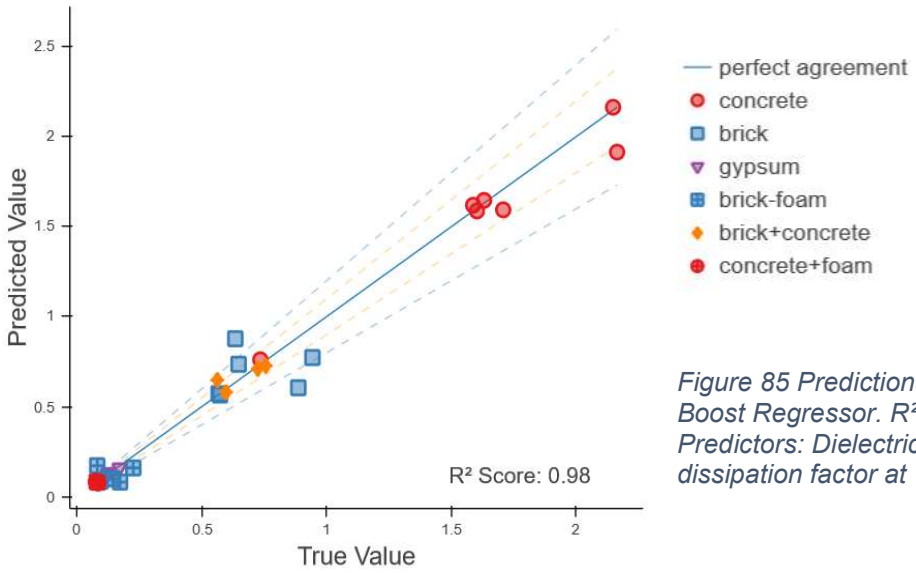

Figure 85 Predictions using Gradient Boost Regressor. R² Score: 0.98, Predictors: Dielectric constant and dissipation factor at 100 kHz

11.5 The Case of Naturally Occurring Stones

Four stones were considered for this study. These ae granite, sandstone, marble and Taxila stone as seen in Figure 75. Figure 86 shows their correlation between dielectric constant at 100 kHz and thermal conductivity. It also shows how the stone samples compare with the rest of the ceramic samples described in the previous section. While granite, marble and sandstone present minor anomalies, the Taxila stone's readings deviate from the pattern significantly. The stones have similar densities, but their dielectric constant seems anomalously higher or lower. However, looking at Figure 87, it can be observed that marble, granite and sandstone have a comparatively low dissipation factor accounting for the lower dielectric constant. The Taxila stone has a phenomenally higher dissipation factor, accounting for the significantly higher dielectric constant. The dissipation factor indicates the presence of moisture content or highly electrically polarizable minerals.

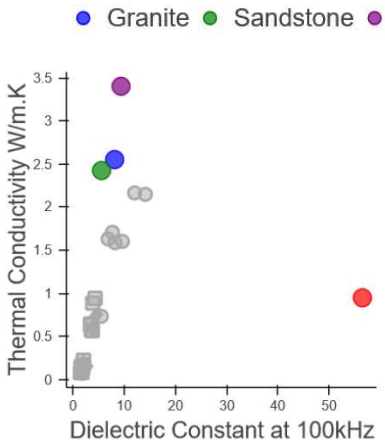

Figure 86 Stone correlation for dielectric constant vs thermal conductivity

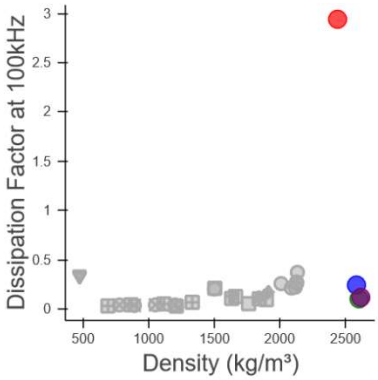

Figure 87 Stone correlation for density vs dissipation factor

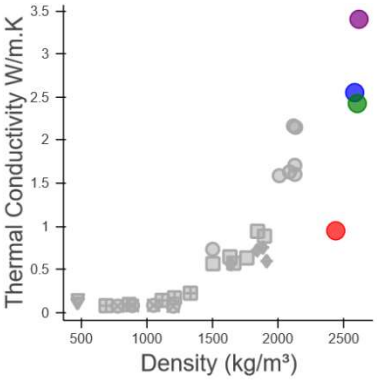

Figure 88 Stone correlation for density vs thermal conductivity

As shown in Figure 88, the Taxila stone has an anomalously low thermal conductivity given its density. This might be explainable by the anisotropy of the material. The stone is made up of several layers, some colored differently than others. See Figure 89 for a picture of the stone where its veins are visible. The measurements were taken in the transverse direction, perpendicular to the grain. If the thermal conductivity measurement was to be taken in the direction parallel to the grain, the reading is likely to be significantly higher.

Figure 89 The Taxila stone is anisotropic and has veins of variable thickness running through it

11.5.1 Frequency Sweeps with NanoVNA

A VNA (vector network analyzer) is an instrument which measures network parameters of an electrical network. It is used to measure the scatter parameter of electrical circuits at radio frequency range and higher. If the radio frequency circuit parameters are estimated correctly, then it can be used to estimate impedance, which is directly proportional to the scatter parameters [144]. A frequency sweep between 25 kHz and 30 Mhz using one port VNA reflection measurement is shown in Figure 90. This measurement was performed using a new model of VNA's on the market, called nanoVNA. While a VNA may cost thousands, up to a million dollars, this model offers promising results at a low budget. However, its accuracy has not been verified through scholarly endeavors yet.

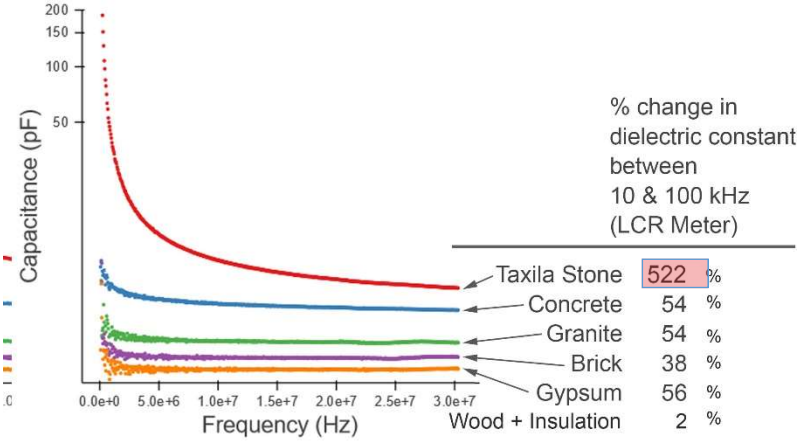

Figure 90 Frequency Sweeps with NanoVNA. Numbers to the right represent average % change in dielectric constant between 10 kHz and 100 kHz as measured by LCR meter

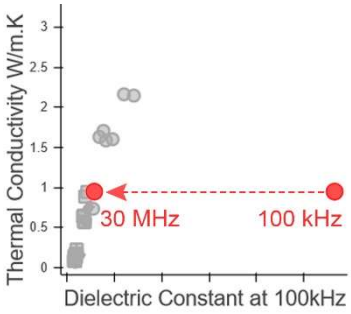

Figure 91 Effect of changing frequency on the correlation of thermal conductivity and dielectric constant

As illustrated in Figure 90, the Taxila stone registers a sharp drop in capacitance (and hence the dielectric constant) when measured in the Megahertz range. Based on the current pattern, its capacitance is likely to continue to decline at higher frequencies, before it stabilizes at around 1 GHz. All previous experimental measurements of this thesis were conducted at 10 and 100 kHz. The shown measurements of Figure 90 are higher, up to 20 Mhz. Other ceramic materials also register a drop in capacitance in this frequency range. However, it is a minor decline in comparison.

The notion that the dielectric constant drops drastically with increased frequency, is reinforced by the results of the LCR Meter. The LCR meter is accurate at 10 kHz and 100 kHz. The results of these readings are also given in Figure 90. These suggest that while other ceramics' dielectric constants register a drop of approximately 56% or lower, the measurement for the Taxila stone registers a huge 522% drop between 10 and 100 kHz. A study related to poplar wood also points out that material with a high moisture content is marked by a rapid decline in its dielectric constant with an increased frequency [145].

The rapidly changing capacitance of the Taxila stone suggests that its thermal conductivity may be accurately predicted at higher frequencies in the mid-Megahertz or the Gigahertz range. See Figure 91. At a higher frequency it will fall in line with the rest of the ceramics without breaking away from the pattern.

11.6 Conclusions

- Unlike wood, the thermal conductivity of clay bricks and concrete is not easily predictable using density and moisture content. Dielectric properties offer a superior solution to the problem.
- While most ceramics could be reliably predicted using the dielectric constant and dissipation factor at 100 kHz, the characterization of stones presented additional challenges. The suitability of higher frequencies to measure dielectric properties was identified. It was seen that the pattern is not clear at 100 kHz, but these irregularities iron out in the mid Megahertz range or higher.
- An interesting case of the Taxila stone was studied, which has a significantly low thermal conductivity given its density. However, it is concluded that this anomaly can be contributed to the anisotropy of the material. If measured parallel to the grain, a higher thermal conductivity is likely to be found.
- The anomalously higher dielectric constant and dissipation factor of the Taxila stone at 100 kHz may be attributed to mineral content which is highly electrically polarizable, or a high moisture level. The rapid decline in the dielectric constant in the Kilohertz range was observed, which could help characterize the stone's material properties.

12 Summary of Conclusions and Future Work

12.1 Consolidating all Experimental Studies: Can Concrete Learn from Wood?

This section demonstrates that even if the family of a construction material is unknown; it is still possible to predict its thermal conductivity based on its dielectric properties. This conclusion follows from the reasoning that if the same set of equations can predict all material types, then any sample's thermal conductivity can be predicted regardless of its density, moisture content and family. In previous chapters the results of various sets of experiments were illustrated, but each set of materials correlations were shown independent of other materials. This section uses the data collected from all experiments and focuses on an analysis which shows that even when the exact contents of a construction wall are unknown, its thermal conductivity can still be accurately predicted.

While the question of whether plastic can learn from wood was addressed in a previous chapter (Section 4.2), this Section asks the relevant question of whether concrete can learn from wood and vice versa using machine learning. It is demonstrated using the graph in Figure 92 that this is indeed possible. This graph shows the results of predicting thermal conductivity of materials belonging to the wood-frame construction as well as the ceramic based construction. The predictive model is trained on data from both the material types to get a result where the R2 score is 0.99. 64% of the predicted datapoints lie in the ±10% accuracy range, and 90% lie in the ±20% accuracy range.

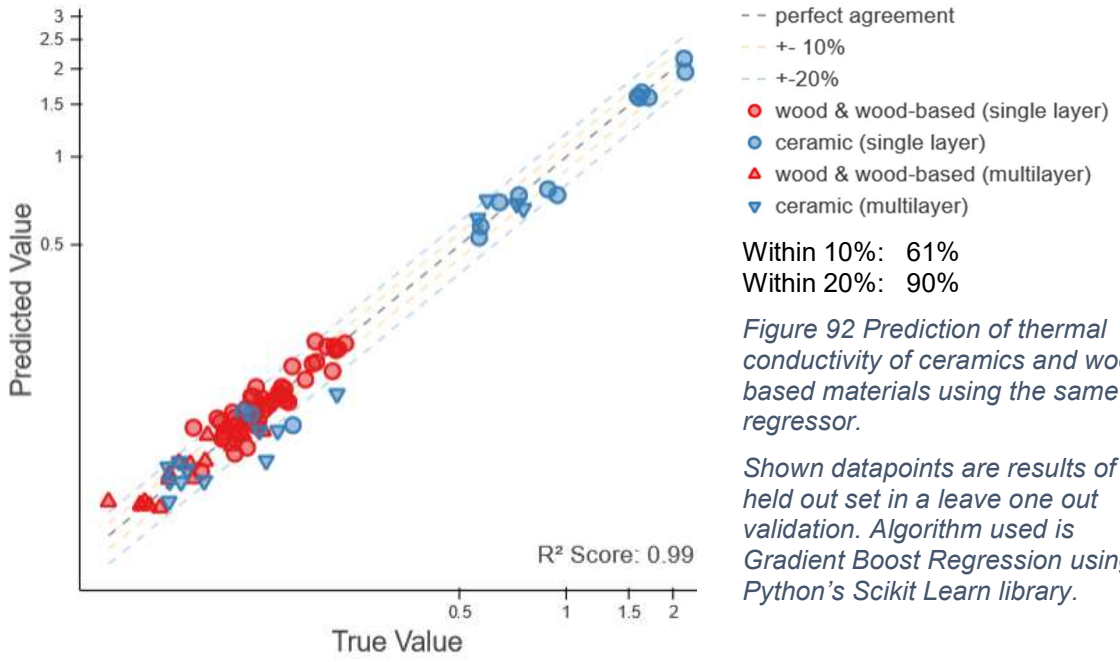

Figure 92 Prediction of thermal conductivity of ceramics and wood-based materials using the same regressor.

Shown datapoints are results of the held out set in a leave one out validation. Algorithm used is Gradient Boost Regression using Python's Scikit Learn library.

Figure 92 shows the results of leave one out validation where the predicted values of the held-out set are plotted against the true value found by experimentation. The feature space contains three material properties. These are the log of, each of, the dielectric constant, dissipation factor and magnitude of the complex impedance. The algorithm used is a boosting algorithm called gradient boosted decision tree. This specific algorithm was chosen

because it is the best performing algorithm as seen in the analysis performed on the dataset related to existing literature (see Chapter 4). The data collected from existing literature served as the validation set, where the hyperparameters were finetuned and a predictive model was built. In this way, a dataset distinct from experimental data was used to build, evaluate and fine tune the predictive model. This method enabled an unbiased estimate of the model's effectiveness, thereby avoiding the bias which would have resulted if the model had been built on the experimental data.

A study of the results shown in Figure 92 suggests that wood and concrete can be predicted using the same regression equations. The used data contains datapoints from the wood and wood-based single layer and multiple layers, as well as the results from the ceramic single and multiple layer experiments with a few exceptions. A few datapoints were excluded from this dataset and are expected. These are expected to map well at higher frequencies. The cleaned outliers are the materials like the four stones belonging to the ceramic family as mentioned in Section 11.5 etc. Further it does not include the materials from the wood moisture study. Datapoints related to the stone, ceramic and the wood at 10% moisture content have been plotted in Figure 93 and Figure 94. The materials from the wood multi-layer experiment have also been plotted here for the sake of comparison.

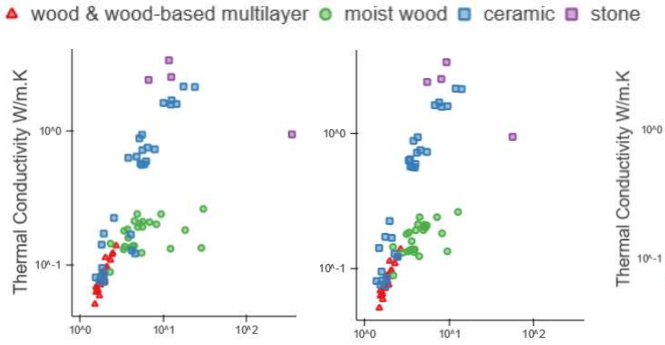

Figure 93 Dielectric Constant at 10 kHz (left) and 100 kHz (right) plotted against thermal conductivity

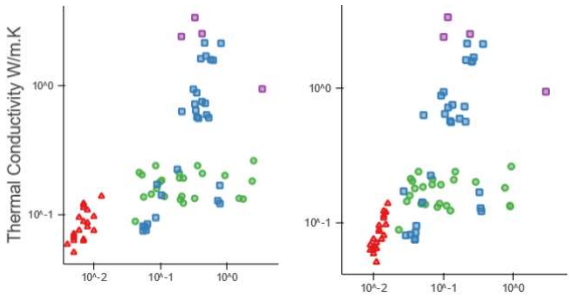

Figure 94 Dissipation Factor at 10 kHz (left) and 100 kHz (right) plotted against thermal conductivity

Figure 93 and Figure 94 show a comparison of dielectric properties at 10 kHz and 100 kHz. In Figure 93, it can be seen that the dielectric constant of the moist wood (green circles) at 10 kHz is more scattered, but these start to pull back at 100 kHz. Similarly, in Figure 94 the dissipation factor of the moist wood seems to shrink back, while that of the wood multiple layer materials seems to move forward. The dissipation factor for the multilayered materials seems a more unified line at 100 kHz. The same is true for the stone for both the dielectric constant and dissipation factor. In contrast, the wood multilayered materials which have a very low moisture content are not seen to have any significant change in dielectric constant between 10 and 100 kHz. The continuously changing behavior of the materials over a change in frequency is thus demonstrated in these graphs. This trend is expected to continue into higher frequencies, and the trend is confirmed by the results of the NanoVNA as shown in Figure 90 of Section 11.5.1.

The shown trend points to a potentially stronger one-on-one correlation between thermal conductivity and dielectric properties at higher frequencies in the Megahertz and Gigahertz

range. It is observed that materials with a high moisture content have a significantly higher rate of decrease in dielectric constant with an increase in frequency. On the other hand, materials with low moisture levels exhibit a modest decrease in their dielectric constant. It is speculated that these datapoints will line-up at a higher frequency. Consequently, this will lead to a higher accuracy in predictions.

12.2 Significance of Work

It is concluded from the experiments of this thesis, that enough information is encoded in the dielectric properties of materials, to accurately predict thermal conductivity. The proposed method to compute thermal conductivity is superior to any other currently used method for measuring thermal conductivity in-situ. A summary of key benefits of using this method and the significance of work is given below:

- **Removal of Reliance on Environmental Conditions**: The measurement of dielectric material properties is free from restrictive environmental conditions. Other measurement methods rely on environmental conditions like the need for a temperature difference of at least 10°C between indoors and outdoors. In some cases, cloud cover, wind speed, presence of heat generating objects inside the building contribute can lead to inaccuracies. This means that measurements through steady state conditions may not be achieved during the summers or for freely ventilated buildings. However, the climate is not a factor if measuring the dielectric material properties.

- **Short Measurement Time**: Removing the need to create steady state conditions would drastically reduce measurement time from up to a month to less than an hour.

- **Readily Available Technology**: Any technology used to measure dielectric properties may be used for predicting thermal conductivity of materials reliably. The technology to measure dielectric properties of architectural walls is already developed, well-practiced and readily available. It could be used to make thermal conductivity measurements without the additional work to develop new tools.

- **Potential for a Cost Effective Gadget for Lay Use**: There are methods to measure relative permittivity, which range from expensive and technical to inexpensive and easy [146]. There is potential to develop a gadget which is easy to operate for the lay person. This would remove the technical aspect of the measurement, bringing it to the non-technical person.

- **Unique Dataset**: As yet, the relationship between thermal conductivity and dielectric properties of construction materials has not been systematically studied. The considerably large dataset generated by this thesis is of immense value, because statistics of this nature are not available. The data can be useful for material science engineers whose work concerns analysis of material properties in a computational way.
- **Acceptable margin of error**: The uncertainty of the proposed method is comparable to existing methods of measurement. The heat flow meter method as described by the ASTM is attributed to have an expected error between 11% and 28% [27] depending on the environmental conditions. For thermography, the expected error is

between 5% and 200% [4,96–98]. In both cases the error is reduced if the environmental conditions are more conducive for the measurement. The proposed measurement method is independent of environmental conditions and shows promise of error margins within ±20% with potential for further reduced error with more data collection and better quality data collection.

- **Potential for predicting thermal conductivity of materials regardless of material type or moisture content** (Possible with additional work): It was demonstrated in the previous section that a unified set of parameters for regression can be defined which can predict materials from both wood-frame and ceramic based construction. This implies that a material's thermal conductivity can be predicted even if the contents of a construction wall are unknown. While a potential future gadget could be calibrated to be more accurate towards a set of material types, it could also be workable if the material type is left unspecified. But it was also seen that this might be possible if data related to dielectric properties could be gathered at higher frequencies.

For a comparison of the proposed method for predicting thermal conductivity with heat flow meter method and thermography, see Table 5, which is presented in Appendix G. This table presents a summary of the advantages and disadvantages of the main methods of measuring in-situ thermal conductivity and how they compare with the approach presented in this thesis.

12.3 Summary of Conclusions from all Experiments

This work demonstrates that thermal conductivity can be predicted by measuring the dielectric properties of building envelopes in-situ. The data gathered in this thesis is useful for prediction, given that the family of the material under study is known. Summary of Conclusions from all experiments is listed below:

Wood and Wood-Based Materials: Single Layers: The results of the experiments show a strong correlation between thermal conductivity and the relative dielectric constant. The potential for predicting thermal conductivity using dielectric material properties was demonstrated.

Sound: Data collection related to sound is tedious and time consuming with high uncertainty. Predictions using dielectric properties were found superior, and so this metric was dropped from future experiments.

Wood and Wood-Based Materials: Multilayers: Thermal conductivity for multilayered materials was predicted from dielectric properties effectively. This implies that that contact resistance does not distort the correlation in significant ways. Suitability to use of dielectric properties to predict thermal conductivity of cavity walls was identified.

Ceramics: For the ceramic family, the suitability of using dielectric properties at higher frequencies to predict thermal conductivity was identified. Rate of change in dielectric properties, with a change in frequency was identified as having a strong potential to identify moisture content. This metric was also identified as having a strong potential as an additional metric for predicting thermal conductivity.

Moisture Studies: Presence of moisture inside materials complicates thermal conductivity prediction. However, using machine learning algorithms, and including impedance in the feature space enables the prediction of thermal conductivity for moist wood and wood-based materials effectively.

Unified Approach: In the final chapter of conclusions, it was demonstrated that a unified set of regression parameters could be specified, so that all construction material's thermal conductivity could be predicted from its dielectric properties using the same regressor. The advantage of such an approach is that thermal conductivity can be predicted even if the contents of a construction wall are unknown.

12.4 Future Work

While much has been achieved in this study, a viable gadget predicting thermal conductivity for in-situ walls still requires significant work. Future work is to have two streams. The first is for further data collection, and the second is for development of the gadget. These are described in the following sections.

12.4.1 Data Collection

While the collected data suggests clear correlations, more experimental data would increase the accuracy further. Future data collection is to focus on two things:

- Future data collection is proposed to be on multilayered materials having layers in the ratio, which is expected to be found in modern day construction. While several material samples were studied as multi-layered systems, these were not layered in realistic proportions. Study of materials as close to real life situations would give better predictability of thermal conductivity of existing buildings.
- Data collection to be targeted towards the range of thermal conductivity which is expected to be found in the buildings that are meant to be measured.
- Data collection to be geared towards materials more commonly, used in construction. While many materials related to wood-frame and ceramic based construction were studied, a lot of effort went into the study of solid wood. Study of the behavior of solid wood enabled establishing the correlation, however, high density solid wood is not part of building construction. Further studies are to focus only on the wood species which are commonly used in the construction industry.
- The potential for a better-quality correlation was identified in studying dielectric properties at higher frequencies. Due to certain limitations, work could only be conducted for 10 kHz and 100 kHz frequencies for this thesis. This short fall needs to be addressed in future work by measuring materials at higher frequencies.

12.4.2 Development of Device

Future work entails development of a gadget which can output thermal conductivity values by measuring dielectric properties of walls in-situ. Future work is to have three workable components. One being the reader, which can make the dielectric measurement. The other must be its processing power, which can translate the measured dielectric properties into thermal conductivity. The third component is the interface meant for the user to interact with the device.

Reader: Several technologies have been used in the past to measure dielectric properties of walls of buildings. These devices include radars, GPR systems and VNAs. A VNA works by measuring the scatter parameter of a sent and received signal. Several researchers have used a free space transmission technique using horn antennas connected to a VNA for dielectric measurement [141,144,147]. In this system, an antenna is placed at a short distance from the target wall to send a signal, and a second antenna is placed on the reverse side to receive the signal. Others have used patch antennas, which may be applied directly to wall under measurement. Lazaro developed a chipless dielectric constant sensor for characterizing civil materials [148]. While the technology for measurement of dielectric properties of construction materials and walls is well developed and easily accessible, the most viable option for the proposed gadget still needs to be explored.

Processing: Advanced machine learning techniques may be explored to improve results for future work. If enough data relevant to the project has been gathered, then a model needs to be developed which can output predictions of thermal conductivity. While this thesis has demonstrated several models to predict thermal conductivity, additional data would require additional work in this regard. Thus far the feature space only consisted of two to five columns and the predictions were based on a single frequency. If data is collected for a range of frequencies, then doing so would change the structure of the predictive model.

Interface: The future work for a device is to include an interface for the user to interact with. The true power of the project is in developming of a device designed for a lay person who can use it successfully without much formal training. An important component of future work must be towards taking the gadget to the non-technical person, to make the measurement ubiquitous, user-friendly and accessible.

References

[1] R.W. Powell, Y.S. Touloukian, Thermal Conductivities of the Elements, Sci. New Ser. 181 (1973) 999–1008. http://www.jstor.org/stable/1736681.

[2] Energy Technology Perspectives, International Energy Agency, 2017.

[3] T.M. Tritt, ed., Thermal conductivity: theory, properties, and applications, Kluwer Academic/Plenum Publishers, New York, 2004.

[4] I. Nardi, E. Lucchi, T. de Rubeis, D. Ambrosini, Quantification of heat energy losses through the building envelope: A state-of-the-art analysis with critical and comprehensive review on infrared thermography, Build. Environ. 146 (2018) 190–205. https://doi.org/10.1016/j.buildenv.2018.09.050.

[5] R. Albatici, A.M. Tonelli, Infrared thermovision technique for the assessment of thermal transmittance value of opaque building elements on site, Energy Build. 42 (2010) 2177–2183. https://doi.org/10.1016/j.enbuild.2010.07.010.

[6] A.-H. Deconinck, S. Roels, Comparison of characterisation methods determining the thermal resistance of building components from onsite measurements, Energy Build. 130 (2016) 309–320. https://doi.org/10.1016/j.enbuild.2016.08.061.

[7] F. Asdrubali, F. D'Alessandro, G. Baldinelli, F. Bianchi, Evaluating in situ thermal transmittance of green buildings masonries—A case study, Case Stud. Constr. Mater. 1 (2014) 53–59. https://doi.org/10.1016/j.cscm.2014.04.004.

[8] E. Cayre, B. Allibe, M.-H. Laurent, D. Osso, There are people in the house! How the results of purely technical analysis of residential energy consumption are misleading for energy policies, (n.d.) 9.

[9] S. Doran, Field investigations of the thermal performance of construction elements as built, 2001, report for DETR, BRE East Kilbride, Glasgow, 2001.

[10] A. Prada, F. Cappelletti, P. Baggio, A. Gasparella, On the effect of material uncertainties in envelope heat transfer simulations, Energy Build. 71 (2014) 53–60. https://doi.org/10.1016/j.enbuild.2013.11.083.

[11] D. Majcen, L.C.M. Itard, H. Visscher, Theoretical vs. actual energy consumption of labelled dwellings in the Netherlands: Discrepancies and policy implications, Energy Policy. 54 (2013) 125–136. https://doi.org/10.1016/j.enpol.2012.11.008.

[12] D. Majcen, L. Itard, H. Visscher, Actual and theoretical gas consumption in Dutch dwellings: What causes the differences?, Energy Policy. 61 (2013) 460–471. https://doi.org/10.1016/j.enpol.2013.06.018.

[13] J.D. MacLean, Thermal Conductivity of wood, Heat. Piping Air Cond. 13 (1941) 380–391.

[14] J.F. Siau, Transport Processes in Wood, Springer Berlin Heidelberg, Berlin, Heidelberg, 1984. https://doi.org/10.1007/978-3-642-69213-0.

[15] W.L. James, Electric moisture meters for wood, U.S. Department of Agriculture, Forest Service, Forest Products Laboratory, Madison, WI, 1988. https://doi.org/10.2737/FPL-GTR-6.

[16] S.O. Nelson, D.S. Trabelsi, Sensing grain and seed moisture and density from dielectric properties, Int. J. Agric. Biol. Eng. 4 (2011) 75–81. https://doi.org/10.3965/j.issn.1934-6344.2011.01.075-081.

[17] S. Trabelsi, A.M. Paz, S.O. Nelson, Microwave dielectric method for the rapid, non-destructive determination of bulk density and moisture content of peanut hull pellets, Biosyst. Eng. 115 (2013) 332–338. https://doi.org/10.1016/j.biosystemseng.2013.04.003.

[18] M. Solar, A. Solar, Non-destructive determination of moisture content in hazelnut (Corylus avellana L.), Comput. Electron. Agric. 121 (2016) 320–330. https://doi.org/10.1016/j.compag.2016.01.002.
[19] A. Venkateswaran, A note on the relationship between electrical properties and thermal conductivity of woods, Wood Sci. Technol. 8 (1974) 50–55.
[20] United States Census Bureau, Characteristics of new housing, (2019). https://www.census.gov/construction/chars/ (accessed June 14, 2020).
[21] A.A. Shubbar, M. Sadique, P. Kot, W. Atherton, Future of clay-based construction materials – A review, Constr. Build. Mater. 210 (2019) 172–187. https://doi.org/10.1016/j.conbuildmat.2019.03.206.
[22] S.P. Venkateshan, Measurement of Thermo-Physical Properties, in: Mech. Meas., John Wiley & Sons, Ltd, Chichester, UK, 2015: pp. 359–387. https://doi.org/10.1002/9781119115571.ch11.
[23] 14:00-17:00, ISO 9869-1:2014, ISO. (n.d.). https://www.iso.org/cms/render/live/en/sites/isoorg/contents/data/standard/05/96/59697.html (accessed May 1, 2020).
[24] ASTM C1155-95, Standard Practice for Determining Thermal Resistance of Building Envelope Components from the In-Situ Data, ASTM International, West Conshohocken, PA, 2013. https://doi.org/10.1520/C1155-95R13.
[25] C. Luo, B. Moghtaderi, S. Hands, A. Page, Determining the thermal capacitance, conductivity and the convective heat transfer coefficient of a brick wall by annually monitored temperatures and total heat fluxes, Energy Build. 43 (2011) 379–385. https://doi.org/10.1016/j.enbuild.2010.09.030.
[26] T.L. Bergman, F.P. Incropera, eds., Fundamentals of heat and mass transfer, 7th ed, Wiley, Hoboken, NJ, 2011.
[27] I.A. Atsonios, I.D. Mandilaras, D.A. Kontogeorgos, M.A. Founti, A comparative assessment of the standardized methods for the in–situ measurement of the thermal resistance of building walls, Energy Build. 154 (2017) 198–206. https://doi.org/10.1016/j.enbuild.2017.08.064.
[28] G. Desogus, S. Mura, R. Ricciu, Comparing different approaches to in situ measurement of building components thermal resistance, Energy Build. 43 (2011) 2613–2620. https://doi.org/10.1016/j.enbuild.2011.05.025.
[29] C1363-11 Standard Test Method for Thermal Performance of Building Materials and Envelope Assemblies by Means of a Hot Box Apparatus, ASTM International, West Conshohocken, PA, n.d. https://doi.org/10.1520/C1363-11.
[30] E. Sassine, A practical method for in-situ thermal characterization of walls, Case Stud. Therm. Eng. 8 (2016) 84–93. https://doi.org/10.1016/j.csite.2016.03.006.
[31] X. Meng, T. Luo, Y. Gao, L. Zhang, Q. Shen, E. Long, A new simple method to measure wall thermal transmittance in situ and its adaptability analysis, Appl. Therm. Eng. 122 (2017) 747–757. https://doi.org/10.1016/j.applthermaleng.2017.05.074.
[32] R. Albatici, A.M. Tonelli, M. Chiogna, A comprehensive experimental approach for the validation of quantitative infrared thermography in the evaluation of building thermal transmittance, Appl. Energy. 141 (2015) 218–228. https://doi.org/10.1016/j.apenergy.2014.12.035.
[33] E. Grinzato, V. Vavilov, T. Kauppinen, Quantitative infrared thermography in buildings, Energy Build. 29 (1998) 1–9. https://doi.org/10.1016/S0378-7788(97)00039-X.
[34] B. Lehmann, K. Ghazi Wakili, Th. Frank, B. Vera Collado, Ch. Tanner, Effects of individual climatic parameters on the infrared thermography of buildings, Appl. Energy. 110 (2013) 29–43. https://doi.org/10.1016/j.apenergy.2013.03.066.

[35] I. Nardi, D. Paoletti, D. Ambrosini, T. de Rubeis, S. Sfarra, U-value assessment by infrared thermography: A comparison of different calculation methods in a Guarded Hot Box, Energy Build. 122 (2016) 211–221. https://doi.org/10.1016/j.enbuild.2016.04.017.
[36] B. Tejedor, M. Casals, M. Gangolells, X. Roca, Quantitative internal infrared thermography for determining in-situ thermal behaviour of façades, Energy Build. 151 (2017) 187–197. https://doi.org/10.1016/j.enbuild.2017.06.040.
[37] L.S. Sørensen, Energy Renovation of Buildings Utilizing the U-value Meter, a New Heat Loss Measuring Device, Sustainability. 2 (2010) 461–474. https://doi.org/10.3390/su2020461.
[38] L. Sørensen, Heat Transmission Coefficient Measurements in Buildings Utilizing a Heat Loss Measuring Device, Sustainability. 5 (2013) 3601–3614. https://doi.org/10.3390/su5083601.
[39] M.R. Mitchell, R.E. Link, B. Pilkington, S. Goodhew, P. deWilde, In Situ Thermal Conductivity Measurements of Building Materials with a Thermal Probe, J. Test. Eval. 38 (2010) 102636. https://doi.org/10.1520/JTE102636.
[40] A. Rasooli, L. Itard, C.I. Ferreira, A response factor-based method for the rapid in-situ determination of wall's thermal resistance in existing buildings, Energy Build. 119 (2016) 51–61. https://doi.org/10.1016/j.enbuild.2016.03.009.
[41] A. Rasooli, L. Itard, In-situ rapid determination of walls' thermal conductivity, volumetric heat capacity, and thermal resistance, using response factors, Appl. Energy. 253 (2019) 113539. https://doi.org/10.1016/j.apenergy.2019.113539.
[42] J.P. Holman, ed., Heat transfer, McGraw-Hill, New York, 1997.
[43] Ashrae, 2013 ASHRAE handbook: fundamentals., ASHRAE, Atlanta, GA., 2013.
[44] J.A. Clarke, P.P. Yaneske, A rational approach to the harmonisation of the thermal properties of building materials, Build. Environ. 44 (2009) 2046–2055. https://doi.org/10.1016/j.buildenv.2009.02.008.
[45] P. Baker, U-values and traditional buildings. In situ measurements and their comparisons to calculated values, Glasgow Caledonian University, Glasgow, 2011. www.historic-scotland.gov.uk/technicalpapers.
[46] S. Doran, Thermal transmittance of walls of dwellings before and after application of cavity wall insulation, BRE, 2008.
[47] S. Martin, History of Thermometer, Utah Mon. Mag. 7 (1891) 391.
[48] Early History of Thermometer, Am. Gas Light J. 51 (1889) 347.
[49] F.B. Rowley, Thermal conductivity of wood at angles to the principal anatomical directions, Heat. Piping Air Cond. 5 (1933) 313–323.
[50] F. Wangaard, Transverse Heat Conductivity of Wood, Heat. Piping Air Cond. 12 (1940) 459–464.
[51] K.E. Wilkes, Thermophysical properties data base activities at Owens-Corning fiberglass, American Society of Heating, Refrigerating and Air-Conditioning Engineers Inc., Atlanta, GA, 1981.
[52] A. TenWolde, J.D. McNatt, L. Krahn, Thermal Properties of wood and wood panel products for use in buildings, USDA, Forest Products Laboratory, 1988.
[53] R. Bergman, Z. Cai, C.G. Carll, C. Clausen, Wood Handbook, Wood as an Engineering Material, U.S. Department of Agriculture, Forest Service, Forest Products Laboratory, Madison, WI, 2010.
[54] T. Cardenas, G. Bible, The Thermal Properties of Wood—Data Base, in: F. Powell, S. Matthews (Eds.), Therm. Insul. Mater. Syst., ASTM International, 100 Barr Harbor Drive, PO Box C700, West Conshohocken, PA 19428-2959, 1987: pp. 238-238–45. https://doi.org/10.1520/STP18485S.

[55] F.B. Rowley, A.B. Algren, THERMAL CONDUCTIVITY OF BUILDING MATERIALS, (n.d.) 144.
[56] T. Maku, Studies on the Heat Conductin In Wood, (n.d.) 80.
[57] F.F.P. Kollmann, Physics of Wood, in: Princ. Wood Sci. Technol. I, Springer Verlag, Berlin, 1968: pp. 160–291.
[58] T. Harada, T. Hata, S. Ishihara, Thermal constants of wood during the heating process measured with the laser flash method, J. Wood Sci. 44 (1998) 425–431. https://doi.org/10.1007/BF00833405.
[59] Z.-T. Yu, X. Xu, L.-W. Fan, Y.-C. Hu, K.-F. Cen, Experimental Measurements of Thermal Conductivity of Wood Species in China: Effects of Density, Temperature, and Moisture Content, For. Prod. J. 61 (2011) 130–135. https://doi.org/10.13073/0015-7473-61.2.130.
[60] W.C. Lewis, Thermal Conductivity of Wood-Base Fiber and Particle Panel Materials, USDA Forest Service, Forest Products Laboratory, Madison, WI, 1967.
[61] L.M.K. Boelter, Heat Transfer Notes, University of California, Berkeley, 1946.
[62] G.R. Jones, Fundamental Properties of Materials, (n.d.) 8.
[63] D. Narain Singh, S.J. Kuriyan, K. Chakravarthy Manthena, A generalised relationship between soil electrical and thermal resistivities, Exp. Therm. Fluid Sci. 25 (2001) 175–181. https://doi.org/10.1016/S0894-1777(01)00082-6.
[64] J. Wang, X. Zhang, L. Du, A laboratory study of the correlation between the thermal conductivity and electrical resistivity of soil, J. Appl. Geophys. 145 (2017) 12–16. https://doi.org/10.1016/j.jappgeo.2017.07.009.
[65] S. Avramidis, L. Iliadis, PREDICTING WOOD THERMAL CONDUCTIVITY USING ARTIFICIAL NEURAL NETWORKS, WOOD FIBER Sci. 37 (2005) 9.
[66] G. Pia, U. Sanna, Intermingled fractal units model and electrical equivalence fractal approach for prediction of thermal conductivity of porous materials, Appl. Therm. Eng. 61 (2013) 186–192. https://doi.org/10.1016/j.applthermaleng.2013.07.031.
[67] C. Skaar, Wood-Water Relations, Springer Berlin Heidelberg, Berlin, Heidelberg, 1988. https://doi.org/10.1007/978-3-642-73683-4.
[68] G.I. Torgovnikov, Dielectric Properties of Wood and Wood-Based Materials, Springer Berlin Heidelberg, Berlin, Heidelberg, 1993. https://doi.org/10.1007/978-3-642-77453-9.
[69] H. Sahin, N. Ay, Dielectric properties of hardwood species at microwave frequencies, J. Wood Sci. 50 (2004) 375–380. https://doi.org/10.1007/s10086-003-0575-1.
[70] A-to-Z Guide to Thermodynamics, Heat and Mass Transfer, and Fluids Engineering: AtoZ, Begellhouse, 2006.
[71] Y. Popov, V. Tertychnyi, R. Romushkevich, D. Korobkov, J. Pohl, Interrelations Between Thermal Conductivity and Other Physical Properties of Rocks: Experimental Data, Pure Appl Geophys. 160 (2003) 26.
[72] P. Mielke, K. Bär, I. Sass, Determining the relationship of thermal conductivity and compressional wave velocity of common rock types as a basis for reservoir characterization, J. Appl. Geophys. 140 (2017) 135–144. https://doi.org/10.1016/j.jappgeo.2017.04.002.
[73] N. Gegenhuber, J. Schoen, New approaches for the relationship between compressional wave velocity and thermal conductivity, J. Appl. Geophys. 76 (2012) 50–55. https://doi.org/10.1016/j.jappgeo.2011.10.005.
[74] L. Pimienta, J. Sarout, L. Esteban, C.D. Piane, Prediction of rocks thermal conductivity from elastic wave velocities, mineralogy and microstructure, Geophys. J. Int. 197 (2014) 860–874. https://doi.org/10.1093/gji/ggu034.

[75] L. Esteban, L. Pimienta, J. Sarout, C.D. Piane, S. Haffen, Y. Geraud, N.E. Timms, Study cases of thermal conductivity prediction from P-wave velocity and porosity, Geothermics. 53 (2015) 255–269. https://doi.org/10.1016/j.geothermics.2014.06.003.
[76] G. Concu, B. De Nicolo, M. Valdes, Prediction of Building Limestone Physical and Mechanical Properties by Means of Ultrasonic P-Wave Velocity, Sci. World J. 2014 (2014) 1–8. https://doi.org/10.1155/2014/508073.
[77] E. Vasanelli, A. Calia, V. Luprano, F. Micelli, Ultrasonic pulse velocity test for non-destructive investigations of historical masonries: an experimental study of the effect of frequency and applied load on the response of a limestone, Mater. Struct. 50 (2017) 38. https://doi.org/10.1617/s11527-016-0892-7.
[78] E. Vasanelli, M. Sileo, A. Calia, M.A. Aiello, Non-destructive Techniques to Assess Mechanical and Physical Properties of Soft Calcarenitic Stones, Procedia Chem. 8 (2013) 35–44. https://doi.org/10.1016/j.proche.2013.03.006.
[79] G. Vasconcelos, P.B. Lourenço, C.A.S. Alves, J. Pamplona, Ultrasonic evaluation of the physical and mechanical properties of granites, Ultrasonics. 48 (2008) 453–466. https://doi.org/10.1016/j.ultras.2008.03.008.
[80] G. Trtnik, F. Kavčič, G. Turk, Prediction of concrete strength using ultrasonic pulse velocity and artificial neural networks, Ultrasonics. 49 (2009) 53–60. https://doi.org/10.1016/j.ultras.2008.05.001.
[81] K. Amini, M. Jalalpour, N. Delatte, Advancing concrete strength prediction using non-destructive testing: Development and verification of a generalizable model, Constr. Build. Mater. 102 (2016) 762–768. https://doi.org/10.1016/j.conbuildmat.2015.10.131.
[82] J.A. Clarke, P.P. Yaneske, A.A. Pinney, The harmonisation of thermal properties of building materials., Building Research Establishment, Building Environmental Performance Analysis Club (BEPAC), Garston, UK, 1991.
[83] N. Saeed, Experimental data correlating thermal conductivity and dielectric properties of wood and wood-based materials, Submitt. Data Brief. (Submitted: Under review) (n.d.).
[84] N. Saeed, J.A. Malen, M. Chamanzar, R. Krishnamurti, Experimental correlation of thermal conductivity with dielectric properties of wood: Towards enabling rapid in-situ evaluation of building energy efficiency, Energy Build. (Submitted, Under review) (n.d.).
[85] N. Saeed, Evaluating building energy efficiency: Experiments correlating thermal conductivity using dielectric properties for multilayered materials related to wood-frame construction, Build. Environ. (Work in progress, to be submitted) (n.d.).
[86] C1045 - 07 Practice for Calculating Thermal Transmission Properties Under Steady-State Conditions, ASTM International, West Conshohocken, PA, n.d. https://doi.org/10.1520/C1045-07R13.
[87] ASTM C518-17, Standard Test Method for Steady-State Thermal Transmission Properties by Means of the Heat Flow Meter Apparatus, ASTM International, West Conshohocken, 2017. https://doi.org/10.1520/C0518-17.
[88] A.H. Scott, H.L. Curtis, Edge correction in the determination of dielectric constant, J. Res. Natl. Bur. Stand. 22 (1939) 747. https://doi.org/10.6028/jres.022.008.
[89] ASTM D150-18 Standard Test Methods for AC Loss Characteristics and Permittivity (Dielectric Constant) of Solid Electrical Insulation, (2018). https://doi.org/10.1520/D0150-18.
[90] ASTM D4442-16 Standard Test Methods for Direct Moisture Content Measurement of Wood and Wood-Based Materials, ASTM International, West Conshohocken, PA, 2016. https://doi.org/10.1520/D4442-16.
[91] J.R. Taylor, An introduction to error analysis: the study of uncertainties in physical measurements, 2nd ed, University Science Books, Sausalito, Calif, 1997.

[92] F.F.P. Kollmann, E.W. Kuenzi, A.J. Stamm, Principles of Wood Science and Technology, Springer Berlin Heidelberg, Berlin, Heidelberg, 1975. https://doi.org/10.1007/978-3-642-87931-9.
[93] F.F.P. Kollmann, W.A. Côté, Principles of Wood Science and Technology: I Solid Wood, 1968. https://doi.org/10.1007/978-3-642-87928-9 (accessed March 23, 2020).
[94] K.Ch. Varada Rajulu, B.N. Mohanty, Dielectric and Conductivity Properties of Some Wood Composites, Int. J. Eng. Technol. 8 (2016) 51–60. https://doi.org/10.18052/www.scipress.com/IJET.8.51.
[95] G. Ficco, F. Iannetta, E. Ianniello, F.R. d'Ambrosio Alfano, M. Dell'Isola, U-value in situ measurement for energy diagnosis of existing buildings, Energy Build. 104 (2015) 108–121. https://doi.org/10.1016/j.enbuild.2015.06.071.
[96] G. Dall'O', L. Sarto, A. Panza, Infrared Screening of Residential Buildings for Energy Audit Purposes: Results of a Field Test, Energies. 6 (2013) 3859–3878. https://doi.org/10.3390/en6083859.
[97] V.P. Vavilov, A pessimistic view of the energy auditing of building structures with the use of infrared thermography, Russ. J. Nondestruct. Test. 46 (2010) 906–910. https://doi.org/10.1134/S1061830910120065.
[98] E. Grinzato, P. Bison, G. Cadelano, F. Peron, R-value estimation by local thermographic analysis, in: R.B. Dinwiddie, M. Safai (Eds.), Orlando, Florida, 2010: p. 76610H. https://doi.org/10.1117/12.850729.
[99] K. Pentoś, D. Łuczycka, T. Wysoczański, Dielectric Properties of Selected Wood Species in Poland, WOOD Res. 62 (2017) 10.
[100] S. Razafindratsima, Z.M. Sbartaï, F. Demontoux, Permittivity measurement of wood material over a wide range of moisture content, Wood Sci. Technol. 51 (2017) 1421–1431. https://doi.org/10.1007/s00226-017-0935-4.
[101] R. Olmi, M. Bini, A. Ignesti, C. Riminesi, Dielectric Properties of Wood from 2 to 3 GHz, J. Microw. Power Electromagn. Energy. 35 (2000) 135–143. https://doi.org/10.1080/08327823.2000.11688430.
[102] M.F. Kabir, K.B. Khalid, W.M. Daud, S.H.A. Aziz, Dielectric properties of rubber wood at microwave frequencies measured with an open-ended coaxial line, Wood Fiber Sci. (1996) 6.
[103] E. Peyskens, M. de Pourcq, M. Stevens, J. Schalck, Dielectric properties of softwood species at microwave frequencies, Wood Sci. Technol. 18 (1984) 267–280. https://doi.org/10.1007/BF00353363.
[104] M. Deshpande, K. Dudley, Estimation of Complex Permittivity of Composite Multilayer Material at Microwave Frequency Using Waveguide Measurements, (2003) 80.
[105] E.H. Ridouane, M. Bianchi, Thermal Performance of Uninsulated and Partially Filled Wall Cavities: Preprint, in: NREL, National Renewable Energy Laboratory, Montral Quebec, 2011.
[106] ISO 15099:2003 Thermal performance of windows, doors and shading devices: Detailed calculations, (2011).
[107] A.-J.N. Khalifa, Natural convective heat transfer coefficient: a review II. Surfaces in two and three dimensional enclosures, Energy Convers. Manag. (2001) 13.
[108] A.-J.N. Khalifa, Natural convective heat transfer coefficient: a review I. Isolated vertical and horizontal surfaces, Energy Convers. Manag. (2001) 14.
[109] V.V. Komarov, Handbook of dielectric and thermal properties of materials at microwave frequencies, Artech House, Boston, 2012.
[110] J.H. Richmond, Efficient Recursive Solutions for Plane and Cylindrical Multilayers, Defense Technical Information Center, Fort Belvoir, VA, 1965. https://doi.org/10.21236/AD0624191.

[111] M.G. Amin, Through-the-Wall Radar Imaging, Taylor & Francis, Boca Raton, FL, 2011.
[112] L. Chen, ed., Microwave electronics: measurement and materials characterisation, John Wiley, Chichester, 2004.
[113] W. Honcharenko, H.L. Bertoni, Transmission and reflection characteristics at concrete block walls in the UHF bands proposed for future PCS, IEEE Trans. Antennas Propag. 42 (1994) 232–239. https://doi.org/10.1109/8.277217.
[114] C.L. Holloway, P.L. Perini, R.R. DeLyser, K.C. Allen, Analysis of composite walls and their effects on short-path propagation modeling, IEEE Trans. Veh. Technol. 46 (1997) 730–738. https://doi.org/10.1109/25.618198.
[115] R.C. de Vekey, Non-Destructive Test Methods for Masonry Structures, in: Dublin, Ireland, 1988: pp. 1673–1681.
[116] R. de Vekey, 9.5 Buildings, in: Ground Penetrating Radar, 2nd ed., Institution of Engineering and Technology, London, UK, 2004.
[117] C. Maierhofer, J. Wostmann, C. Hennen, Non-destructive investigation of complex historic masonry structures with impulse radar, in: Non-Destr. Test. Civ. Eng., Federal Institute for Materials Research and Testing (BAM), Berlin, 2003. http://www.ndt.net/article/ndtce03/papers/p063/p063.htm.
[118] R. Thallon, Graphic guide to frame construction, 3rd ed., rev.updated, Taunton Press, Newtown, CT, 2008.
[119] W.L. James, Dielectric Properties of Wood and Hardboard: Variation with Temperature, Frequency, Moisture Content, and Grain Orientation, USDA Forest Service, Forest Products Laboratory, Madison, WI, 1975.
[120] R. and A.-C.E. American Society of Heating, Heat, Air, and Moisture Control in Building Assemblies (Chapter 26), in: 2017 ASHRAE Handb. Fundam. SI Ed., ASHRAE, 2017, ©2017, Atlanta, GA, 2017.
[121] H.Y. Song, X.X. Cheng, L. Chu, Effect of Density and Ambient Temperature on Coefficient of Thermal Conductivity of Heat-Insulated EPS and PU Materials for Food Packaging, Appl. Mech. Mater. 469 (2013) 152–155. https://doi.org/10.4028/www.scientific.net/AMM.469.152.
[122] W.A. Lotz, Facts about thermal insulation, ASHRAE J. 11 (1969) 83–84.
[123] M. Mehta, W. Scarborough, D. Armpriest, Building construction: principles, materials, and systems, 2009 update, Prentice Hall, Boston, 2010.
[124] L. Rusiniak, Electrical properties of water. New experimental data in the 5 Hz - 13 MHz frequency range, Acta Geophys. Pol. 52 (2004) 63–76.
[125] A. Andryieuski, S.M. Kuznetsova, S.V. Zhukovsky, Y.S. Kivshar, A.V. Lavrinenko, Water: Promising Opportunities For Tunable All-dielectric Electromagnetic Metamaterials, Sci. Rep. 5 (2015) 13535. https://doi.org/10.1038/srep13535.
[126] W.J. Ellison, K. Lamkaouchi, J.-M. Moreau, Water: a dielectric reference, J. Mol. Liq. 68 (1996) 171–279. https://doi.org/10.1016/0167-7322(96)00926-9.
[127] I. Asadi, P. Shafigh, Z.F.B. Abu Hassan, N.B. Mahyuddin, Thermal conductivity of concrete – A review, J. Build. Eng. 20 (2018) 81–93. https://doi.org/10.1016/j.jobe.2018.07.002.
[128] R. Demirboga, A. Kan, Thermal conductivity and shrinkage properties of modified waste polystyrene aggregate concretes, Constr. Build. Mater. 35 (2012) 730–734. https://doi.org/10.1016/j.conbuildmat.2012.04.105.
[129] R. Demirboğa, R. Gül, Thermal conductivity and compressive strength of expanded perlite aggregate concrete with mineral admixtures, Energy Build. 35 (2003) 1155–1159. https://doi.org/10.1016/j.enbuild.2003.09.002.

[130] F. Blanco, P. García, P. Mateos, J. Ayala, Characteristics and properties of lightweight concrete manufactured with cenospheres, Cem. Concr. Res. 30 (2000) 1715–1722. https://doi.org/10.1016/S0008-8846(00)00357-4.
[131] H.C. Robinson, R.A. Ayres, S.G. Barton, T.W. Bremner, W.I. Brooks, A.C. Carter, R.A. Cook, N.A. Cumming, C.L. Dodl, F.G. Erskine, J.H. Faber, L. Gorsline, J.A. Hanson, S.B. Helms, T.A. Holms, W.W. Hotaling, J.G. Kluball, Guide for Structural Lightweight Aggregate Concrete, (n.d.) 27.
[132] J. García Ten, M.J. Orts, A. Saburit, G. Silva, Thermal conductivity of traditional ceramics. Part I: Influence of bulk density and firing temperature, Ceram. Int. 36 (2010) 1951–1959. https://doi.org/10.1016/j.ceramint.2010.05.012.
[133] L. Aouba, C. Bories, M. Coutand, B. Perrin, H. Lemercier, Properties of fired clay bricks with incorporated biomasses: Cases of Olive Stone Flour and Wheat Straw residues, Constr. Build. Mater. 102 (2016) 7–13. https://doi.org/10.1016/j.conbuildmat.2015.10.040.
[134] M.L. Gualtieri, A.F. Gualtieri, S. Gagliardi, P. Ruffini, R. Ferrari, M. Hanuskova, Thermal conductivity of fired clays: Effects of mineralogical and physical properties of the raw materials, Appl. Clay Sci. 49 (2010) 269–275. https://doi.org/10.1016/j.clay.2010.06.002.
[135] M. Sutcu, Influence of expanded vermiculite on physical properties and thermal conductivity of clay bricks, Ceram. Int. 41 (2015) 2819–2827. https://doi.org/10.1016/j.ceramint.2014.10.102.
[136] M. Dondi, F. Mazzanti, P. Principi, M. Raimondo, G. Zanarini, Thermal Conductivity of Clay Bricks, J. Mater. Civ. Eng. 16 (2004) 8–14. https://doi.org/10.1061/(ASCE)0899-1561(2004)16:1(8).
[137] M. Jamil, M.K. Hassan, H.M.A. Al-Mattarneh, M.F.M. Zain, Concrete dielectric properties investigation using microwave nondestructive techniques, Mater. Struct. 46 (2013) 77–87. https://doi.org/10.1617/s11527-012-9886-2.
[138] N. Piladaeng, N. Angkawisittpan, S. Homwuttiwong, Determination of Relationship between Dielectric Properties, Compressive Strength, and Age of Concrete with Rice Husk Ash Using Planar Coaxial Probe, Meas. Sci. Rev. 16 (2016) 14–20. https://doi.org/10.1515/msr-2016-0003.
[139] X. Jin, M. Ali, Simple empirical formulas to estimate the dielectric constant and conductivity of concrete, Microw. Opt. Technol. Lett. 61 (2019) 386–390. https://doi.org/10.1002/mop.31577.
[140] K. Chung, L. Yuan, S. Ji, L. Sun, C. Qu, C. Zhang, Dielectric Characterization of Chinese Standard Concrete for Compressive Strength Evaluation, Appl. Sci. 7 (2017) 177. https://doi.org/10.3390/app7020177.
[141] P. D'Atanasio, A. Zambotti, S. Pisa, E. Pittella, E. Piuzzi, Complex Permittivity Measurements for Moisture and Salinity Characterization of Building Materials, (2017) 5.
[142] Z. Hlavá, ELECTRICAL PROPERTIES OF SOME BUILDING MATERIALS, (2007) 7.
[143] D.Q.A. Sattar, D.T.S. Hamadi, Dielectric Properties of Iraqi Clay; Effect of Alumina Content, (n.d.) 5.
[144] M.S. Venkatesh, G.S.V. Raghavan, An overview of dielectric properties measuring techniques, Can. Biosyst. Eng. 47 (2005) 16.
[145] X. He, J. Xie, X. Xiong, Y. Li, Y. Wei, P. Quan, Q. Mou, X. Li, Study on Dielectric Properties of Poplar Wood over an Ultra-wide Frequency Range, BioResources. 12 (2017) 5984–5995. https://doi.org/10.15376/biores.12.3.5984-5995.
[146] S. Yahya, A Modified Complex Permittivity Measurement Technique at Microwave Frequency, Int. J. New Comput. Archit. Their Appl. IJNCAA. 2 (2012) 390–402.

[147] D.K. Ghodgaonkar, V.V. Varadan, V.K. Varadan, A free-space method for measurement of dielectric constants and loss tangents at microwave frequencies, IEEE Trans. Instrum. Meas. 38 (1989) 789–793. https://doi.org/10.1109/19.32194.
[148] A. Lazaro, R. Villarino, F. Costa, S. Genovesi, A. Gentile, L. Buoncristiani, D. Girbau, Chipless Dielectric Constant Sensor for Structural Health Testing, IEEE Sens. J. 18 (2018) 5576–5585. https://doi.org/10.1109/JSEN.2018.2839689.
[149] Gplastics, (n.d.). www.gplastics.com (accessed January 10, 2018).
[150] Quadrant Plastics, (n.d.). www.quadrantplastics.com (accessed January 10, 2018).
[151] Professional Plastics, (n.d.). www.professionalplastics.com. (accessed January 10, 2018).
[152] Laminated Plastics, (n.d.). www.laminatedplastics.com (accessed January 10, 2018).
[153] H. Sahin, Thermal and dielectric properties of pine wood in the transverse direction, BioResources. (2009) 1663–1669.
[154] B.M. Suleiman, J. Larfeldt, B. Leckner, M. Gustavsson, Thermal conductivity and diffusivity of wood, Wood Sci. Technol. 33 (1999) 465–473. https://doi.org/10.1007/s002260050130.
[155] A. Jankowska, P. Kozakiewicz, Comparison of thermal properties of selected wood species intended to woodwork windows production, (n.d.) 5.
[156] P.O. Kettunen, Wood structure and properties, Trans Tech Publications Ltd, Uetikon-Zuerich ; Enfield, N.H, 2006.
[157] W.P. Goss, R.G. MUler, Thermal Properties of Wood and Wood Products, (n.d.) 11.
[158] O. Vay, K. De Borst, C. Hansmann, A. Teischinger, U. Müller, Thermal conductivity of wood at angles to the principal anatomical directions, Wood Sci. Technol. 49 (2015) 577–589. https://doi.org/10.1007/s00226-015-0716-x.
[159] T. Kawasaki, S. Kawai, Thermal insulation properties of wood-based sandwich panel for use as structural insulated walls and floors, J. Wood Sci. 52 (2006) 75–83. https://doi.org/10.1007/s10086-005-0720-0.
[160] K. Prałat, Research on Thermal Conductivity of the Wood and Analysis of Results Obtained by the Hot Wire Method, Exp. Tech. 40 (2016) 973–980. https://doi.org/10.1007/s40799-016-0096-7.
[161] R.E. Zarr, NIST US dept of commerce, NIST Stand. Ref. Database 81 NIST Heat Transm. Prop. Insul. Build. Mater. (2018). https://srdata.nist.gov/ (accessed January 10, 2018).
[162] J. Zhou, H. Zhou, C. Hu, S. Hu, Measurements of Thermal and Dielectric Properties of Medium Density Fiberboard with Different Moisture Contents, BioResources. 8 (2013) 4185–4192. https://doi.org/10.15376/biores.8.3.4185-4192.
[163] V. Bucur, Handbook of Materials for String Musical Instruments, Springer International Publishing, Cham, 2016. https://doi.org/10.1007/978-3-319-32080-9.
[164] W.W. Barkas, Mechanical properties of wood and paper, North-Holland Pub. Co.; Interscience Publishers, Amsterdam, New York, 1953. //catalog.hathitrust.org/Record/000226233.
[165] E.V. Bachtiar, S.J. Sanabria, J.P. Mittig, P. Niemz, Moisture-dependent elastic characteristics of walnut and cherry wood by means of mechanical and ultrasonic test incorporating three different ultrasound data evaluation techniques, Wood Sci. Technol. 51 (2017) 47–67. https://doi.org/10.1007/s00226-016-0851-z.
[166] G. Han, Q. Wu, X. Wang, Stress-wave velocity of wood-based panels: Effect of moisture, product type, and material direction, For. Prod. J. (2006) 6.
[167] M. Roohnia, Wood: Vibration and Acoustic Properties, in: Ref. Module Mater. Sci. Mater. Eng., Elsevier, 2019: p. B9780128035818020000. https://doi.org/10.1016/B978-0-12-803581-8.01996-2.

[168] H. Yang, L. Yu, L. Wang, Effect of moisture content on the ultrasonic acoustic properties of wood, J. For. Res. 26 (2015) 753–757. https://doi.org/10.1007/s11676-015-0079-z.
[169] V. Bucur, Acoustics of wood, 2nd ed, Springer, Berlin ; New York, 2006.
[170] T. Ozyhar, S. Hering, S.J. Sanabria, P. Niemz, Determining moisture-dependent elastic characteristics of beech wood by means of ultrasonic waves, Wood Sci. Technol. 47 (2013) 329–341. https://doi.org/10.1007/s00226-012-0499-2.

Appendix A

Comparison of various mathematical models for the length of time (in days) needed to calculate thermal conductivity during various seasons as shown by Deconinck et al [6]

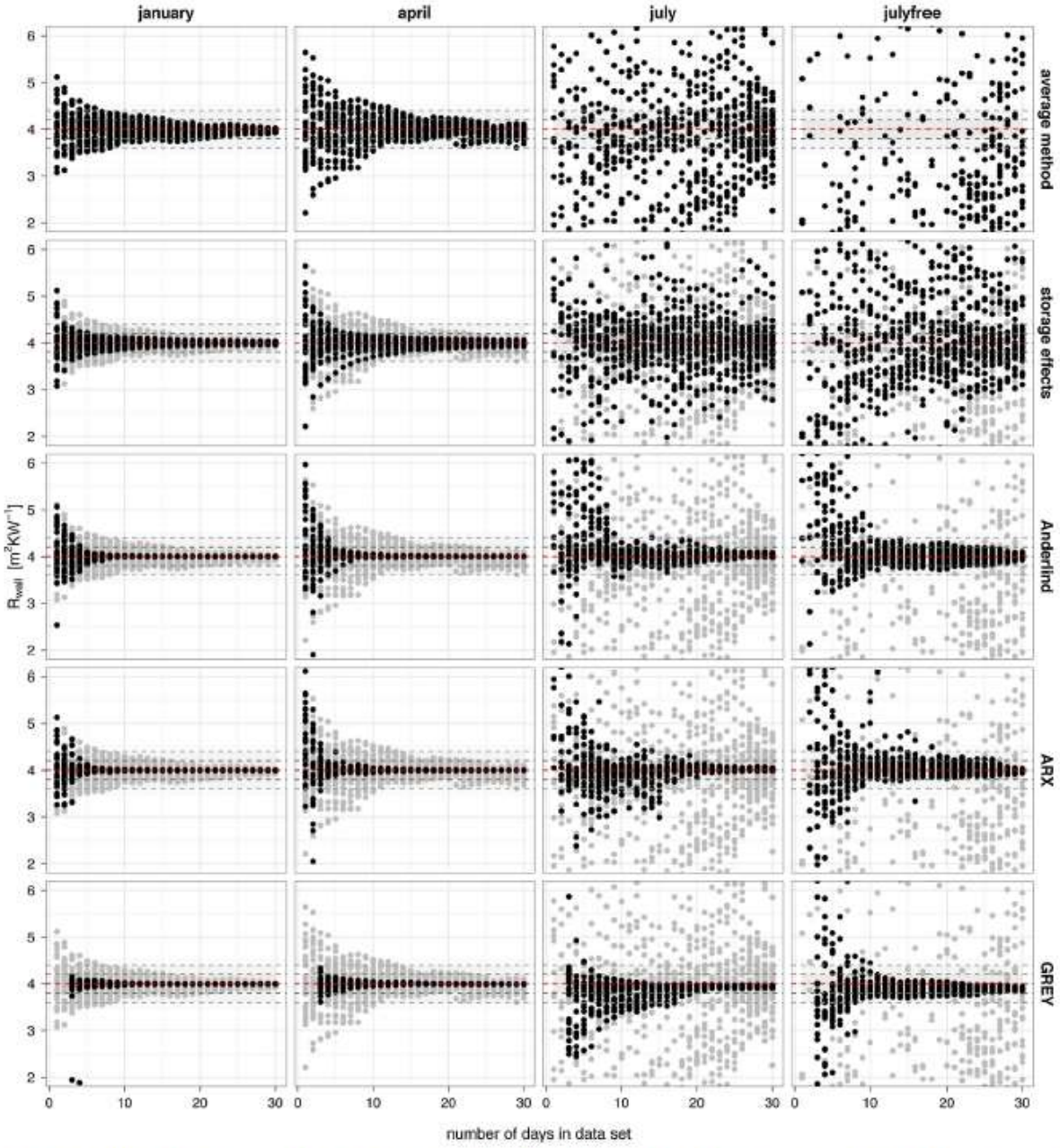

Fig. 3. Comparison of the different analysis techniques regarding the data set length and period. The red dotted line represents the reference value for the thermal resistance of the cavity wall. The grey dotted lines and areas correspond to the 5% and 10% accuracy bands. (For interpretation of the references to color in this figure legend, the reader is referred to the web version of the article.)

Appendix B

A page from the ASHRAE Fundamentals 2013 (Chapter 26) showing material properties, and their sources. A lot of sources predate 1989 (approximately 50%) and most are based on work by a single scientist [43].

Table 1 Building and Insulating Materials: Design Values[a] (*Continued*)

Description	Density, kg/m³	Conductivity[b] k, W/(m·K)	Resistance R, (m²·K)/W	Specific Heat, kJ/(kg·K)	Reference[l]
	1760	0.71 to 0.85	—	—	Valore (1988)
	1600	0.61 to 0.74	—	—	Valore (1988)
	1440	0.52 to 0.62	—	—	Valore (1988)
	1280	0.43 to 0.53	—	—	Valore (1988)
	1120	0.36 to 0.45	—	—	Valore (1988)
Clay tile, hollow					
1 cell deep 75 mm	—	—	0.14	0.88	Rowley and Algren (1937)
100 mm	—	—	0.20	—	Rowley and Algren (1937)
2 cells deep 150 mm	—	—	0.27	—	Rowley and Algren (1937)
200 mm	—	—	0.33	—	Rowley and Algren (1937)
250 mm	—	—	0.39	—	Rowley and Algren (1937)
3 cells deep 300 mm	—	—	0.44	—	Rowley and Algren (1937)
Lightweight brick	800	0.20	—	—	Kumaran (1996)
	770	0.22	—	—	Kumaran (1996)
Concrete blocks[f, g]					
Limestone aggregate					
~200 mm, 16.3 kg, 2200 kg/m³ concrete, 2 cores	—	—	—	—	
with perlite-filled cores	—	—	0.37	—	Valore (1988)
~300 mm, 25 kg, 2200 kg/m³ concrete, 2 cores	—		—	—	
with perlite-filled cores	—	—	0.65	—	Valore (1988)
Normal-weight aggregate (sand and gravel)					
~200 mm, 16 kg, 2100 kg/m³ concrete, 2 or 3 cores…	—	—	0.20 to 0.17	0.92	Van Geem (1985)
with perlite-filled cores	—	—	0.35	—	Van Geem (1985)
with vermiculite-filled cores	—	—	0.34 to 0.24	—	Valore (1988)
~300 mm, 22.7 kg, 2000 kg/m³ concrete, 2 cores	—	—	0.217	0.92	Valore (1988)
Medium-weight aggregate (combinations of normal and lightweight aggregate)					
~200 mm, 13 kg, 1550 to 1800 kg/m³ concrete, 2 or 3 cores	—	—	0.30 to 0.22	—	Van Geem (1985)
with perlite-filled cores	—	—	0.65 to 0.41	—	Van Geem (1985)
with vermiculite-filled cores	—	—	0.58	—	Van Geem (1985)
with molded-EPS-filled (beads) cores	—	—	0.56	—	Van Geem (1985)
with molded EPS inserts in cores	—	—	0.47	—	Van Geem (1985)
Low-mass aggregate (expanded shale, clay, slate or slag, pumice)					
~150 mm, 7 1/2 kg, 1400 kg/m² concrete, 2 or 3 cores	—	—	0.34 to 0.29	—	Van Geem (1985)
with perlite-filled cores	—	—	0.74	—	Van Geem (1985)
with vermiculite-filled cores	—	—	0.53	—	Van Geem (1985)
200 mm, 8 to 10 kg, 1150 to 1380 kg/m² concrete	—	—	0.56 to 0.33	0.88	Van Geem (1985)
with perlite-filled cores	—	—	1.20 to 0.77	—	Van Geem (1985)
with vermiculite-filled cores	—	—	0.93 to 0.69	—	Shu et al. (1979)
with molded-EPS-filled (beads) cores	—	—	0.85	—	Shu et al. (1979)
with UF foam-filled cores	—	—	0.79	—	Shu et al. (1979)
with molded EPS inserts in cores	—	—	0.62	—	Shu et al. (1979)
300 mm, 16 kg, 1400 kg/m³, concrete, 2 or 3 cores	—	—	0.46 to 0.40	—	Van Geem (1985)
with perlite-filled cores	—	—	1.6 to 1.1	—	Van Geem (1985)
with vermiculite-filled cores	—	—	1.0	—	Valore (1988)
Stone, lime, or sand	2880	10.4	—	—	Valore (1988)
Quartzitic and sandstone	2560	6.2	—	—	Valore (1988)
	2240	3.46	—	—	Valore (1988)
	1920	1.88	—	0.88	Valore (1988)
Calcitic, dolomitic, limestone, marble, and granite	2880	4.33	—	—	Valore (1988)
	2560	3.17	—	—	Valore (1988)
	2240	2.31	—	—	Valore (1988)
	1920	1.59	—	0.88	Valore (1988)
	1600	1.15	—	—	Valore (1988)
Gypsum partition tile					
75 by 300 by 760 mm, solid	—	—	0.222	0.79	Rowley and Algren (1937)
4 cells	—	—	0.238	—	Rowley and Algren (1937)
100 by 300 by 760 mm, 3 cells	—	—	0.294	—	Rowley and Algren (1937)
Limestone	2400	0.57	—	0.84	Kumaran (2002)

Appendix C

Results by Mielke et al showing Cross plots of thermal conductivity and compressional wave velocity of all tested rock types at dry condition [72].

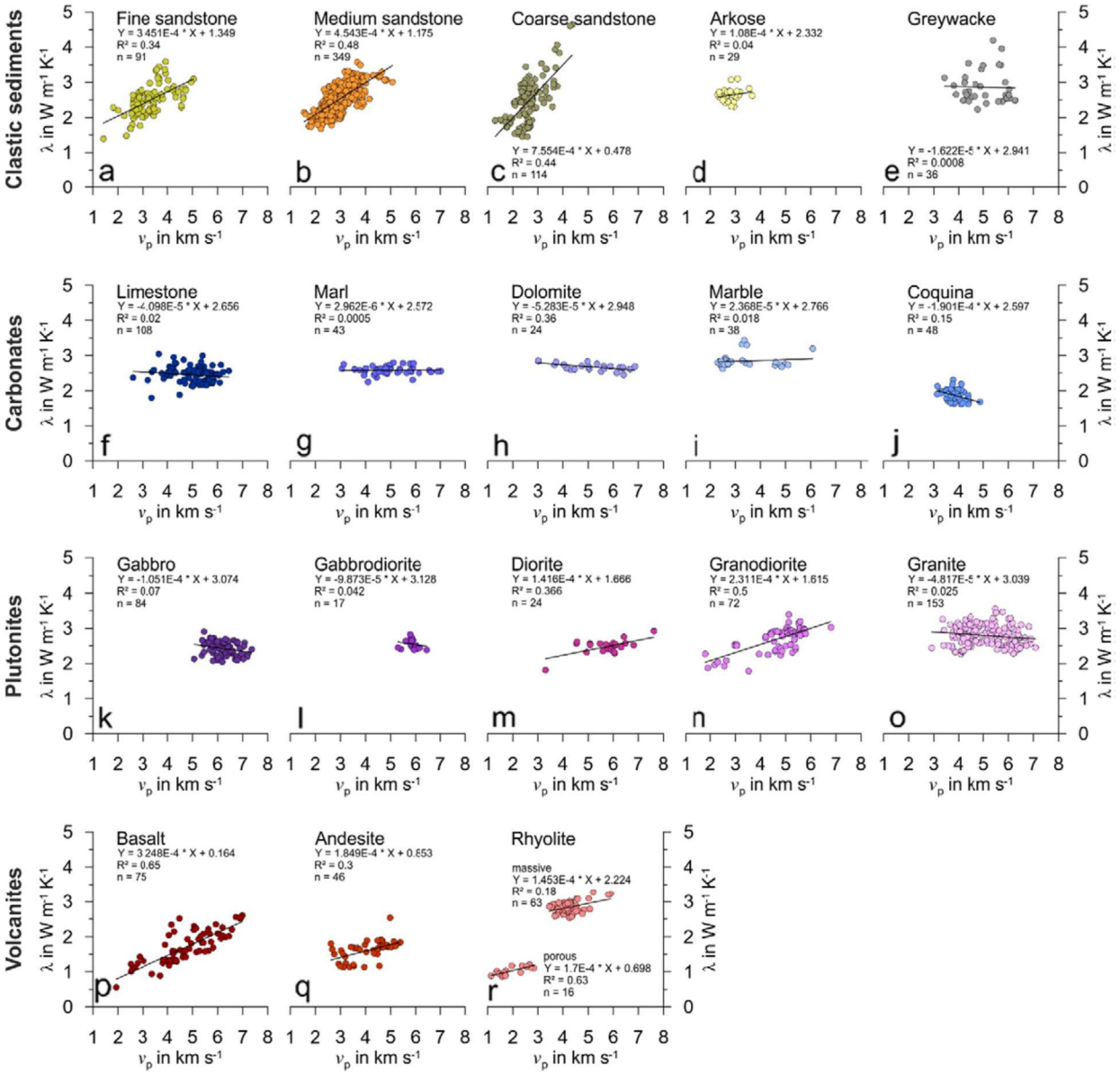

Appendix D

Table 4 Sources used for data collection for analysis described in Chapter 4

No.	Ref.	Reference	Number of Data Points	Material Studied*	Property
1	[149]	(Material Properties, 2018)	6	0	All
2	[150]	(Quadrant Plastics, 2018)	26	0	All
3	[151]	(Professional Plastics, 2018)	44	0	All
4	[152]	(Laminated Plastics, 2018)	54	0	All
5	[153]	(Sahin H. K., 2009)	4	1	Dielectric
6	[69]	(Sahin & Ay, 2004)	36	1	Dielectric
7	[119]	(James, 1975)	64	2	Dielectric
8	[68]	(Torgovnikov, 1993)	324	1	Dielectric
9	[154]	(Suleiman, Larfeldt, Leckner, & Gustavsson, 1999)	3	1	Thermal
10	[153]	(Sahin H. K., 2009)	4	1	Thermal
11	[155]	(Jankowska & Kozakiewicz, 2014)	4	1	Thermal
12	[156]	(Kettunen, 2006)	5	1	Thermal
13	[157]	(Goss & Miller, 1992)	6	2	Thermal
14	[158]	(Vay, De Borst, Hansmann, Teischinger, & Muller, 2015)	9	1	Thermal
15	[159]	(Kawasaki & Kawai, 2006)	12	2	Thermal
16	[160]	(Pralat, 2015)	12	1	Thermal
17	[161]	https://srdata.nist.gov/ NIST US dept of commerce	41	2	Thermal
18	[54]	(Cardenas & Bible, 1987)	547	1	Thermal
19	[162]	(Zhou, Zhou, Hu, & Hu, 2013)	12	2	Thermal & dielectric
20	[163]	(Bucur, Handbook of Materials for String Musical Instruments, 2016)		1	Velocity
21	[164]	(Barkas, Hearmon, & Rance, 1953)	6	1	Velocity
22	[93]	(Kollman & Cote, 1968)	7	1	Velocity
23	[165]	(Bachtiar, Sanabria, Mittig, & Niemz, 2016)	8	1	Velocity
24	[166]	(Han, Wu, & Wang, 2006)	14	2	Velocity
25	[167]	(Roohnia, 2016)	17	1	Velocity
26	[168]	(Yang, Yu, & Wang, 2015)	36	1	Velocity
27	[169]	(Bucur, Springer Series in Wood Science: Acoustics of wood, 2006)	73	1	Velocity
28	[170]	(Ozyhar, Hering, Sanabria, & Niemz, 2013)	6	1	Velocty
		TOTAL	**1380**		

* 0- Plastic, 1-Wood, 2-Wood Derivatives

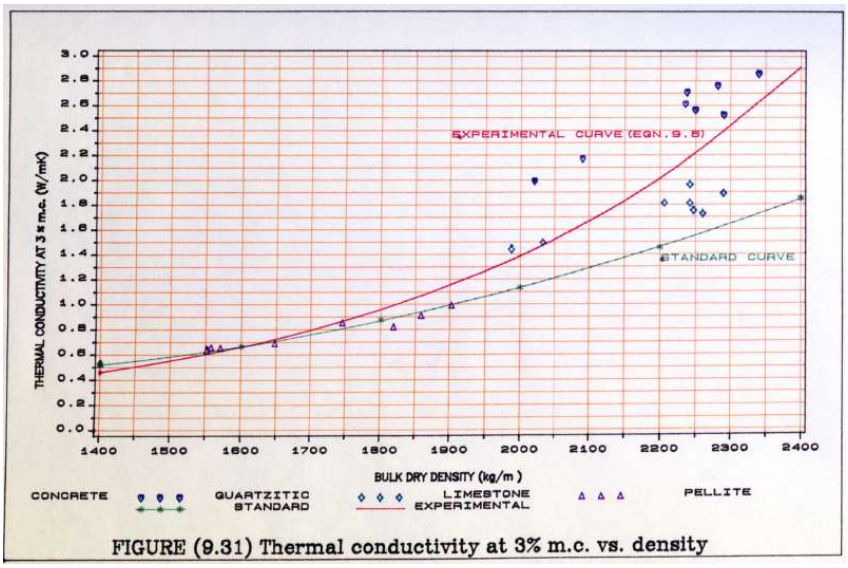

Figure 95 Ganjian's work on thermal conductivity of concrete and its density

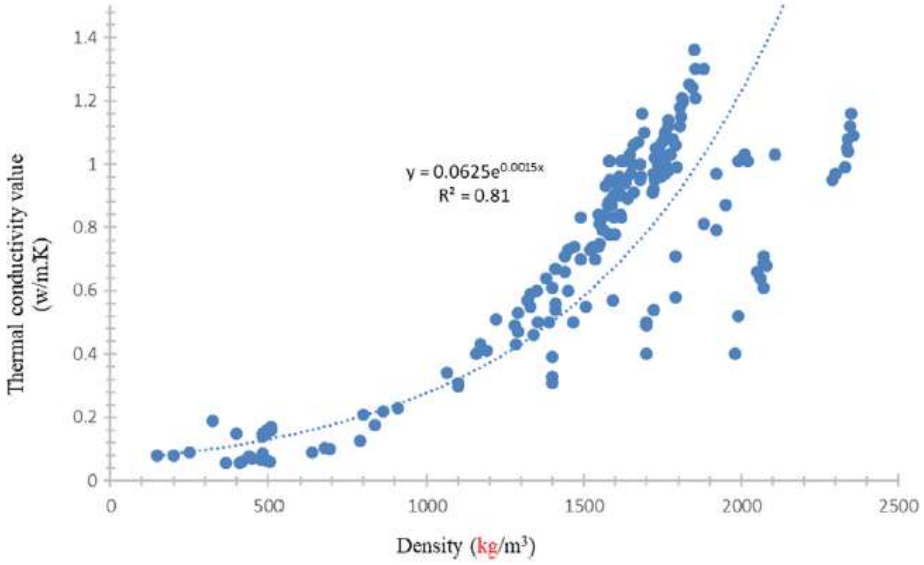

Figure 96 Asadi's [115] data and equation for the correlation of density and thermal conductivity for lightweight concrete

Appendix F

Work of scientists to correlate thermal conductivity with density of clay bricks. Very low scores for linear regression are shown.

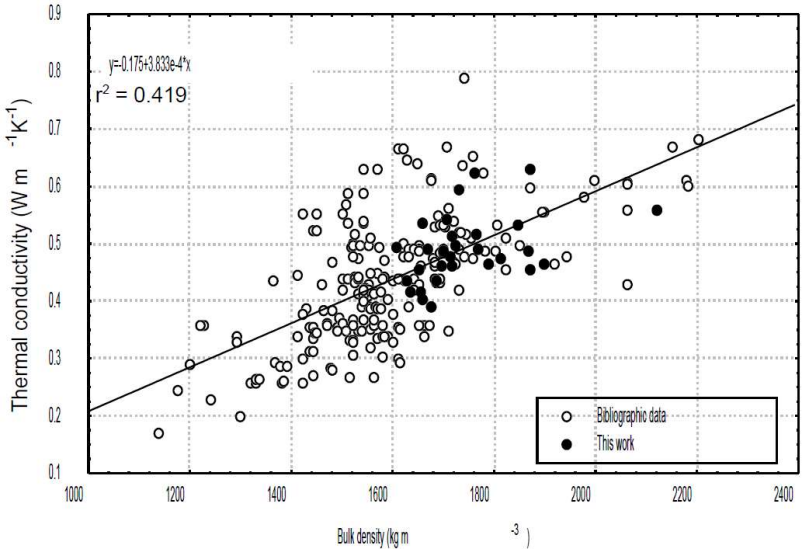

$R^2 = 0.419$

Figure 97 Correlation of bulk density and thermal conductivity of clay bricks as shown by Dondi et al [136]

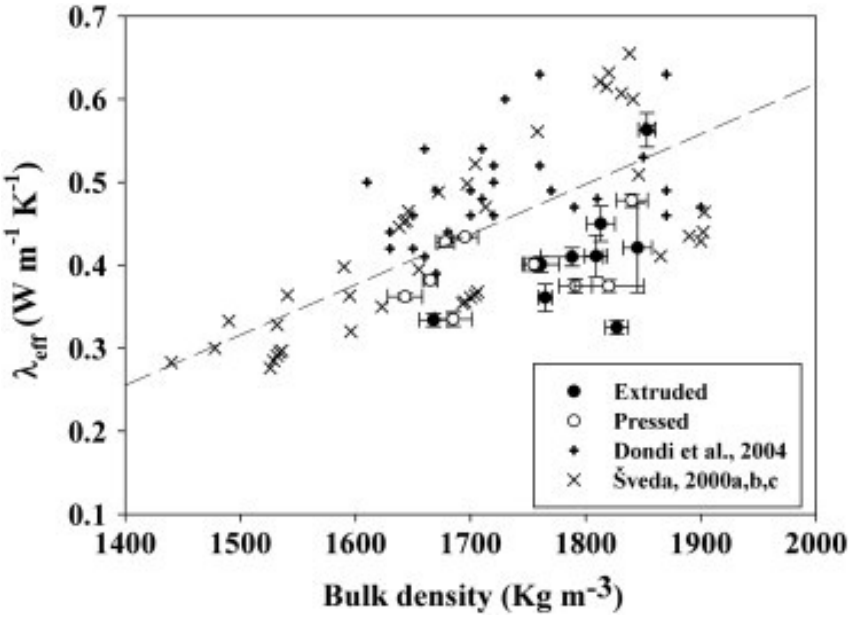

$R^2 = 0.54$

Figure 98 Correlation of bulk density and thermal conductivity for clay bricks as shown by Lassinantti et al [134]

Appendix G

Table 5 Advantages of using the computational approach to thermal conductivity as proposed in this thesis over other commonly used methods

	Heat Flow Meter Method	Infra-red Thermography	Computational Approach
Environmental Conditions	Requires steady state conditions. Needs temperature difference of at least 10°C between indoors and outdoors	Requires steady state conditions. Needs temperature difference of at least 10°C between indoors and outdoors	None
Weather bound	Need for temperature difference implies that freely ventilated buildings cannot be measured in summers	Affected by cloud cover, wind speed, temperature, building occupancy. Freely ventilated buildings may not be measured in summers	None
Ease of measurement	Requires advanced technical knowledge and training	Requires advanced technical knowledge and training	Potential for development of non-technical device
Bulky equipment	No	Yes	No
Cavity Walls	Yes	No	Yes
Ceramic / Heavy Walls	Yes	No	Yes
Measurement Time	3 days to 30 days	Few hours to 3 days	Less than an hour
Expected Error	11% to 28% [27]. Improves with better environmental conditions	5% to 200% [4,96–98] Improves with better environmental conditions	Up to ±20% Can improve with more data and better quality data
Cost effective	Ranges from inexpensive to high end.	Expensive	Ranges from inexpensive to high end